NON-NEWTONIAN FLUID FLOW IN ANNULI

BY

SIJUN YU, B. Eng., M. Eng.

A Thesis

Submitted to the School of Graduate Studies

McMaster University

in Partial Fulfilment of the Requirements

for the Degree of

Doctor of Philosophy

July 1994

DOCTOR OF PHILOSOPHY(1994) McMaster University

(Mechanical Engineering) Hamilton, Ontario

TITLE: Non-Newtonian Fluid Flow in annuli

AUTHOR: SIJUN YU, B.Eng., M.Eng. (Beijing University of Science and Technology)

SUPERVISOR: Dr. G.F. ROUND

NUMBER OF PAGES: xiii, 149

ACKNOWLEDGEMENTS

I wish to express my sincere gratitude to my supervisor, Dr. G.F. Round, for his helpful advice, valuable discussions and suggestions and continuous encouragement throughout this research, and for his great help in all aspects of my graduate studies since the very first day I arrived at McMaster University. All of these made the completion of this work possible.

A special appreciation is extended to the menbers of my supervisory committee, Dr. M. Shoukri and Dr. J. Vlachopoulos.

TABLE OF CONTENTS

ABSTRACT

The flow of non-Newtonian fluids in both concentric and eccentric annuli was investigated in this thesis. The model for generalized Bingham (Herschel-Bulkley) fluids was used in the studies, which included fully developed flow, entrance flow, start-up flow and pulsating flow in a concentric annulus and start-up flow in an eccentric annulus. A set of mathematical formulations has been developed for fully developed flow of generalized Bingham fluids in a concentric annulus. Velocity profiles are presented by using a numerical scheme to solve the equations. The position of the unsheared plug in the annulus may be determined by the solutions. The equations of motion for entrance flow and unsteady flow of generalized Bingham fluids in a concentric annulus have been derived with a group of dimensionless variables. A control volume based finite difference technique was used to solve the governing equations. The effects of generalized Bingham number Pl, flow index n and radius ratio s on velocity profiles and pressure drop in the annulus are presented. Velocity profiles of start-up flow of generalized Bingham fluids in an eccentric annulus were obtained from finite difference solutions of the equation of motion after transformation into bipolar coordinates. The effects of eccentricity were also considered.

LIST OF FIGURES

Nomenclature

d_h	hydraulic diameter $2(r_o-r_i)$
e	eccentricity, distance between the centres of inner and outer cylinders
E	dimensionless eccentricity, $E=e/d_h$
k	consistency factor
n	flow behaviour index
p	pressure
p_0	pressure at entry section of the annulus
P	dimensionless pressure $(p-p_0)/\rho u_0^2$
Pl	generalized Bingham number $(\tau_0 d_h^n)/(ku_0^n)$
Q	volume flow rate in the annulus
r	radial coordinate
r_i, r_o	inner and outer radii of the annulus
r_n, r_p	inner and outer boundaries of the unsheared plug
R	dimensionless radius $4r/d_h$
R_i, R_o, R_n, R_p	dimensionless variables of r_i, r_o, r_n, r_p respectively
Re	Reynolds number $(\rho d_h^n u_0^{2-n})/k$
s	radius ratio r_i/r_o
t	time
T	dimensionless time

u, v	velocity components in axial and radial directions respectively
u_0	axial velocity at the entry section of the annulus
U, V	dimensionless velocity components $U=u/u_0$, $V=R_c v/u_0$
x,y,z	coordinates
X,Y,Z	dimensionless coordinates $X=x/d_h$, $Y=y/d_h$, $Z=z/[(d_h/4)R_c]$

Greek symbols

β	frequency parameter
ϵ	pressure amplitude
η,ξ	bipolar coordinates
$\dot{\gamma}$	shear rate $\partial u/\partial r$
ρ	density of the fluid
τ	shear stress
τ_0	yield stress

CHAPTER 1

INTRODUCTION

Non-Newtonian fluids are found everywhere in the industrial world: examples of such non-Newtonian materials are polymer solutions and melts, various slurries and suspensions, cement, greases, oils, petroleum preparations, drilling mud, pastes, paper pulp, paints, and many food products such as tomato sauces and margarine. Such non-Newtonian behaviour is characterized by the shear stress being not linearly related to the rate of strain. In many cases non-Newtonian behaviour is time-independent. Non-Newtonian fluids are classified according to their response to the application of shear stress. The most common classification is:

I) power law fluids;

II) ideal Bingham fluids;

III) generalized Bingham (Herschel-Bulkley) fluids.

Figure 1.1 shows the behaviour of flowing materials by means of flow curves, that is, plots of shear stress versus strain rate. The curve (A) represents Newtonian behavior

whereas curves (B)- (E) depict various non-Newtonian fluids.

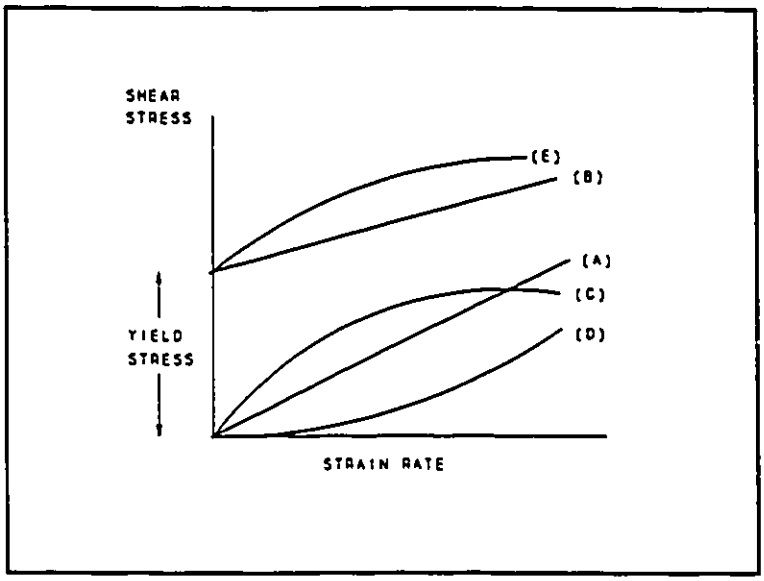

Figure 1.1 Flow curves for model inelastic materials. (A) Newtonian fluids; (B) Ideal Bingham fluids; (C) Power law fluids (n > 1); (D) Power law fluids (n < 1)); (E) Generalized Bingham fluids.

The study of flow of non-Newtonian fluids in pipes and annuli is of importance because of various engineering applications in chemical, petroleum, biomedical and food processes. Examples that may be cited are the extrusion process of polymer melts, blood circulation in the human cardiovascular system, and coal-water slurry transportation. Studies have found that entry region in a concentric annulus

has significant effects on the so called " Shark Skin" problem in polymer product manufacturing. Another typical example from the petroleum industry of non-Newtonian fluid flow in eccentric annuli is drilling mud and cement slurry flowing between the drillpipe and the casing in an oilwell. An understanding of the characteristics of non-Newtonian fluid flow in an annulus is of considerable interest in many areas of science and engineering. Knowledge of the velocity distribution during flow is necessary to predict the pressure drop required to obtain a desired flow rate, and to determine the rates of heat and mass transfer accompanying such flow. The trend towards a more scientific approach to engineering design has brought about the need for fundamental information concerning the behaviour of non-Newtonian fluids in motion. One of the main objectives of the present study is to present more detailed information about the behaviour of non-Newtonian fluids flowing in both concentric and eccentric annuli.

In the present work, the non-Newtonian fluids which we are dealing with are time-independent generalized Bingham fluids (Herschel-Bulkley fluids) whose rheological behaviour can be described by the equation:

$$\tau=\tau_0\pm k\left|\dot{\gamma}\right|^{n-1}\dot{\gamma} \qquad 1.1$$

where τ is the shear stress, τ_0 is the yield stress, k is the

consistency factor, $\dot{\gamma}$ is the shear rate and $\dot{\gamma} = \partial u/\partial r$, n is the flow behaviour index. " + " is for $\dot{\gamma} > 0$ and " - " is for $\dot{\gamma} < 0$. The engineering reality of the yield stress has been discussed by many researchers (Astarita, 1990). The behaviour of a generalized Bingham fluid is an empirical combination of an ideal Bingham plastic and power-law behaviour. If $\tau_0 = 0$ and $n \neq 1$, it reduces to a power-law fluid. If $\tau_0 \neq 0$ and $n = 1$, an ideal Bingham plastic fluid results. Generalized Bingham fluids are also referred to as yield power law fluids. Although the model of generalized Bingham fluids can be used to represent most viscous non-Newtonian flows, very little has been reported in the literature on developing and unsteady flows of fluids for this model in ducts.

Because of the nonlinear relationship between shear stress and shear rate, the equations of motion of non-Newtonian fluids are nonlinear. Therefore, in the majority of cases of interest it is impossible to find exact analytical solutions, and numerical methods have to be used to solve such problems. The primary concerns of the present work are the numerical solutions of both entrance developing flow and unsteady flow of non-Newtonian fluids in annuli. A control volume based finite difference marching integration technique was used to solve the nonlinear equations of motion. For Bingham fluids flowing in a concentric annulus, because of the

characteristics of the yield stress, there exists an unsheared plug flowing in the annulus. The location of the plug is not symmetric between the inner and outer walls of the annulus and the inner and outer radii of the unsheared plug should be obtained as the boundary conditions for both the entrance developing flow and the unsteady flow. Therefore, a numerical procedure was developed to calculate the fully developed flow of generalized Bingham fluids in concentric annuli and the inner and outer boundary radii can be determined from the results. Because the flow in an eccentric annulus is not axisymmetric, the geometry of the eccentric annulus is described by using a bipolar coordinate system. The transformation from rectangular to bipolar coordinates allows the eccentric annulus to be mapped into a rectangular region, therefore a finite difference method can be applied to solve the problems.

In Chapter 4, a general method for the practical calculation of the fully developed flow of generalized Bingham fluids in a concentric annulus is presented. The analysis is worked for Newtonian fluids, power-law fluids, ideal Bingham fluids and generalized Bingham fluids, but it is readily extended to other rheological models. Dimensionless Velocity profiles, volumetric flow rates and the inner and outer boundary radii of the unsheared plug for the Bingham fluids can be obtained from the numerical calculation.

In Chapter 5, a control volume based finite difference marching integration technique is used to solve the two dimensional boundary layer equations which represent the entrance flow of generalized Bingham fluids in a concentric annulus. The velocity profiles and pressure drop profiles in the entrance region are presented.

Chapter 6 provides detailed information about the unsteady flow of generalized Bingham fluids in concentric annuli, which includes start-up flow and pulsating flow. The governing equations derivation, dimensional analysis, numerical calculating procedures and results are presented. The effects of radius ratio, fluid properties and flow parameters are discussed.

Unsteady flow of generalized Bingham fluids in an eccentric annulus is studied in chapter 7. Details of the transformation of momentum equation from rectangular to bipolar coordinates are presented. A finite difference method is developed to obtain the velocity profiles. The effects of eccentricities, radius ratio and fluid properties are discussed in this study.

CHAPTER 2

LITERATURE REVIEW

2.1. Fully developed flow in a concentric annulus

Calculations on fully developed, laminar, axial flow of non-Newtonian fluids through a concentric annulus are commonly needed in many industrial situations such as the design of equipment handling non-Newtonian fluids, and they are important references for studies of more complicated flows. For instance, in this study, from the calculations of the fully developed flow of Bingham fluids, the inner and outer boundary radii of the unsheared plug in the annulus were obtained, which were used in the calculations of entrance flow and unsteady flow in concentric annuli as boundary conditions that simplified the numerical procedures.

For non-Newtonian fluid flow in concentric annuli, Fredrickson and Bird (1958) analyzed fully developed flow of ideal Bingham and power law fluids in a concentric annulus. The relationship between flow rate and frictional pressure gradient was published in theform of a set of plots. Rotem

(1962), McEachern (1966), Mishra and Mishra (1976), Hanks and Larsen (1979) have theoretically analyzed fully developed laminar flow of power law fluids. An analytical expression for the volume rate of flow of a power law non-Newtonian fluid through a concentric annulus was found by Hanks and Larsen as:

$$Q=\frac{n\pi r_o^3}{1+3n}\left(\frac{dp/dzr_o}{2k}\right)^{\frac{1}{n}}\left[(1-\lambda^2)^{\frac{n+1}{n}}-s^{\frac{n-1}{n}}(\lambda^2-s^2)^{\frac{n+1}{n}}\right] \qquad 2.1$$

where n is flow behaviour index, r_o outer radius, k is consistency factor, s is ratio of radius of inner cylinder to that of outer cylinder $s=r_i/r_o$, $\lambda=r^*/r_o$, at $r=r^*$ the shear stress $\tau = 0$. Figure 2.1 shows the schematic representation of coordinates describing axial flow in a concentric annulus.

In 1979, Hanks published results for the fully developed flow of generalized Bingham fluids in a concentric annulus, and gave useful engineering design charts to make practical calculations quite easy. Fordham, Bittleston and Tehrani (1991) presented the calculations of fully developed flow in a concentric annulus with Casson, Herschel-Bulkley and Robertson-Stiff rheological models.

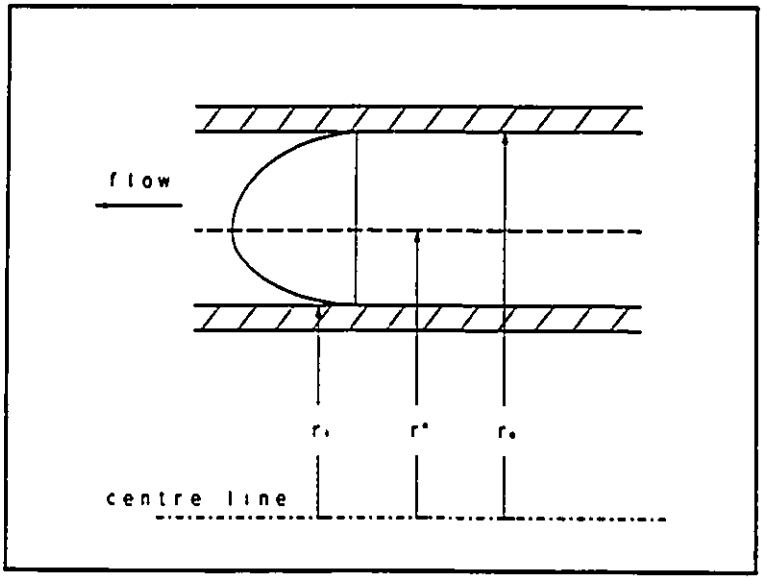

Figure 2.1 Schematic representation of coordinates describing axial flow in a concentric annulus.

Pressure drop and velocity profiles from given volumetric flow rates were presented. Gucuyener and Mehmetoglu (1992) further developed the method of Hanks. They analyzed and calculated the fully developed flow of generalized Bingham fluids (called yield-pseudo-plastic fluids in the paper) in a concentric annulus. An analytical solution for the volumetric flow rate of the fluids was presented. Practical examples were provided to give insight into the use of their development.

In this study, the governing equations of the fully developed flow of generalized Bingham fluids are made

dimensionless with the same nondimensional variables used in developing flow and unsteady flow, so that the results of calculations are consistent with such flows. A similar numerical method to Fordham's was used in this study.

2.2. Entrance and developing flow in ducts

When a fluid enters a duct in laminar flow through an abrupt contraction, it undergoes a change in flow pattern from an initial condition close to a flat velocity profile at the inlet, to a fully developed condition at a certain distance downstream. This is commonly known as entrance flow or developing flow. The distance from the inlet to the point where the maximum velocity is 98% of its fully developed value is defined as the entrance length. The length of the entrance region depends on the geometry of the duct, the Reynolds number and the rheological characteristics of the fluid. In many practical applications, the flow may not become fully developed and the effect of the entrance region may be significant. Therefore, a knowledge of the entrance flow of non-Newtonian fluids in ducts is important in order to predict the pressure drop required to obtain a desired flow rate and to determine the rates of heat and mass transfer accompanying such flow. Flow in the entrance region of ducts constitutes a problem of fundamental interest in engineering applications such as in heat exchange devices and in polymer processing

industries. The behaviour of the fluid in the entrance region may play a significant part in the total length of the duct and the pressure drop may be markedly greater than for the case where the flow is regarded as fully developed throughout the duct. Many industrial applications of non-Newtonian fluids are described in a review by Bird, Dai and Yarusso(1983).

For entrance flow (developing flow) in a pipe or an annulus, the flow field is taken to be composed of the two regions: a boundary layer region and an inviscid core region. As the flow proceeds, the thickness of the boundary layer region-where the viscous effects dominate-increases and correspondingly the inviscid core thickness decreases. Therefore, for high Reynolds numbers (greater than 200, Gupta and Garg 1981, Mehrotra and Patience 1990), the steady, laminar entrance flow problem is often treated as a two dimensional boundary layer problem, and instead of using Navier-Stokes equations, Prandtl's boundary layer equations are used to solve the problem (e.g. Mckillop et al. 1970, Liu and Shah 1975, Lin and Shah 1978, Gupta and Garg 1981, Matras and Nowak 1982, Gupta 1987, Batra and Jena 1990, Cho and Hyun 1990).

A number of authors have studied entrance flow of non-Newtonian fluids in ducts. The entrance region flow of power-law fluids in pipes was investigated by Bogue (1959), Collins and Schowalter (1963), Matras and Nowak (1983) and Mehrotra

and Patience (1990). Using different approximation methods, the velocity and pressure profiles in the entrance region as well as the entrance lengths were obtained. Chen, Fan and Hwang (1970), Shah and Soto (1975) and Nowak and Gajdeczko (1983) studied the entrance flow of ideal Bingham fluids in pipes. The effects of the yield stress on the velocity profiles and the pressure drop in the entrance region were also investigated. Soto and Shah (1976), Batra and Kandasamy (1990) studied the entrance flow of generalized Bingham fluids in pipes. However, in Batra and Kandasamy's solution, the inertia terms in the governing equation were neglected. Non-Newtonian blood flow in the entrance region of a tube was investigated by Shah and Soto (1974). The flow characteristics of blood were assumed to obey Casson's stress-strain relation

$$\sqrt{\tau}=\sqrt{\tau_0}+\sqrt{k|\dot{\gamma}|} \qquad 2.2$$

Tiu and Bhattacharya (1973, 1974) presented both numerical calculations and experimental results for developing flow of power law fluids in a concentric annulus. Mishra and Mishra (1977) employed a linearized approach for predicting loss coefficients in entrance region flows of power law fluids in a concentric annular duct. Entrance flow of ideal Bingham fluids in a concentric annulus was studied by Mishra, Kumar

and Mishra (1985). Results were obtained for dimensionless boundary layer thickness, center core velocity, pressure drop and the entrance length. Liu and Shah (1975), and Batra and Jena (1990) investigated the entrance region flow of blood and Casson fluids in concentric annuli. To our knowledge, developing laminar flow and fully developed flow of generalized Bingham fluids (Hershel- Bulkley fluids) in concentric annuli has not been reported in the literature.

For an incompressible, steady, laminar, isothermal, axisymmetric entrance flow, the conservation equations of continuity and motion in a pipe or an annulus may be expressed as:

$$\frac{\partial u}{\partial z}+\frac{\partial}{r\partial r}(rv)=0 \qquad 2.3$$

and

$$u\frac{\partial u}{\partial z}+v\frac{\partial u}{\partial r}=-\frac{1}{\varrho}\frac{dp}{dz}-\frac{1}{\varrho r}\frac{\partial}{\partial r}(r\tau) \qquad 2.4$$

where x and r are the coordinates in the axial and radial directions respectively, u and v are the axial and radial components of velocity, ϱ is the density of the fluid, p is the pressure.

The governing differential equations 2.3 and 2.4 for entrance flow are nonlinear; no exact analytical solutions

have been obtained even for Newtonian fluids. Many approximate methods for entrance developing flow in ducts have been developed, in which the momentum integral method and finite difference methods are most used.

The momentum integral method for the entrance region flow of a Newtonian fluid was first developed by Schiller (1922). He assumed a parabolic velocity profile in the boundary layer with a thickness $\delta(x)$ and a uniform velocity profile outside the boundary layer. The pressure gradient was related to the velocity outside the boundary layer by

$$U\frac{dU}{dZ}=-\frac{1}{\rho}\frac{dP}{dZ} \qquad 2.5$$

where U is a function of x. Integrating the equation of motion with these assumptions and after further numerical procedures, the velocity and pressure profiles could be obtained. This method was used by Bogue (1959) for the entrance flow of Power-law fluids in pipes, Tiu and Bhattacharyya (1973) for the entrance flow of power-law fluids in annuli, Mishra and Kumar (1985) for the entrance region flow of ideal Bingham fluids in concentric annuli, and Batra and Jena (1990) for the entrance flow of blood in concentric annuli.

The major drawback of the momentum integral method is the assumption of an inviscid core of fluid outside the boundary

layers. The calculation of pressure drop is done simply from inviscid flow considerations. This assumption may be valid near the entry where the viscous effect is important only in the regions near the walls, but becomes unrealistic in the downstream region near the fully developed flow region. Campbell and Slattery (1963) first modified the classical momentum integral method for the entrance flow problem of Newtonian fluids in circular tubes by using the macroscopic momentum balance equation and incorporating the overall macroscopic mechanical energy balance to account for the viscous dissipation within the boundary layers.

The macroscopic momentum balance equation may be written as:

$$\frac{d}{dz}\int_0^R u^2 r dr+\frac{1}{\varrho}\frac{dp}{dz}\int_0^R r dr+\frac{1}{\varrho}[\tau_{rz}]\,|_{r=R}=0 \qquad 2.6$$

The macroscopic mechanical energy balance equation may be written as:

$$\frac{1}{2}\varrho\int_0^R u^3 r dr-\frac{1}{4}\varrho U_0^3 R^2+p\int_0^R u r dr-\frac{1}{2}p_0 U_0 R^2 +\mu\int_0^z\int_0^R\left(\frac{\partial u}{\partial r}\right)^2 r dr dz=0 \qquad 2.7$$

Using the assumption of the parabolic velocity profile in the boundary layers, Eqns. 2.6 and 2.7 can be solved numerically, and the velocity and pressure profiles in the entrance region can be obtained. This method was employed by Chen, Fan and Hwang (1970) for the entrance region flow of ideal Bingham fluids in a circular pipe and by Tiu and Bhattacharyya (1973) for the entrance region flow of power-law fluids in annuli.

One of the drawbacks of these integration methods is the assumption of a velocity profile - this can introduce some error into the results. With the development of computer and numerical computing techniques, finite difference methods were developed for the problem of the entrance flow. Using finite difference methods to solve the problem of the entrance region flow; velocity and pressure distributions may be obtained directly without assuming the form of velocity profile within the boundary layer. The finite difference method was first developed by Bodoia and Osterle (1961) for the entrance flow of Newtonian fluids between two parallel plates. Without linearizing assumptions for the original difference equations of fluid motion, the governing equations for the developing flow were directly solved by a finite difference marching procedure. The velocity and pressure profiles in the entrance region were obtained. This method was also used by Hornbeck (1964) for the entrance flow of Newtonian fluids a pipe, and very good results obtained. Patankar and Spalding (1968,

1970) developed a similar finite difference marching-integration procedure based on the control volume approach to solve the general two dimensional boundary equations. In their method, the governing equations were expressed in finite difference forms by the integration of a control volume at every step, the nonlinear inertia terms in the governing equations were evaluated from the upstream values of the control volume. Therefore, the velocities and pressure at any axial position were determined by using values upstream from the position. By step-wise repetition of this basic operation, the whole region could be investigated. Because the finite difference marching-integration technique is very convenient for dealing with the nonlinear terms in the governing equations, this method was popularly used by many investigators to solve the problem of developing flow of Newtonian fluids and extended to the non-Newtonian fluids flow in the entrance region. Shah and Farnia (1974), Gupta and Garg (1981) used the finite difference procedure of Patankar and Spalding for the entrance flow of Newtonian fluids in a concentric annulus. Shah and Farnia presented some values of local and apparent friction factors in figures for the entrance region. Gupta and Garg provided the velocity and pressure profiles for developing flow through annular ducts. Soto and Shah (1975, 1976) employed the finite difference method of Patankar and Spalding for the problems of developing

flow of ideal Bingham fluids and yield-power law fluids in pipes. The values of local friction factor, apparent friction factor and center line velocity were determined and presented graphically. The effects of yield stress and the flow behaviour index on the velocity and friction factors profiles were also investigated. Liu and Shah (1975) using Patankar and Spalding's finite difference method obtained the numerical solution of the entrance flow in an annular tube for a non-Newtonian fluid obeying the Casson's relation. The effects of yield stress on friction factors were presented and results for entrance flow of Newtonian fluids in annuli presented. Mehrotra and Patience (1990) using the Patankar (1980) control volume approach investigated entrance flow of power law fluids in pipes. A staggered grid block system was used, in which the primary variables of radial velocity, axial velocity and pressure were evaluated at different locations in each grid block. Center line velocity profiles and entry lengths were obtained.

Matras and Nowak (1983) introduced an approach called a "transformation method" for predicting changes in pressure drop in laminar isothermal entry flow of power-law fluids in circular tubes. In their method, a "pseudo-Newtonian" fluid model was adopted to describe the power law fluid model by introducing some transformation variables. The behaviour of power law fluids in the entrance region of circular tubes was

obtained by studying a hydrodynamical analogy of Newtonian fluids. Use of the integral forms of equations of motion with an appropriate velocity distribution led to simple expressions boundary layer and pressure distribution in the developing region. Gupta (1987, 1990) using a similar method investigated laminar power law fluid flow development in a straight channel.

In the present program, the finite difference marching integration approach will be used to solve the entrance region flow of generalized Bingham fluids in pipes and in annuli.

2.3. Unsteady flow of non-Newtonian fluids in ducts

In both industry and nature, the time-dependent unsteady motion of fluids as part of some process is quite common. Three aspects of unsteady, laminar motion of non-Newtonian fluids in ducts are considered by many investigators. These are:

(a) Start-up flow --- in a duct following the sudden application of an axial pressure gradient to a fluid at rest.

(b) Oscillatory flow --- in which the fluid is subjected to a periodic pressure gradient having a mean value of zero. There is no net flow of fluid in the duct. The fluid merely oscillates backward and forward.

(c) Pulsating flow --- in which the fluid is subjected to a periodic pressure gradient having a non-zero mean value and

there is a net flow of fluid through the duct.

Actually, start-up flow and oscillatory flow are special cases of pulsating flow. The pressure gradient for a sinusoidal pulsating flow may be written as:

$$-\frac{\partial p}{\partial z}=\left(\frac{dp}{dz}\right)_s+\left(\frac{dp}{dz}\right)_o \sin(\omega t) \qquad 2.8$$

where $(dp/dx)_s$ is the steady component of the pressure gradient, and $(dp/dx)_o$ is the oscillatory component. If $(dp/dx)_o=0$, we get the condition for start-up flow. If $(dp/dx)_s=0$, the problem reduces to oscillatory flow. For all three types of unsteady flow in long pipes or annuli where entry and exit effects are negligible, the equation of motion may be written as:

$$\varrho\frac{\partial u}{\partial t}=-\frac{dp}{dz}-\frac{1}{r}\frac{\partial}{\partial r}(r\tau) \qquad 2.9$$

The treatment of non-linear partial differential equations of unsteady flow of non-Newtonian fluids generally leads to the use of numerical methods.

Because the unsteady flow of non-Newtonian fluids in ducts has many practical applications, considerable investigations have been made in this field. Barnes, Townsend

and Walters (1969) have presented experimental data on the pulsating flow of power law fluids. Under a pulsating pressure gradient, it was observed that the addition of oscillations increased the mean flow rate above that given by the steady pressure gradient along. They also presented a theoretical analysis of pulsating flow of power law fluids in pipes. The predicted increases in flow rate showed the same trends as the experiment results. Edwards, Nellist and Wilkinson (1972) studied the unsteady laminar flow of power law fluids in pipes. Start-up flow, oscillatory flow and pulsating flow were considered and a finite difference technique was developed to solve the equation of motion; typical velocity profiles were presented. The effects of the major parameters which influenced these flows were demonstrated. Duggins (1972) studied the start-up flow of ideal Bingham fluids in pipes. Velocity profiles for start-up flow of ideal Bingham fluids were derived by using Patankar and Spalding's finite difference methods. The pulsating flows of solid-liquid suspensions in pipelines were studied by Round (1974, 1981); Round, Latto and Lau (1976); Round and El-Sayed (1985, 1986). The possibility for large energy saving in slurry pipelines by the superposition of low frequency regular pulses on a steady flow was investigated. Experiments were carried out using laboratory-scale pipelines involving flow systems using periodic total interruption of flow and an air pulsing device.

Ly and Bellet (1976) developed a technique for dealing with the time-dependent pipe flow of power-law fluids called the "multiviscous" approximation. This method breaks the flow field into N distinct layers of fluid with N different constant Newtonian viscosities. The constant viscosity values were obtained from approximating the non-Newtonian shear stress/shear rate curve by N straight lines. The momentum equations expressed in terms of shear stress were then solved consecutively across the layers. The velocity profiles for oscillatory flow and pulsating flow were obtained. The results were concordant compared with other numerical procedures.

Several different numerical methods were used for unsteady flows of non-Newtonian fluids by Balmer and Fiorina (1980), Gorla and Madden (1984), Nakamura and Sawada (1987, 1990). Balmer et al. studied the unsteady flow of power law fluids in a tube. The momentum equations were solved numerically using an implicit finite difference technique for the time-dependent velocity profiles for both start-up and pulsating pressure gradients. Dimensionless curves were presented showing the velocity profile development and phase angle variation for a variety of power-law index values. Gorla et al. adopted a semi-direct variational method of Kantovorich to analyze the unsteady flow of power-law fluids in a circular tube. The results were reported on the effect of a triangular pressure pulse on the development and transient response of

the flow field of a power-law fluid. Laminar pulsatile flow of slurries was studied numerically by Nakamura and Sawada (1987) with the slurry being described as a ideal Bingham fluid. The Crank-Nicolson method was adopted to solve the governing equations of motion. The flow enhancement rates, the extra power required to pulsate the flow were investigated. Nakamura and Sawada also investigated unsteady blood flow through a stenosis. The two-dimensional starting and stopping flows of the non-Newtonian fluids through an axisymmetric stenosis were calculated using the finite element method.

Laminar pulsating flow of a clay slurry in a circular pipe was studied experimentally by Kajiuchi and Saito (1984). The flow behaviour of the slurry was approximated as that of an ideal Bingham fluid. The addition of sinusoidal pulsating fluctuation to a steady pressure gradient resulted in enhancement of the flow rate, because of the non-Newtonian behaviour of the slurry. The enhancement increased with the following conditions: (1) an increase in pulsating amplitude, (2) a decrease in pulsating frequency and (3) a decrease in the mean pressure gradient. An experiment on the pulsatile flow of ideal Bingham fluids in a high Reynolds number region was carried out by Nakamura and Sawada (1990).

It appears that there is nothing published in the open literature on the unsteady flow of non-Newtonian (power law, ideal Bingham and generalized Bingham) fluids in a concentric

annulus, and few papers have been published on the unsteady flow of generalized Bingham fluids in pipes.

In the present program, the finite difference marching integration approach will be adopted to deal with the unsteady flow of non-Newtonian fluids (including generalized Bingham fluids) in pipes and in annuli.

2.4. Non-Newtonian fluid flow in an eccentric annulus

Fluids flow through an annular space is an often-encountered engineering problem. For most of the cases, it is treated as a concentric annular flow. However, in some cases the annular space is not concentric but eccentric, i.e., the axes of inner and outer tubes do not coincide with each other. For example, in the petroleum industry, during a drilling operation, the drillpipe is usually positioned eccentrically in the wellbore, especially in a deviated wellbore where the drillpipe has a strong tendency to offset toward the low side because of gravitational effects.

A bipolar coordinate system is often adopted to describe the geometry of eccentric annuli. In bipolar coordinates, the eccentric annulus is represented by two coordinates, which are two sets of orthogonal circles. This coordinate system is obviously useful, since the walls of the eccentric annulus are represented by two constant values in one coordinate. The transformation from rectangular to bipolar coordinates allows

the eccentric annulus to be a rectangular region. Using bipolar coordinate system and Green's function, Heyda (1959) presented analytical solutions for Newtonian fluids flow in an eccentric annulus. Heyda obtained the velocity profile in the form of an infinite series. Redberger and Charles (1962) applied bipolar coordinates and the finite difference method to solve the differential equation of motion for the velocity profiles, and the flow rates was obtained as a function of the pressure gradient and conduit geometry of Newtonian fluids in an eccentric annulus. Their velocity profile agreed with Heyda's analytical solution. Snyder and Goldstein (1965) also analyzed Newtonian fluid flow in an eccentric annulus using a technique similar to Heyda's. From the solution of velocity profile, they developed expressions for shear stress at the inner and outer surface of the annulus and related these to friction factor calculations.

For non-Newtonian fluid flow in an eccentric annulus, there are only limited number of studies having been carried out. Mitsuishi and Aoyagi (1973) presented a comparison of the experimental data with the conventional variational method analysis for fluid flow in an eccentric annulus, using the Sutterby model as a non-Newtonian model. An equation was given to predict the relation between flow rate and pressure drop in an eccentric annulus in terms of experimental fluid flow data in a circular tube. Guckes (1975) investigated the laminar

flow of power-law fluids and ideal Bingham fluids in eccentric annuli. The volumetric flow rate for the steady flow was presented as a series of dimensionless plots. The plots covered a broad range of fluid properties, pipe diameters, eccentricity and pressure drop. These relationships were obtained by numerically integrating the velocity profile resulting from a finite difference solution of the equations of continuity and motion after transformation into bipolar coordinates.

Although the bipolar coordinate methods were adopted to solve the problem of eccentric flow, it is still very complicated. Some simple approximate methods were developed to solve the problem of eccentric flow. One approximate solution to predict the relationship between volume flow rate and pressure drop for steady-state laminar flow of non-Newtonian fluids in an eccentric annulus was described by Iyoho and Azar (1981). An eccentric annulus was modeled as a slot of variable height (see Figure 2.2). They derived a complete equation for the variable slot height:

$$h=(r_o^2-\epsilon^2c^2\sin^2\theta)^{1/2}-r_i+\epsilon c\cos\theta \qquad 2.10$$

where $c = r_o - r_i$

$\epsilon = e / c$

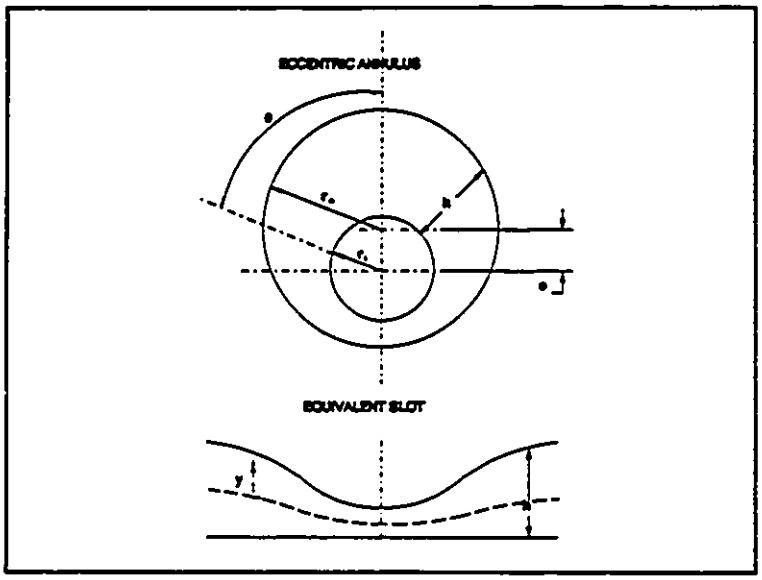

Figure 2.2 Slot equivalent of eccentric annuli

Using the velocity equation for a channel flow, the velocity profiles of power law fluids in eccentric annuli were solved with different eccentricity. However, they calculated the volume rate of flow by using the modified version of the formula given by Skelland (1967) in which the eccentricity was not taken into account. Uner, Ozgen and Tosun (1987) also used the slot flow approximation. A solution to predict the relationship between volume rate of flow and pressure drop for steady state laminar flow of power law and ideal Bingham fluids in an eccentric annulus was described as a function of

eccentricity and radius ratio. The accuracy of the solution was limited only for the radius ratio larger than 0.5. Walton and Bittleston (1991) presented a similar method analyzed the axial flow of a ideal Bingham fluid in a narrow eccentric annulus. Analytical solutions were obtained by expanding in power of δ, the ratio of the difference in radii of the bounding cylinders to their mean. Noting that the slot model is in essence a modified model for flow between parallel plates, which will result in unrealistic symmetric profiles of the shear-stress/ shear-rate magnitudes and the velocity, Luo and Peden (1990) developed another approximate method for the flow of non-Newtonian fluids through eccentric annuli. In their method, an eccentric annulus is treated as being composed of an infinite number of concentric annuli with variable outer radii, which were described as:

$$r_o{}^e = e\cos\theta + \sqrt{r_o{}^2 - [e\sin\theta]^2} \qquad 2.11$$

Instead of using the velocity equation of channel, the velocity profiles for the concentric annuli flow were used in this method to approximate the flow. The solutions for the shear stress, shear rate, velocity profiles and volumetric flow rate/pressure were obtained. Power-law fluids and ideal Bingham fluids were considered.

However, both the slot model and the model presented by

Luo and Peden failed to give accurate solutions of velocity profiles even for Newtonian fluids flowing in an eccentric annulus, because the equation of motion they used could not correctly describe the flow situation in an eccentric annulus. The greater the eccentricity, the greater the error. Using a bipolar coordinate system would here give more accurate solutions. Using this technique to solve the problem of flow in eccentric annuli is even more complicated for non-Newtonian fluids.

Haciislamoglu and Langlinais (1990) first presented studies dealing with fully developed flow of generalized Bingham fluids (named yield-power law fluids in their paper) in eccentric annuli by adopting a bipolar coordinate system and a finite difference technique. The velocity profiles,the viscosity profiles, and the flow rate versus frictional pressure loss gradient relationship were demonstrated for different eccentricities. In their numerical procedure, a non-uniform grid point distribution in bipolar coordinates was introduced, which could give a more realistic distribution of grid points in physical coordinates.

It appears that, there is no literature published for either entrance flow or unsteady flows of non-Newtonian fluids in an eccentric annulus.

CHAPTER 3

SCOPE OF INVESTIGATION

The literature review in Chapter 2 has indicated that the flow of non-Newtonian fluids in concentric or eccentric annuli has considerable industrial applications. However, as a typical non-Newtonian fluid, generalized Bingham fluids, where behaviour is an empirical combination of ideal Bingham fluids and power law fluids, have not been given enough attention. As mentioned in Chapter 2, fully developed flow and developing flow of generalized Bingham fluids (Herschel-Bulkley or Yield power law fluids) in concentric annuli have not been reported in the literature, and it appears that there is nothing published in the open literature on the unsteady flow of non-Newtonian fluids (power law, ideal Bingham and generalized Bingham fluids) in concentric or eccentric annuli. These effects have prompted the present research, which includes following:

1. Fully developed flow of generalized Bingham fluids in

a concentric annulus. Equations of velocity and flow rate were derived. A numerical procedure was developed to solve the velocity profiles. The location of the unsheared plug was determined.

2. Entrance flow of generalized Bingham fluids in a concentric annulus. The equation of motion for generalized Bingham fluids in the entrance region was numerical solved by a finite difference method. Velocity and pressure drop profiles were obtained.

3. Unsteady flow of non-Newtonian fluids in a concentric annulus. The equation of motion of non-Newtonian fluids was solved for both start up flow and pulsating flow. Velocity profiles were obtained.

4. Unsteady flow of non-Newtonian fluids in an eccentric annulus. Bipolar coordinate system and finite difference technique were used to solve the equation of motion for the start up flow in an eccentric annulus. Velocity profiles were obtained.

CHAPTER 4

FULLY DEVELOPED FLOW OF GENERALIZED BINGHAM FLUIDS IN CONCENTRIC ANNULI

4.1. Derivation of governing equations

For Bingham fluid flow in a concentric annulus, because of the yield shear stress τ_0, (see Figure 4.1), the pressure gradient has to be sufficient to overcome the yield stress τ_0 so that the fluid can flow; where $|\tau(r)| > \tau_0$, an unsheared plug flow region with two yield boundaries r_a and

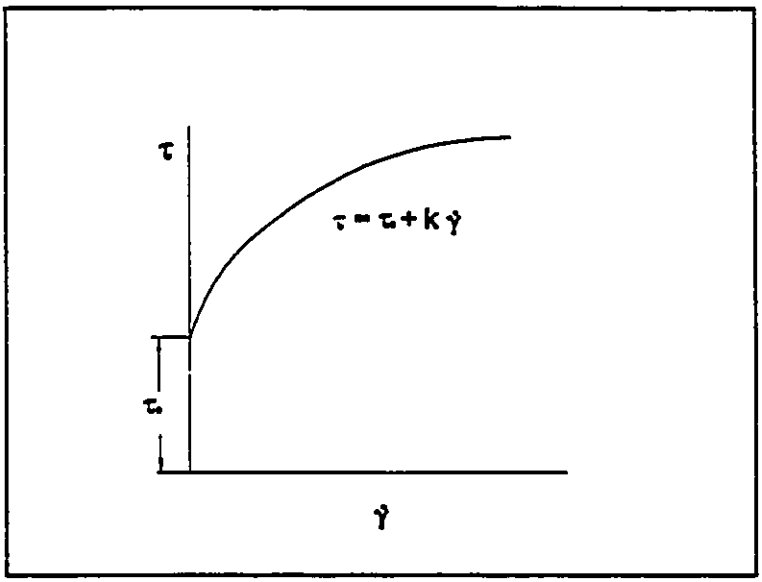

Figure 4.1 τ- $\dot{\gamma}$ relation for a generalized Bingham fluid

r_p (where $r_i < r_a < r_p < r_o$) exists in the concentric annular flow and the inner and outer yield boundary radii are determined by the condition $|\tau(r)| = \tau_0$ at $r = r_a$ and at $r = r_p$. Figure 4.2 shows a sketch of the characteristic velocity distribution for Bingham fluid axial laminar flow in a concentric annulus. In the region of $r_i < r < r_a$; $\dot{\gamma} > 0$, and in the region of $r_p < r < r_o$; $\dot{\gamma} < 0$. The values of r_a and r_p can be determined by calculating the fully developed flow situation.

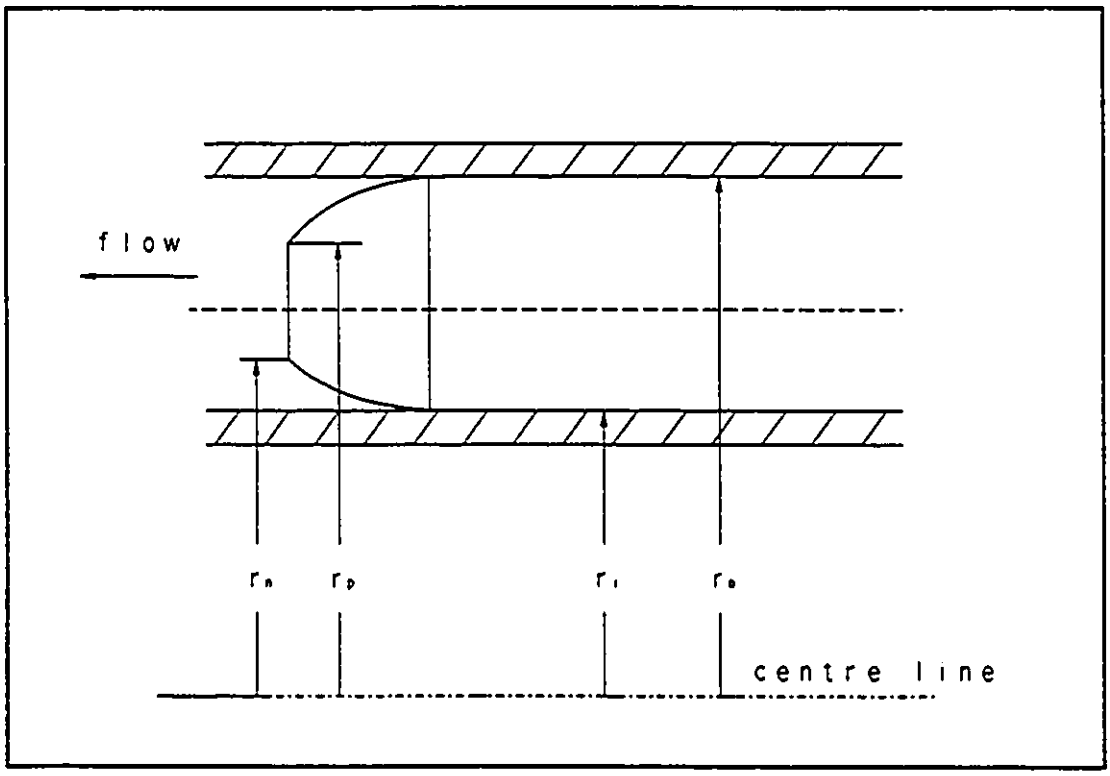

Figure 4.2 Nomenclature for Bingham fluid flow in concentric annulus

Notice that the shear rate $\dot{\gamma} = -\partial u/\partial r$, equation 1.1 for

generalized Bingham fluids may be expressed as:

$$\tau=\tau_0\pm k\left|\frac{\partial u}{\partial r}\right|^{n-1}\frac{\partial u}{\partial r} \qquad 4.1$$

for $r_i \le r \le r_n$, and $r_p \le r \le r_o$

and

$$\frac{\partial u}{\partial r}=0 \qquad 4.2$$

for $r_n < r < r_p$

where r_i and r_o are respectively the inner and outer radii of the annulus.

For the fully developed flow of incompressible fluids through a concentric annulus, the equation of motion can be integrated in cylindrical coordinates to yield:

$$r\tau+\frac{1}{2}\frac{dp}{dz}r^2=C \qquad 4.3$$

where C is an integration constant, and dp/dx is the pressure

gradient in the annulus ($dp/dz < 0$). Substituting of the boundary conditions,

$$\tau=\tau_0 \quad \text{at } r=r_n$$

$$\tau=\tau_0 \quad \text{at } r=r_p$$

into the Eqn. 4.3, and we obtain

$$\tau=\frac{\tau_0 r_n}{r}-\frac{1}{2}\frac{dp}{dz}\left(\frac{r_n^2}{r}-r\right) \qquad 4.4$$

$$r_i \le r \le r_n$$

$$\tau=\frac{\tau_0 r_p}{r}+\frac{1}{2}\frac{dp}{dz}\left(\frac{r_p^2}{r}-r\right) \qquad 4.5$$

$$r_p \le r \le r_o$$

after substituting of Eqn. 4.4 and Eqn. 4.5 into Eqn. 4.1

respectively and integrating the equations, the expressions of the velocity for generalized Bingham fluid flow in a concentric annulus can be written as:

$$u(r)=\int_{r_i}^{r}\left[\frac{\tau_0}{k}\left(\frac{r_n}{r}-1\right)-\frac{1}{2k}\frac{dp}{dz}\left(\frac{r_n^2}{r}-r\right)\right]^{1/n}dr \qquad 4.6$$

$$r_i \le r \le r_n$$

$$u(r)=\int_{r}^{r_o}\left[\frac{\tau_0}{k}\left(1-\frac{r_p}{r}\right)-\frac{1}{2k}\frac{dp}{dz}\left(\frac{r_p^2}{r}-r\right)\right]^{1/n}dr \qquad 4.7$$

$$r_p \le r \le r_o$$

Note: because of the existence of the unsheared plug flow in the annulus,

$$\text{for} \quad r_n \le r \le r_p$$

$$u(r) = u(r_n) = u(r_p) = \text{constant}$$

The volume rate of flow for the generalized Bingham fluid in

the annulus can be expressed by integrating the velocity distribution over the annulus region:

$$Q=2\pi\int_{r_i}^{r_o}u(r)\,r\,dr \qquad 4.8$$

substituting of Eqns. 4.6, 4.7 into Eqn. 4.8 and using the condition of the unsheared plug flow in the annulus, the volume rate of flow expression becomes:

$$Q=\pi\int_{r_i}^{r_n}(r_n^2-r^2)\left[\frac{\tau_0}{k}\left(\frac{r_n}{r}-1\right)-\frac{1}{2k}\frac{dp}{dz}\left(\frac{r_n^2}{r}-r\right)\right]^{1/n}dr$$

$$+\pi\left(r_p^2-r_n^2\right)\int_{r_i}^{r_n}\left[\frac{\tau_0}{k}\left(\frac{r_n}{r}-1\right)-\frac{1}{2k}\frac{dp}{dz}\left(\frac{r_n^2}{r}-r\right)\right]^{1/n}dr$$

$$+\pi\int_{r_p}^{r_o}(r^2-r_n^2)\left[\frac{\tau_0}{k}\left(1-\frac{r_p}{r}\right)-\frac{1}{2k}\frac{dp}{dz}\left(\frac{r_p^2}{r}-r\right)\right]^{1/n}dr \qquad 4.9$$

To calculate the thickness of the unsheared plug in the

annulus, the force balance equation gives:

$$r_p - r_n = -\frac{2\tau_0}{dp/dz} \qquad 4.10$$

4.2. Dimensional analysis

Equations. 4.6, 4.7, 4.9 and 4.10 are made dimensionless by defining the following nondimensional variables:

$$U=\frac{u}{\bar{u}} \qquad R=\frac{r}{d_h/4}$$

$$Re=\frac{\varrho d_h^{\,n}\bar{u}^{2-n}}{k} \qquad Pl=\frac{\tau_0 d_h^{\,n}}{k\bar{u}^{n}} \qquad f=-\frac{dp}{dz}\frac{d_h}{\varrho\bar{u}^2/2}$$

where Re and Pl are respectively defined as a generalized Reynolds number and a generalized Bingham number, f is the Darcy-Weisbach friction factor, $\bar{u}$ is the average velocity of the annulus, d_h is the hydraulic diameter of the annulus.

$$d_h = 2(r_o - r_i)$$

In terms of these nondimensional variables, Eqns. 4.6 and 4.7

become:

$$U(R) = \int_{R_i}^{R} \left[\frac{Pl}{4^n} \left(\frac{R_n}{R} - 1 \right) + \frac{fRe}{4^{n+2}} \left(\frac{R_n^2}{R} - R \right) \right]^{1/n} dR \qquad 4.11$$

$$R_i \leq R \leq R_n$$

$$U(R) = \int_{R}^{R_o} \left[\frac{Pl}{4^n} \left(1 - \frac{R_p}{R} \right) + \frac{fRe}{4^{n+2}} \left(\frac{R_p^2}{R} - R \right) \right]^{1/n} dR \qquad 4.12$$

$$R_p \leq R \leq R_o$$

The dimensionless form of Eqn. 4.9 results in the equation:

$$R_o^2 - R_i^2 = \int_{R_i}^{R_n} -R^2 \left[\frac{Pl}{4^n} \left(\frac{R_n}{R} - 1 \right) + \frac{fRe}{4^{n+2}} \left(\frac{R_n^2}{R} - R \right) \right]^{1/n} dR$$

$$+ \int_{R_p}^{R_o} R^2 \left[\frac{Pl}{4^n} \left(1 - \frac{R_p}{R} \right) + \frac{fRe}{4^{n+2}} \left(\frac{R_p^2}{R} - R \right) \right]^{1/n} dR \qquad 4.13$$

The dimensionless form of Eqn. 4.10 becomes

$$R_p - R_n = \frac{8Pl}{fRe} \qquad 4.14$$

4.3. Numerical procedures

Equations 4.11, 4.12 and 4.13 are the basic results of the flow analysis, which illustrate nondimensional velocity and volume rate of flow of generalized Bingham fluid flow in a concentric annulus. In these equations, the boundary radii of the unsheared plug R_n and R_p are unknown. In order to obtain the details of the velocity profiles and volume rate of flow in the annulus, the values of R_n and R_p have to be determined first. To get the values of R_n and R_p, Eqns. 4.11, 4.12 and 4.13 have to be solved by using numerical integration and iteration methods.

According to the conditions

$$U(R_n) = U(R_p),$$

and

$$R_p = R_n + (8Pl)/(fRe),$$

a function of R_n, $F_1(R_n)$, can be obtained by substituting these

conditions into Eqns. 4.11 and 4.12 and subtracting Eqn. 4.12 from Eqn. 4.11:

$$F_1(R_n) = \int_{R_i}^{R_n} \left[\frac{Pl}{4^n} \left(\frac{R_n}{R} - 1 \right) + \frac{fRe}{4^{n+2}} \left(\frac{R_n^2}{R} - R \right) \right]^{1/n} dR$$

$$- \int_{R_p}^{R_o} \left[\frac{Pl}{4^n} \left(1 - \frac{R_p}{R} \right) + \frac{fRe}{4^{n+2}} \left(\frac{R_p^2}{R} - R \right) \right]^{1/n} dR \qquad 4.15$$

In Eqn. 4.15, for a specific fluid, if the pressure drop along the annulus is given, the values of the generalized Bingham number Pl and flow index n are known and the product of the Reynolds number and the friction factor f is a constant. However, the value of f is unknown. To solve Eqn. 4.15 to get the value of R_n, we have to find the value of f. Therefore, another equation is needed. From Eqn. 4.13, a function of f can be obtained by subtracting the left side of the Eqn. 4.13 from the right side of the equation:

$$F_2(f) = R_o^2 - R_i^2 + \int_{R_i}^{R_n} R^2 \left[\frac{Pl}{4^n} \left(\frac{R_n}{R} - 1 \right) + \frac{fRe}{4^{n+2}} \left(\frac{R_n^2}{R} - R \right) \right]^{1/n} dR$$

$$- \int_{R_p}^{R_o} R^2 \left[\frac{Pl}{4^n} \left(1 - \frac{R_p}{R} \right) + \frac{fRe}{4^{n+2}} \left(\frac{R_p^2}{R} - R \right) \right]^{1/n} dR \qquad 4.16$$

Now, the computational problem reduces to finding simultaneously the zeroes of two functions. Let $F_1(R_n)=0$, and $F_2(f)=0$, using an interval-chopping algorithm, the radii of the unsheared plug R_n and R_p, and the friction factor f can be determined through iteration of the three simultaneous equations 4.14, 4.15 and 4.16. The numerical procedures are: first, an initial guess of friction factor f is provided in equation 4.15 to calculate R_n by using an interval-chopping root finding method, and using equation 4.14 to calculate R_p; then the current values of R_n and R_p are substituted into equation 4.16 to calculate f by using same root finding algorithm. Comparing the updated value of f (f^n) with the value of f at the last step (f^{n-1}), if $f^n - f^{n-1} > \epsilon$, (where $\epsilon \ll 1$), then go back to the first step with the new updated value

of f and repeat the procedures; if $f^n - f^{n-1} < \epsilon$, then stop the calculation. The final values of f^n, R_a^n, R_p^n are the desired results. Substituting these results into equations 4.11 and 4.12, the velocity profiles of generalized Bingham fluids in a centric annulus are obtained

4.4 Results and discussion

According to the numerical procedures derived previously, a computer program has been developed for fully developed flow of non-Newtonian fluids in concentric annuli. Velocity profiles were obtained for different radius ratios s, power law indices n, and generalized Bingham numbers Pl. Figures 4.3 to figure 4.6 show velocity profiles of radius ratios s = 0.02, 0.2, 0.4 and 0.6 with n = 0.7 and Pl = 10. When the radius ratio s is decreased, the maximum velocity (i.e. the velocity of the unsheared plug) in the annulus is increased. The position of the unsheared plug is not symmetric between the inner and outer wall of the annulus, and it is closer to the inner wall. With the radius ratio s decreasing, the unsheared plug is shifted towards the inner wall. When $s \rightarrow 0$, the unsheared plug will be very close to R=0, and becomes an unsheared core with a radius $R_c = 8Pl/fRe$ as in pipe flow. Figure 4.7 shows the velocity profiles of different generalized Bingham number with n=0.7 and s=0.2. With Pl increasing, the maximum velocity in the annulus is decreased, and the unsheared plug region is increased. The accuracy of

the computing was indirectly checked by comparing the results of Newtonian fluids in a concentric annulus with the analytic solutions, which gave very good agreement.

When the boundary radii of the unsheared plug are determined, it will be easier to do further calculations on developing flow or unsteady flow of generalized Bingham fluids in a concentric annulus.

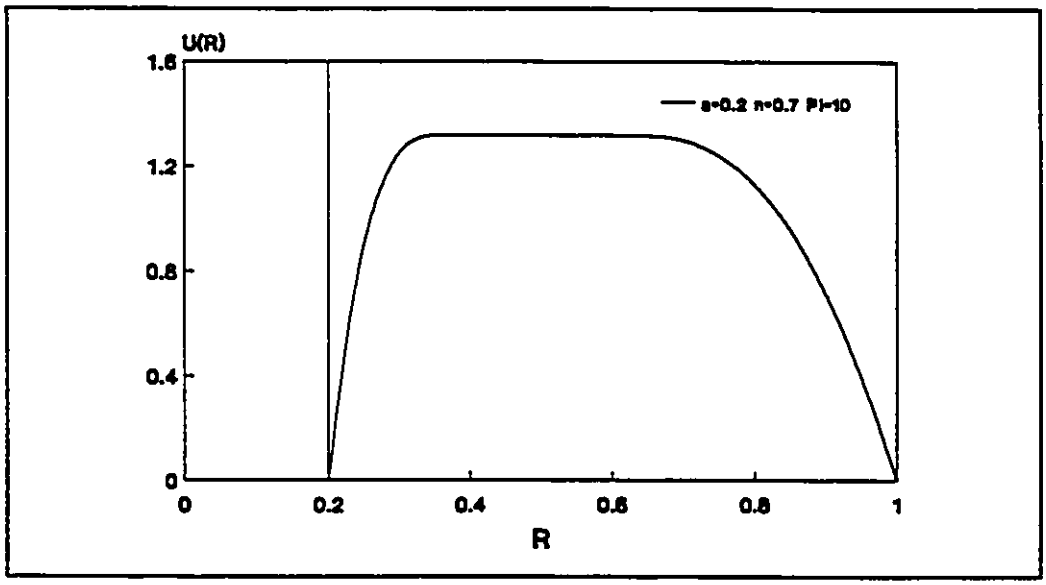

Figure 4.3 Velocity profile of fully developed flow

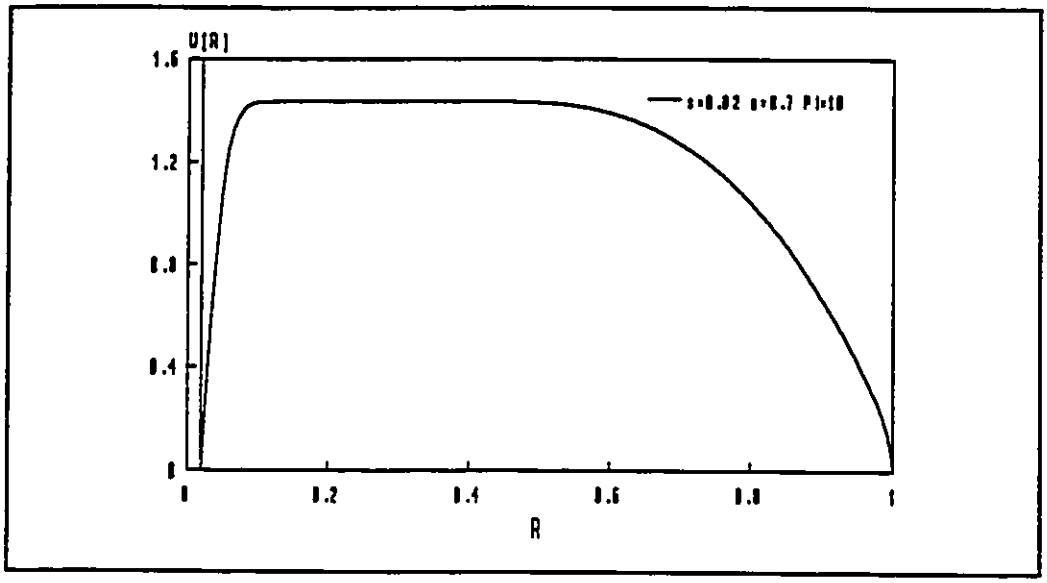

Figure 4.4 Velocity profile of fully developed flow

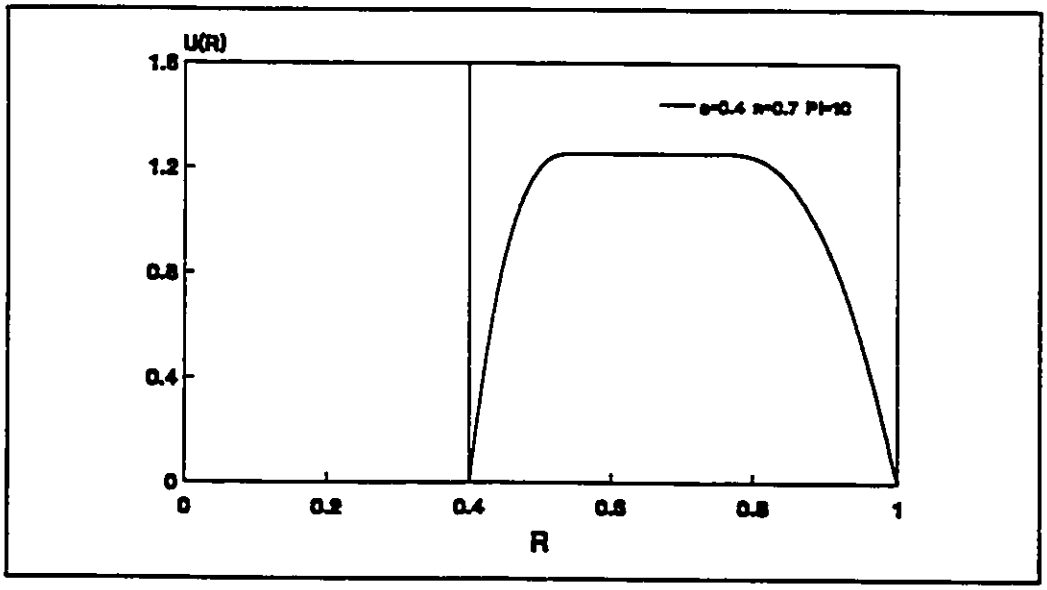

Figure 4.5 Velocity profile of fully developed flow

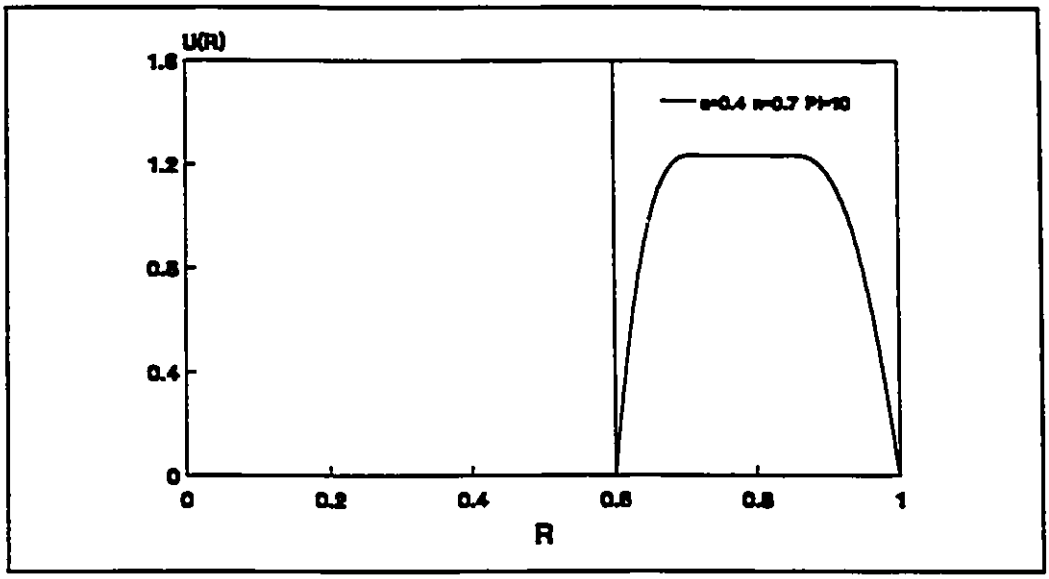

Figure 4.6 Velocity profile of fully developed flow

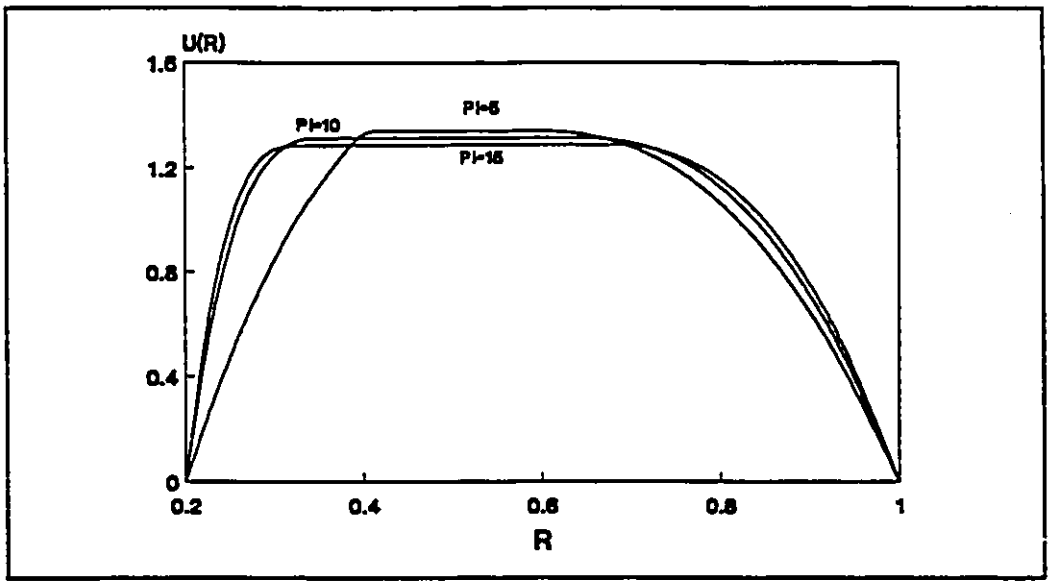

Figure 4.7 Velocity profiles of fully developed flow s=0.2 n=0.7

CHAPTER 5

DEVELOPING FLOW IN CONCENTRIC ANNULI

5.1 Dimensional analysis

For entrance flow (developing flow), in a pipe or an annulus, the flow field is taken to be composed of the two regions: the boundary layer region and the inviscid core region. As the flow proceeds, the thickness of the boundary layer region-where the viscous effects dominate-increases and correspondingly the inviscid core thickness decreases. Therefore, for high Reynolds numbers (greater than 200, Gupta and Garg 1981, Mehrotra and Patience 1990), the steady, laminar entrance flow problem is often treated as a two dimensional boundary layer problem.

For an incompressible, laminar, axisymmetric steady flow, the conservation equations of continuity and motion are:

$$\frac{\partial u}{\partial z}+\frac{\partial}{r\partial r}(rv)=0 \qquad 5.1$$

and

$$u\frac{\partial u}{\partial z}+v\frac{\partial u}{\partial r}=-\frac{1}{\varrho}\frac{\partial p}{\partial z}-\frac{1}{\varrho r}\frac{\partial}{\partial r}(r\tau_{rz})-\frac{1}{\varrho}\frac{\partial \tau_{zz}}{\partial z} \qquad 5.2$$

$$u\frac{\partial v}{\partial z}+v\frac{\partial v}{\partial r}=-\frac{1}{\varrho}\frac{\partial p}{\partial r}-\frac{1}{\varrho r}\frac{\partial}{\partial r}(r\tau_{rr})-\frac{1}{\varrho}\frac{\partial \tau_{rz}}{\partial z} \qquad 5.3$$

for generalized Bingham fluids(Bird, 1960)

$$\tau_{rz}=-\left(\frac{\tau_0}{I_2}+kI_2^{n-1}\right)\left(\frac{\partial u}{\partial z}+\frac{\partial v}{\partial r}\right) \qquad 5.4$$

$$\tau_{zz}=-\left(\frac{\tau_0}{I_2}+2kI_2^{n-1}\right)\left(\frac{\partial u}{\partial z}\right) \qquad 5.5$$

$$\tau_{rr}=-\left(\frac{\tau_0}{I_2}+2kI_2^{n-1}\right)\left(\frac{\partial v}{\partial r}\right) \qquad 5.6$$

where

$$I_2=\left|\sqrt{2\left(\frac{\partial u}{\partial z}\right)^2+\left(\frac{\partial u}{\partial r}+\frac{\partial v}{\partial z}\right)^2+2\left(\frac{\partial v}{\partial r}\right)^2+2\left(\frac{v}{r}\right)^2}\right|$$

For the sake of simplicity, we use a group of nondimensional variables as follows for the dimensional analysis of equations 5.1, 5.2 and 5.3. These nondimensional variables are defined as:

$$U=\frac{u}{u_0} \qquad V=\frac{v}{u_0}Re \qquad R=\frac{r}{d_h/4}$$

$$Z=\frac{z}{(d_h/4)\,Re} \qquad P=\frac{p-p_0}{\varrho u_0^2}$$

$$Re=\frac{\varrho d_h{}^n u_0{}^{2-n}}{k} \qquad Pl=\frac{\tau_0 d_h{}^n}{k u_0{}^n}$$

where Re and Pl are respectively defined as a generalized

Reynolds number and a generalized Bingham number, d_h is the hydraulic diameter of the annulus

$$d_h = 2(r_o - r_i)$$

In terms of these nondimensional variables, and substitute eqns 5.4, 5.5 and 5.6 into Eqns. 5.1, 5.2 and 5.3, the governing equations become:

$$\frac{\partial U}{\partial Z}+\frac{\partial}{R\partial R}(RV)=0 \qquad 5.7$$

$$U\frac{\partial U}{\partial Z}+V\frac{\partial U}{\partial R}=$$

$$-\frac{\partial P}{\partial Z}+\frac{1}{R}\frac{\partial}{\partial R}\{R[(\frac{Pl}{I_2^*}+4^n I_2^{*n-1})(\frac{\partial U}{\partial R}+\frac{1}{Re^2}\frac{\partial V}{\partial Z})]\}$$

$$+\frac{2}{Re^{n-1}}\frac{\partial}{\partial Z}[(\frac{Pl}{I_2^*}+4^n I_2^{*n-1})(\frac{\partial U}{\partial Z}) \qquad 5.8$$

$$\frac{U}{Re^2}\frac{\partial V}{\partial Z}+\frac{V}{Re^2}\frac{\partial V}{\partial R}=$$

$$-\frac{\partial P}{\partial Z}+\frac{2}{Re^2 R}\frac{\partial}{\partial R}\{R[(\frac{Pl}{I_2^*}+4^{n}I_2^{n-1})(\frac{\partial V}{\partial R})]\} \qquad 5.9$$

$$+\frac{1}{Re^2}\frac{\partial}{\partial Z}[(\frac{Pl}{I_2^*}+4^{n}I_2^{*n-1})(\frac{\partial U}{\partial R}+\frac{1}{Re^2}\frac{\partial V}{\partial Z})]$$

where

$$I_2^*=|\sqrt{2(\frac{\partial U}{Re\partial Z})^2+(\frac{\partial U}{\partial R}+\frac{\partial V}{Re^2\partial Z})^2+2(\frac{\partial V}{Re\partial R})^2+2(\frac{V}{ReR})^2}|$$

When the Reynolds number is very large, the terms in the governing equations with $1/Re$, $1/Re^2$ and $1/Re^{n+1}$ orders of magnitude are considered much smaller than other terms in the equations. The momentum equations 5.8 and 5.9 can now be simplified by neglecting the terms which have $1/Re$, $1/Re^2$ and

$1/Re^{n+1}$ orders of magnitude:

$$U\frac{\partial U}{\partial Z}+V\frac{\partial U}{\partial R}=-\frac{\partial P}{\partial Z}-\frac{1}{R}\frac{\partial}{\partial R}\{R[Pl\pm 4^{n}(\frac{\partial U}{\partial R})^{n}]\} \qquad 5.10$$

$$\frac{\partial P}{\partial R}\approx 0 \qquad 5.11$$

Equations 5.7, 5.10 and 5.11 can also be derived from the two dimensional boundary layer equations. Therefore, for a very large Reynolds number, the entrance flow in an annulus can be simplified by using two dimensional boundary layer equations instead of using formal Navier-Stokes equations. Previous studies on entrance flow have shown that a higher order of approximation, including the radial momentum flux but not second derivatives of velocity in axial direction, does not give significantly different results from the boundary layer type of model for Reynolds numbers greater than 200. (Gupta and Garg 1981, Mehrotra and Patience 1990). Since large Reynolds number situations are considered in present studies, a boundary layer model is adopted for the analysis.

5.2. Derivation of governing equations

For an incompressible, laminar, axisymmetric steady flow, the boundary layer equations are:

$$\frac{\partial u}{\partial z}+\frac{\partial}{r\partial r}(rv)=0 \qquad 5.12$$

and

$$u\frac{\partial u}{\partial z}+v\frac{\partial u}{\partial r}=-\frac{1}{\varrho}\frac{dp}{dz}-\frac{1}{\varrho r}\frac{\partial}{\partial r}(r\tau) \qquad 5.13$$

The boundary conditions for a concentric annulus flow are:

$$u(r,\ 0)= u_0, \qquad u(r_i,\ x)=u(r_o,\ x)= 0$$

$$v(r,\ 0)= v(r_i,\ x)= v(r_o,\ x)= 0, \qquad p(0)=p_0$$

where u and v are the axial and radial components of velocity, ϱ is the density of the fluid, p is the pressure, u_0 and p_0 are respectively the velocity and pressure at the inlet section, r_i and r_o are respectively the inner and outer radii of the annulus.

Equation 1.1 for generalized Bingham fluids may be expressed as:

$$\tau=\tau_0\pm k\left|\frac{\partial u}{\partial r}\right|^{n-1}\frac{\partial u}{\partial r} \qquad 5.14$$

for $r_i \le r \le r_n$, and $r_p \le r \le r_o$

$$\frac{\partial u}{\partial r}=0 \qquad 5.15$$

for $r_n \le r \le r_p$

The values of the boundary radii r_n and r_p are determined from the results of the fully developed flow.

Substituting of Eqn. 5.14 into Eqn. 5.13, and the equation of motion becomes:

$$u\frac{\partial u}{\partial z}+v\frac{\partial u}{\partial r}=-\frac{1}{\varrho}\frac{dp}{dz}-\frac{\tau_0}{\varrho r}\pm\frac{k}{\varrho r}\left|\frac{\partial u}{\partial r}\right|^{(n-1)}\frac{\partial u}{\partial r}$$

$$\pm\left[1\pm(n-1)\right]\frac{k}{\varrho}\left|\frac{\partial u}{\partial r}\right|^{(n-1)}\frac{\partial^2 u}{\partial r^2} \qquad 5.16$$

where " - " is for $r_i < r < r_s$, and " + " is for $r_p < r < r_o$. Since the pressure gradient in the entrance region is not a constant, the flow rate continuity equation is needed:

$$Q=2\pi\int_{r_i}^{r_o}u(r)\,r\,dr=const. \qquad 5.17$$

Equations 5.12, 5.16 and 5.17 are made dimensionless by defining the same nondimensional variables used in section 5.1. In terms of these nondimensional variables, Eqns. 5.12, 5.16 and 5.17 become:

$$\frac{\partial U}{\partial Z}+\frac{V}{R}+\frac{\partial V}{\partial R}=0 \qquad 5.18$$

$$U\frac{\partial U}{\partial Z}+V\frac{\partial U}{\partial R}=-\frac{dP}{dZ}-\frac{Pl}{R}\pm\frac{4^n}{R}\left|\frac{\partial U}{\partial R}\right|^{n-1}\frac{\partial U}{\partial R}$$

$$\pm 4^n[1\pm(n-1)]\left|\frac{\partial U}{\partial R}\right|^{n-1}\frac{\partial^2 U}{\partial R^2} \qquad 5.19$$

where " - " is for $R_i < R < R_s$, and " + " is for $R_p < R < R_o$. and

$$2\int_{R_i}^{R_o} U(R)\,R\,dR=1 \qquad 5.20$$

The boundary conditions are

$$U(R_i,\ X)= U(R_o,\ X)= V(R_i,\ X)= V(\ R_o,\ X)= 0$$

$$U(R,\ 0)= 1, \qquad V(R,\ 0)= 0 \qquad P(0)= 0$$

$$\partial U/\partial R= 0 \qquad \text{for} \quad R_s \le R \le R_p$$

5.3. Finite difference approach

For entrance flow in an annulus, the u-velocity component in the axial direction is much larger than the v-velocity

component in the radial direction. The u-velocity component has significant influence on downstream conditions. The conditions at a point in the region are then affected largely by the upstream conditions. A control-volume based upon a finite difference marching integration technique was used in this study to solve the two dimensional boundary layer equations (Eqns. 5.18 and 5.19). This numerical technique was first developed by Patankar and Spalding (1970). Many studies adopted this method to solve entrance flow problems, such as Shah and Soto (1975) for the entrance flow of Bingham fluids in a pipe, and Gupta and Garg (1981) for the developing flow of Newtonian fluids in a concentric annulus. The discretization methods and the solutions of the algebraic equations used in the computer program are also made with reference to the book of "Numerical Heat Transfer and fluid Flow" from Patankar (1983). Because flow in a concentric annulus is axisymmetric to the center line, only half section area along the axis needs to be calculated. Figure 5.1 shows the network of the grid points.

An upwind-difference scheme is applied to each control volume which surrounds a grid point. The values of velocities at each interface of the control volume in axial direction are determined by the values of upstream grid points. Therefore, the momentum equation for each control volume is discretized by using the values of four grid points (see Fig. 5.1). The values of v velocity component in the equation of motion are

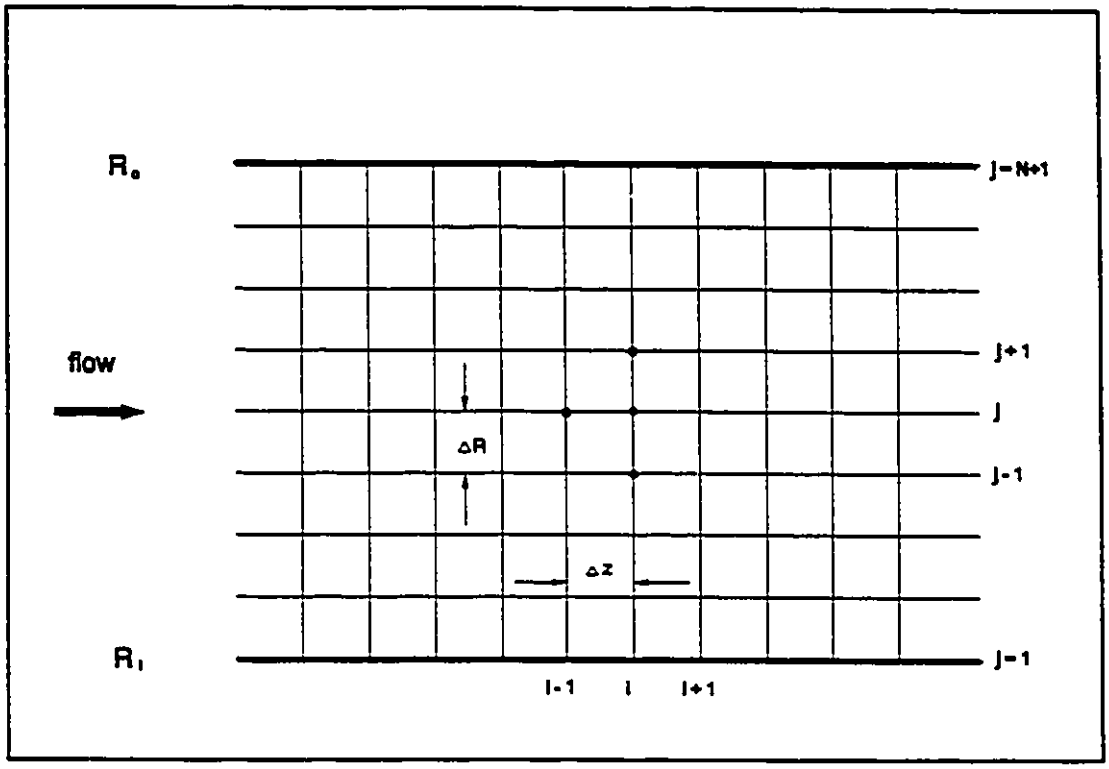

Figure 5.1 Finite difference network

also determined by the values at the upstream station.

The finite difference representations used for various terms in Eqns. 5.18, 5.19 at a grid point (i, j) are:

$$\frac{\partial U}{\partial Z} = \frac{U_{i,j} - U_{i-1,j}}{\Delta Z}$$

$$\frac{V}{R}=\frac{V_{i,j}}{R_j}$$

$$\frac{\partial V}{\partial R}=\frac{V_{i,j+1}-V_{i,j-1}}{2\Delta R}$$

$$U\frac{\partial U}{\partial Z}=U_{i-1,j}\left[\frac{U_{i,j}-U_{i-1,j}}{\Delta Z}\right]$$

$$V\frac{\partial U}{\partial R}=V_{i-1,j}\left[\frac{U_{i,j+1}-U_{i,j-1}}{2\Delta R}\right]$$

$$\frac{\partial P}{\partial Z}=\frac{P_i-P_{i-1}}{\Delta Z}$$

$$\frac{Pl}{R}=\frac{Pl}{R_j}$$

$$\frac{1}{R}\left|\frac{\partial U}{\partial R}\right|^{n-1}\frac{\partial U}{\partial R}=\frac{1}{R_j}\left|\frac{U_{i-1,j+1}-U_{i-1,j-1}}{2\Delta R}\right|^{n-1}\frac{U_{i,j+1}-U_{i,j-1}}{2\Delta R}$$

$$\left|\frac{\partial U}{\partial R}\right|^{n-1}\frac{\partial^2 U}{\partial R^2}=\left|\frac{U_{i-1,j+1}-U_{i-1,j-1}}{2\Delta R}\right|^{n-1}\frac{U_{i,j+1}-2U_{i,j}+U_{i,j-1}}{\Delta R^2}$$

The variables with (i-1) subscript are assumed known as the values at upstream station, while those with (i) subscript are unknown. Using these representations, Eqns. 5.18 and 5.19 become:

$$V_{i,j-1}+\frac{2\Delta R}{R_j}V_{i,j}-V_{i,j+1}=\frac{2\Delta R}{\Delta Z}\left(U_{i-1,j}-U_{i,j}\right) \qquad 5.21$$

and

$$\left(-\frac{V_{i-1,j}}{2\Delta R}+\frac{K_1}{2R_j\Delta R}-\frac{K_2}{\Delta R^2}\right)U_{i,j+1}+\left(\frac{U_{i-1,j}}{\Delta Z}+\frac{2K_2}{\Delta R^2}\right)U_{i,j}$$

$$+\left(\frac{V_{i-1,j}}{2\Delta R}-\frac{K_1}{2R_j\Delta R}-\frac{K_2}{\Delta R^2}\right)U_{i,j-1}+\frac{P_i}{\Delta Z}$$

5.22

$$=\frac{U^2_{i-1,j}}{\Delta Z}+\frac{P_{i-1}}{\Delta Z}-\frac{Pl}{R_j}$$

where

$$K_1=\pm 4^n\left|\frac{U_{i-1,j+1}-U_{i-1,j-1}}{2\Delta R}\right|^{n-1}$$

$$K_2=\pm 4^n[1\pm(n-1)]\left|\frac{U_{i-1,j+1}-U_{i-1,j-1}}{2\Delta R}\right|^{n-1}$$

The finite difference form of Eqn. 5.20 may be written as:

$$\sum_{j=1}^{N}R_jU_{i,j}=\sum_{j=1}^{N}R_jU_{i-1,j} \qquad 5.23$$

Combining Eqns. 5.22 and 5.23, a set of simultaneous linear equations of U_{ij} and P_i are obtained for a group of grid points

along one cross stream line in the entrance region. After solving these equations, eqn. 5.21 may be solved for V_{ij} by using updated results of the u velocity component. Starting from the inlet of the entrance region, the two dimensional boundary layer equations are computed by marching in the axial direction. The velocity and pressure profiles in the whole entrance region of an annulus can be obtained by a step-by-step continuation of the process downstream.

5.4. Results and discussion

Numerical solutions were obtained for different fluids in annuli with different radius ratios. Figures 5.2 and 5.3 show the developing velocity distributions of the generalized Bingham fluid with generalized Bingham number Pl=10 and power law index n=0.7 for radius ratio, s=0.02 and 0.6. It is observed from these figures that the velocity profiles are changed from symmetry about the mid point between the inner and outer walls at the inlet to asymmetry in the entry region. As the radius ratio s decreases, the asymmetry intensifies, and the unsheared plug shifts closer to the inner wall. The velocity at any point between the inner wall and the unsheared plug is greater than that at a point equidistant from the outer wall. Figure 5.3 shows the developing velocity profiles for Pl=15 with n=0.7 and s=0.2 at several axial locations in the entry region. The region of the unsheared plug is proportional to Pl. Figures 5.5 and 5.8 show the development

of maximum velocity (the velocity of the plug) and the pressure profiles in the entrance region for Pl=10, n=0.7 with the radius ratios s=0.02, 0.2, 0.4, 0.6. It can be seen from these figures as s is increased, the values of the maximum velocity and the entry length are decreased, and the values of pressure drop are increased. Figures 5.6, 5.7, 5.9 and 5.10 compare results of the developing velocity of the unsheared plug and pressure drop profiles for n=0.7, 1, and 1.2 with Pl=10 and s=0.2; and for Pl=5, 10, 15 with n=0.7 and s=0.2. It is obvious that when n is increased, the values of the velocity of the unsheared plug, entrance length and pressure drop are also increased. When Pl is increased, the values of the velocity of the unsheared plug and the entrance length are decreased, and the pressure drop in the entry region is increased. The results presented were obtained by using successively small mesh sizes until a sufficient degree of convergence was obtained. The basic mesh sizes used for most of the flow field were $\Delta R=0.025$, and $\Delta Z=0.001$. The comparison of velocities at $X \rightarrow \infty$ with the results of fully developed flow shows that the differences are less than 2%.

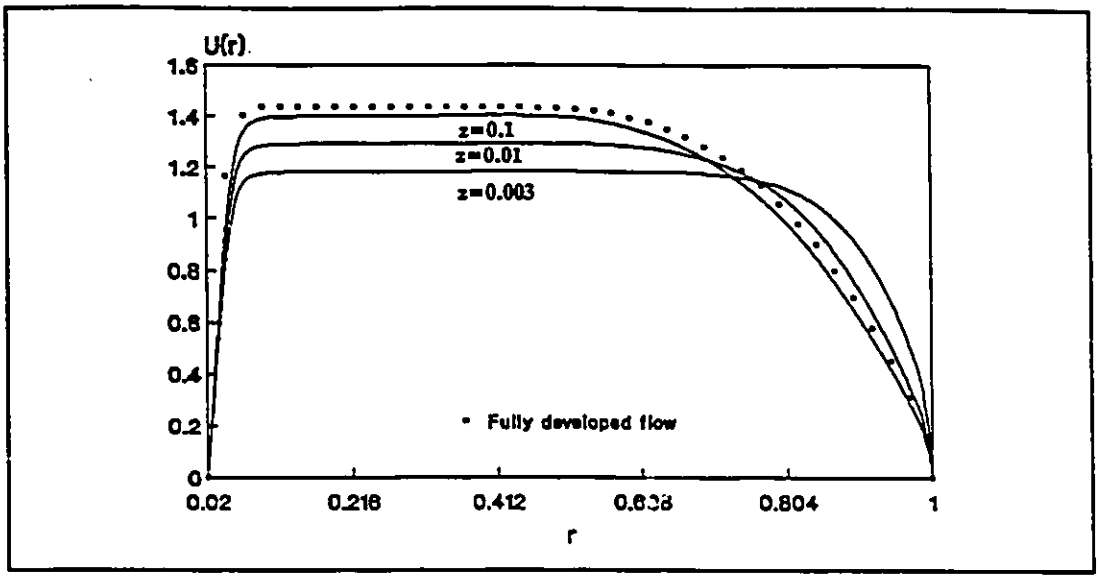

Figure 5.2 Entrance flow in a concentric annulus, velocity profiles Pl=10 n=0.7 s=0.02

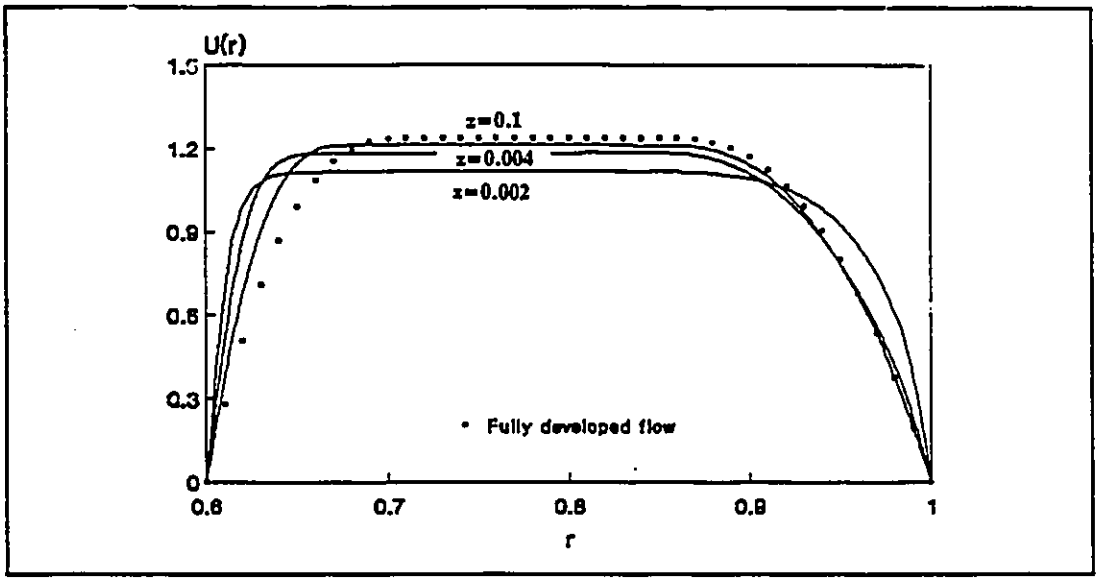

Figure 5.3 Entrance flow in a concentric annulus, velocity profiles Pl= 10 n=0.7 s=0.6

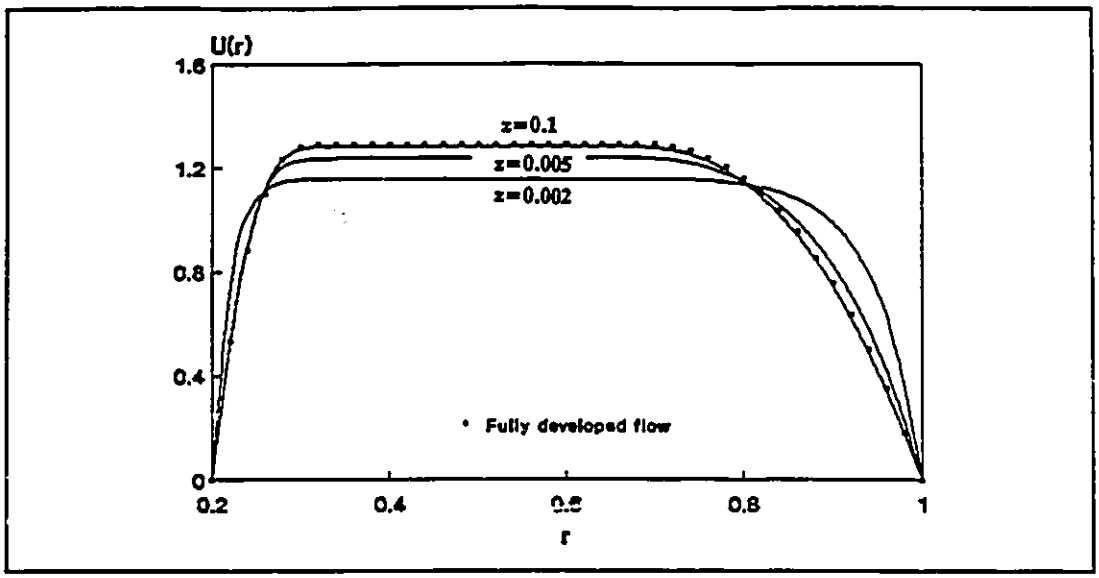

Figure 5.4 Entrance flow in a concentric annulus, velocity profiles Pl =15 n=0.7 s=0.2

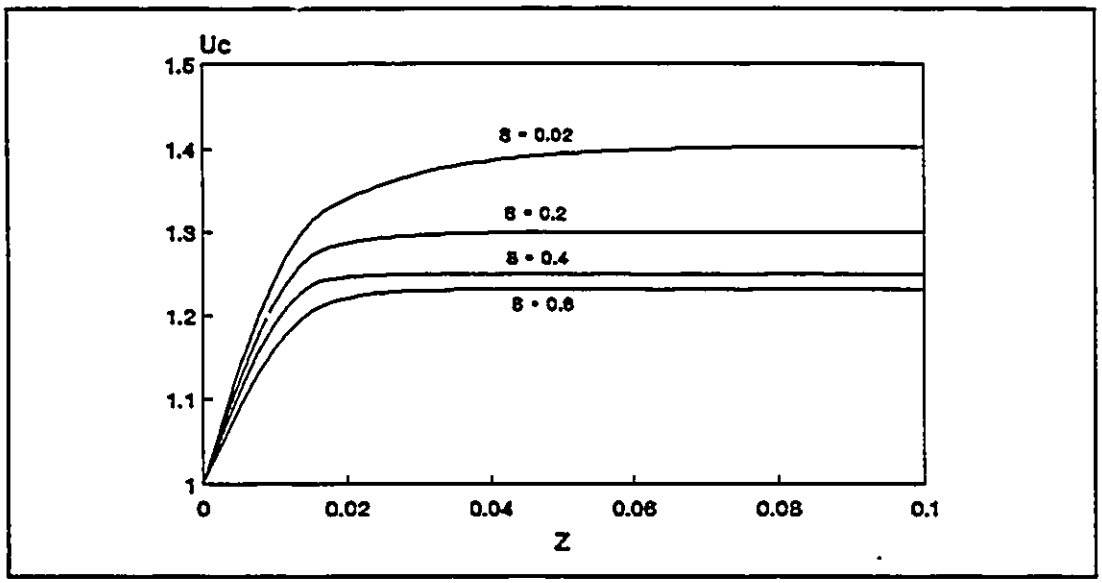

Figure 5.5 Entrance flow in a concentric annulus, unsheared plug velocity profiles Pl=10 n=0.7 with different radius ratio s= r_i/r_o

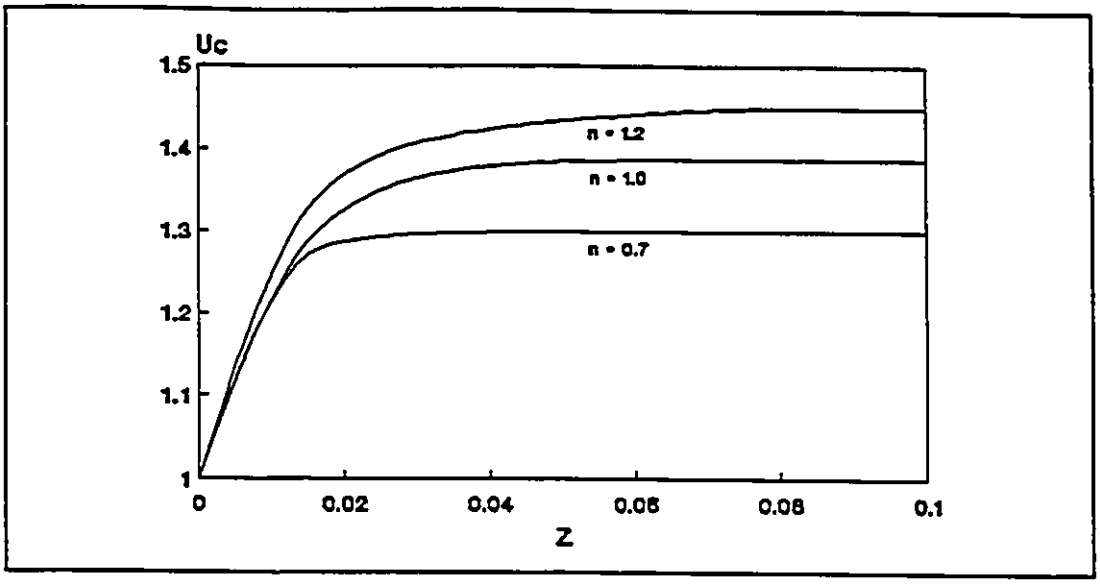

Figure 5.6 Entrance flow in a concentric annulus, unsheared plug velocity profiles Pl=10 s=0.2 with different power law index n

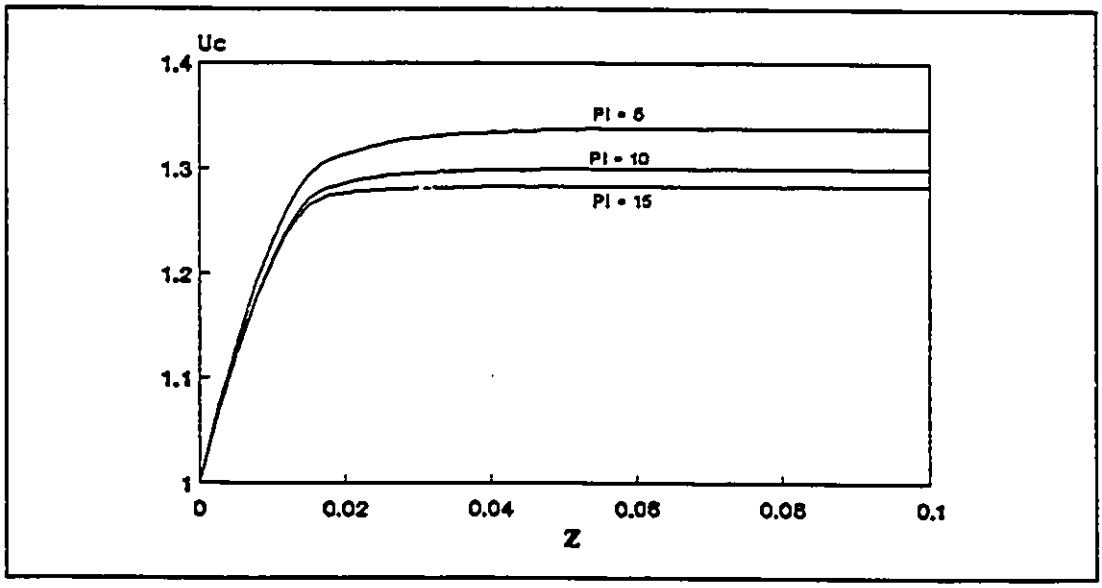

Figure 5.7 Entrance flow in a concentric annulus, unsheared plug velocity profiles n=0.7 s=0.2 with different generalized Bingham number Pl

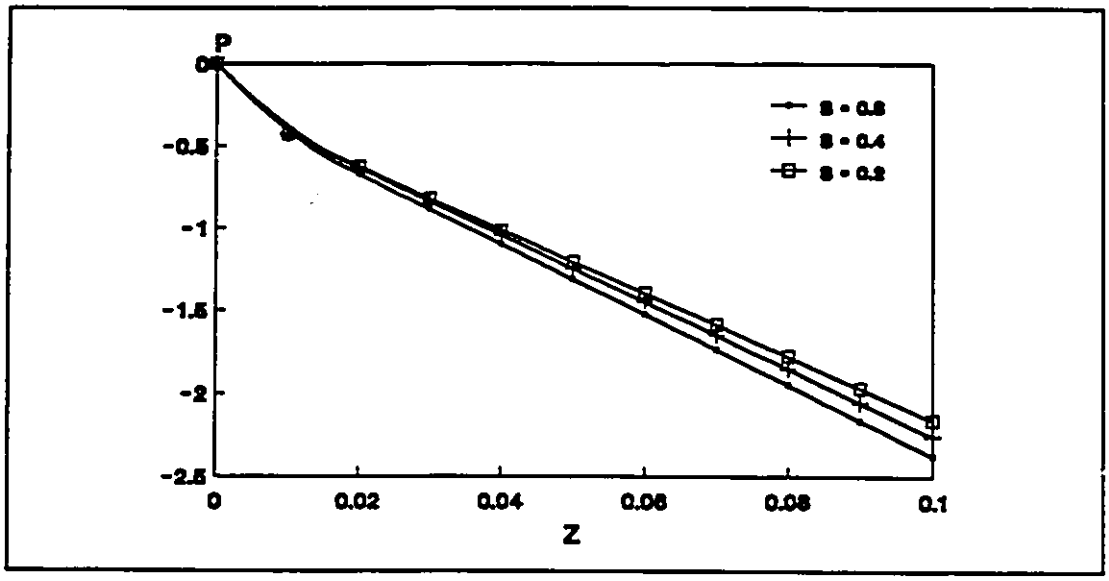

Figure 5.8 Entrance flow in a concentric annulus, pressure drop profiles Pl=10 n=0.7 with different radius ratio $s=r_i/r_o$

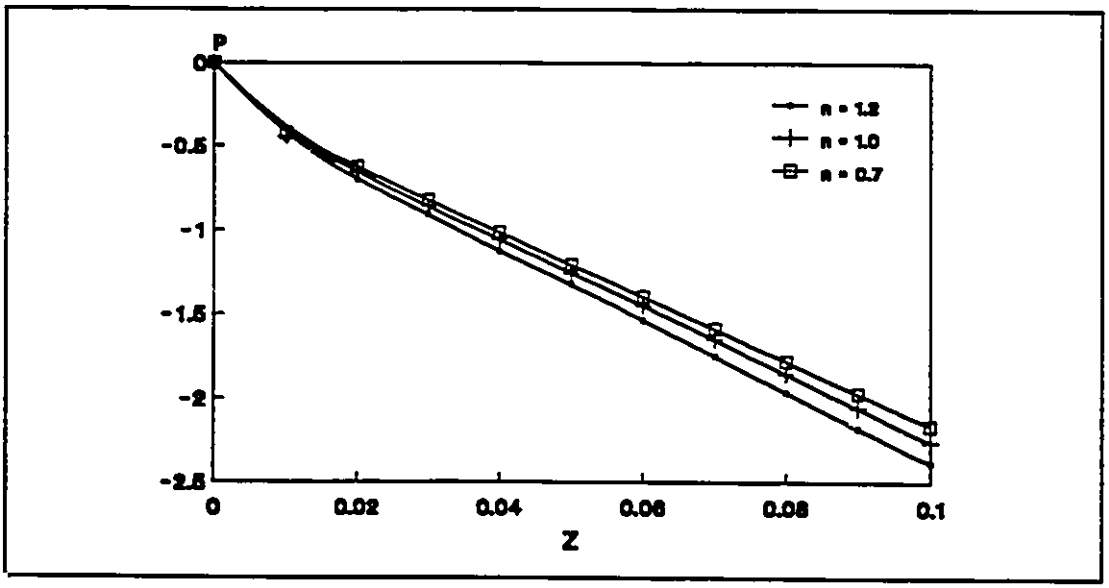

Figure 5.9 Entrance flow in a concentric annulus, pressure drop profiles Pl=10 s=0.2 with different power law index n

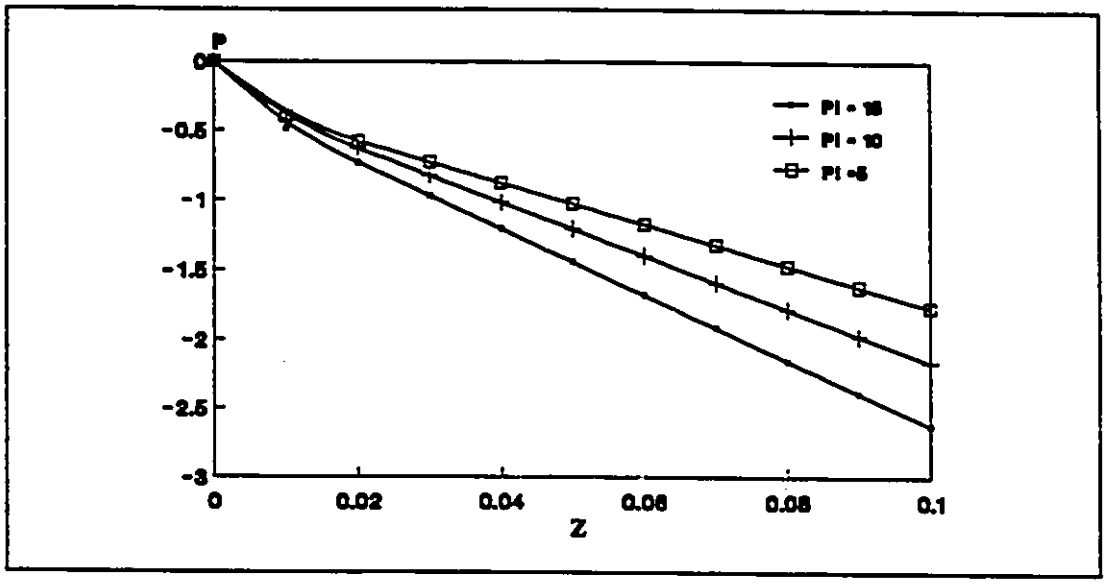

Figure 5.10 Entrance flow in a concentric annulus, pressure drop profiles n=0.7 s=0.2 with different generalized Bingham number Pl

CHAPTER 6

UNSTEADY FLOW IN CONCENTRIC ANNULI

6.1 Derivation of governing equations

For an incompressible, laminar, unsteady, axisymmetric flow, ignoring the effects of entry and exit, the momentum equation of generalized Bingham fluids in a concentric annulus may be written as:

$$\rho \frac{\partial v}{\partial t} = -\frac{\partial p}{\partial z} - \frac{\partial}{r \partial r}(r\tau) \qquad 6.1$$

with

$$\tau = \tau_0 + k \left| \frac{\partial v}{\partial r} \right|^{n-1} \frac{\partial v}{\partial r} \qquad 6.2$$

for $r_i \leq r \leq r_o$ and $\tau_y \leq r \leq r_o$

$$\frac{\partial u}{\partial r}=0 \qquad 6.3$$

for $r_a \leq r \leq r_p$

The pressure gradient is given by:

$$-\frac{\partial p}{\partial z}=\left(\frac{dp}{dz}\right)_s+\left(\frac{dp}{dz}\right)_o \sin(\omega t) \qquad 6.4$$

where $(dp/dx)_s$ is the steady component of the pressure gradient, and $(dp/dx)_o$ is the oscillatory component. Equation. 6.4 can also be written as:

$$-\frac{\partial p}{\partial z}=\frac{dp}{dz}_s (1+\epsilon\sin(\omega t)) \qquad 6.5$$

where $\epsilon = (dp/dx)_o/(dp/dx)_s$

The boundary conditions for unsteady flow are:

$$u(r,0)=0, \qquad u(r_i,t)=u(r_o,t)=0$$

Substituting Eqn. 6.2 into Eqn. 6.4, the momentum equation for unsteady flow of generalized Bingham fluids becomes:

$$\varrho\frac{\partial u}{\partial t}=-\frac{\partial p}{\partial z}-\frac{\tau_0}{r}\pm\frac{k}{r}\left|\frac{\partial u}{\partial r}\right|^{(n-1)}\frac{\partial u}{\partial r}$$

$$\pm[1\pm(n-1)]\,k\left|\frac{\partial u}{\partial r}\right|^{(n-1)}\frac{\partial^2 u}{\partial r^2} \qquad 6.6$$

where " - " is for $r_i < r < r_a$, and " + " is for $r_p < r < r_o$.

6.2. Dimensional analysis

Equation. 6.6 can be made dimensionless by defining the following nondimensional variables:

$$U=\frac{u}{\bar{u}} \qquad R=\frac{r}{d_h/4}$$

$$Re=\frac{\varrho d_h^{\,n}\bar{u}^{2-n}}{k} \qquad Pl=\frac{\tau_0 d_h^{\,n}}{k\bar{u}^{\,n}} \qquad f=-\frac{dp}{dz}_s \frac{d_h}{\varrho\bar{u}^2/2}$$

for start-up flow

$$T=4^{n+1}\frac{t\bar{u}}{d_h Re}$$

for pulsating flow

$$T=\frac{\omega t}{2\pi}$$

where Re and Pl are respectively defined as a generalized Reynolds number and a generalized Bingham number, f is the friction factor, $\bar{u}$ is the average velocity of the annulus, d_h is the hydraulic diameter of the annulus. $d_h = 2(r_o - r_i)$

In terms of these nondimensional variables, Eqn. 6.6 becomes:

for start-up flow

$$\frac{1}{4^{n+1}}\frac{\partial U}{\partial T}=\frac{1}{2^{2n-3}}fRe-\frac{1}{4^n}\frac{Pl}{R}\pm\frac{1}{R}\left|\frac{\partial U}{\partial R}\right|^{n-1}\frac{\partial U}{\partial R}$$

$$\pm[1\pm(n-1)]\left|\frac{\partial U}{\partial R}\right|^{n-1}\frac{\partial^2 U}{\partial R^2} \qquad 6.7$$

for pulsating flow

$$\xi\frac{1}{4^{n+1}}\frac{\partial U}{\partial T}=\frac{1}{2^{2n+3}}fRe(1+\varepsilon\sin(2\pi T))-\frac{1}{4^n}\frac{Pl}{R}\pm\frac{1}{R}\left|\frac{\partial U}{\partial R}\right|^{n-1}\frac{\partial U}{\partial R}$$

$$\pm[1\pm(n-1)]\left|\frac{\partial U}{\partial R}\right|^{n-1}\frac{\partial^2 U}{\partial R^2} \qquad 6.8$$

where

$$\xi=\frac{\omega}{2\pi}\frac{d_h}{\bar{u}}Re$$

and " - " is for $R_i < R < R_n$, and " + " is for $R_p < R < R_o$.

6.3. Numerical procedures

A control-volume based upon a finite difference marching integration technique is used to solve the equation of motion (Eqns. 6.7 and 6.8). Fig. 6.1 shows the finite difference network grid for the unsteady flow problem. The grid in the i direction in the network represents the different time

intervals.

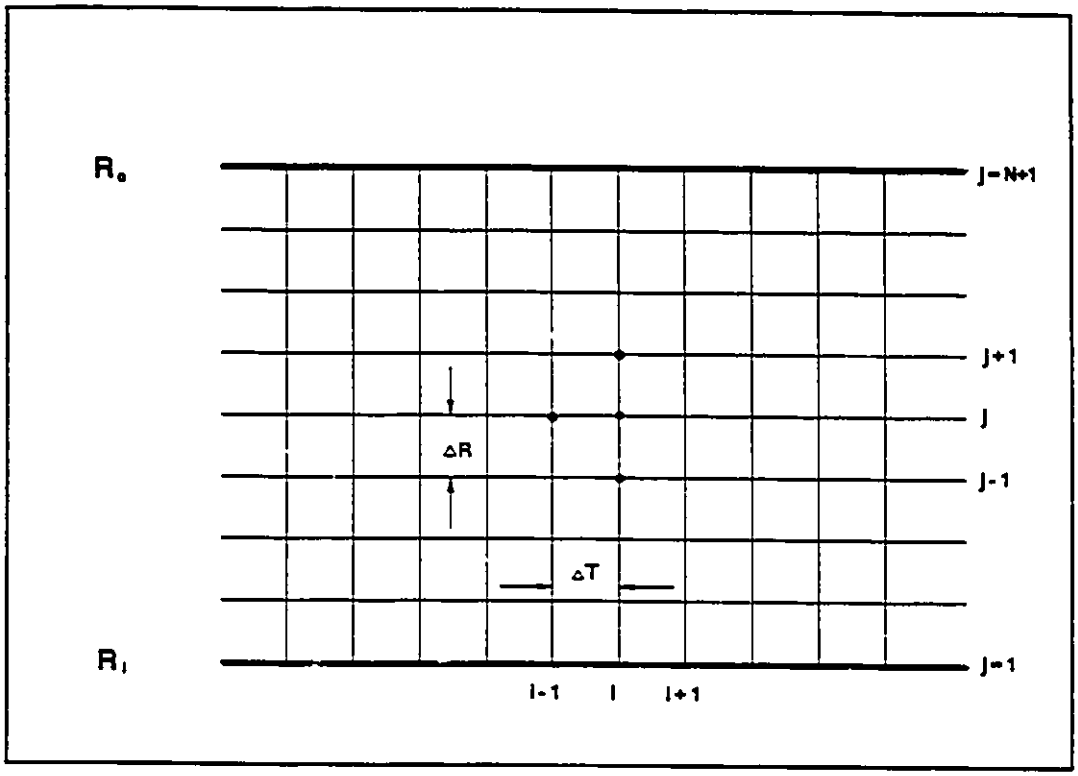

Figure 6.1 Finite difference network

An upwind-difference scheme is applied to each control volume which surrounds a grid point. The value of velocity at each interface of the control volume in i direction is determined by the value of velocity at the grid corresponding to the last half time interval. The finite difference calculating procedure is similar to that used for the developing flow. For the network of grid points shown in figure 6.1, the finite difference representations used for various terms in Eqns. 6.7, 6.8 at a grid point (i, j) are:

$$\frac{\partial U}{\partial T}=\frac{U_{i,j}-U_{i-1,j}}{\Delta T}$$

$$\frac{Pl}{R}=\frac{Pl}{R_j}$$

$$\frac{1}{R}\left|\frac{\partial U}{\partial R}\right|^{n-1}\frac{\partial U}{\partial R}=\frac{1}{R_j}\left|\frac{U_{i-1,j+1}-U_{i-1,j-1}}{2\Delta R}\right|^{n-1}\frac{U_{i,j+1}-U_{i,j-1}}{2\Delta R}$$

$$\left|\frac{\partial U}{\partial R}\right|^{n-1}\frac{\partial^2 U}{\partial R^2}=\left|\frac{U_{i-1,j+1}-U_{i-1,j-1}}{2\Delta R}\right|^{n-1}\frac{U_{i,j+1}-2U_{i,j}+U_{i,j-1}}{\Delta R^2}$$

The variables with (i-1) subscript are assumed known while those with (i) subscript are unknown. Using these representations, Eqns. 6.7 and 6.8 become:

for start-up flow

$$\left(\frac{K_1}{2R_j\Delta R}-\frac{K_2}{\Delta R^2}\right)U_{i,j+1}+\left(\frac{1}{4^{n+1}\Delta T}+\frac{2K_2}{\Delta R^2}\right)U_{i,j}+\left(-\frac{k_1}{R_j 2\Delta R}-\frac{k_2}{\Delta R^2}\right)U_{i,j}$$

$$=\frac{U_{i-1,j}}{4^{n+1}\Delta T}+\frac{1}{2^{2n+3}}fRe-\frac{Pl}{4^n R_j} \qquad 6.9$$

where

$$K_1=\pm\left|\frac{U_{i-1,j+1}-U_{i-1,j-1}}{2\Delta R}\right|^{n-1}$$

$$K_2=\pm\left[1\pm(n-1)\right]\left|\frac{U_{i-1,j+1}-U_{i-1,j-1}}{2\Delta R}\right|^{n-1}$$

for pulsating flow

$$\left(\frac{K_1}{2R_j\Delta R}-\frac{K_2}{\Delta R^2}\right)U_{i,j+1}+\left(\frac{\xi}{4^{n+1}\Delta T}+\frac{2K_2}{\Delta R^2}\right)U_{i,j}+\left(-\frac{k_1}{R_j 2\Delta R}-\frac{k_2}{\Delta R^2}\right)U_{i,j}$$

$$=\xi\frac{U_{i-1,j}}{4^{n+1}\Delta T}+\frac{1}{2^{2n+3}}fRe(1+\varepsilon\sin(2\pi i\Delta T))-\frac{Pl}{4^n R_j} \qquad 6.10$$

From the Eqn. (39) or (40), a set of simultaneous linear equations of velocity U_{ij} can be obtained on the grids across the annulus. Solving these equations step-by-step continually, the velocity profile development with time will be obtained.

6.4. Results and discussion

Velocity profiles of start-up flow and pulsating flow of generalized Bingham fluids in a concentric annulus were obtained by using finite difference methods. Figures 6.2 to 6.6 show velocity profiles of generalized Bingham fluids with generalized Bingham number Pl=5, 10, 15, and radius ratio s=0.2, 0.4 and 0.6 at different time intervals and finally steady state. Figure 6.7 shows the velocity distributions of the unsheared plug in the annulus with different generalized Bingham number Pl=5, 10 and 15 during the start-up flow. A comparison among the velocity distribution curves illustrates the effect of Pl on the time of flow from start to the steady state. The larger the generalized Bingham number, the shorter is the time interval to achieve steady state. The reason for this is that a higher value of yield stress makes the fluids behave like solid material. Once it starts moving, it quickly becoming fully developed flow. Figure 6.8 illustrates the effect of radius ratio s on the start-up flow. Velocity distributions of s=0.2, 0.4 and 0.6 show that the time of the flow from start to steady state is shorter when the radius ratio s is increased. A significant effect of flow index n on

time of the start-up flow from start to the steady state could be observed in fig 6.9. The velocity distributions show that when n is increased from less than unity (i.e. the fluid is much more shear thinning) to larger than unity (i.e. the fluid is much more shear thickening), the time of flow from start to steady flow reduces greatly. The accuracy of the numerical solutions was checked by comparing the velocity profiles at $T \rightarrow \infty$ with the results of fully developed flow with the same conditions. Figure 6.10 shows the velocity distributions of start-up flow with different mesh size in the radial direction. Grid refinement brings the numerical solutions closer to the value of velocity of unsheared plug of fully developed flow in a concentric annulus. Figures 6.11 and 6.12 show the velocity distributions of pulsating flow of unsheared plug in a concentric annulus with generalized Bingham number Pl = 5, 10, 15 and flow index n = 0.7, 1.0 and 1.2. The results indicate that both Pl and n have effects on the velocity profile and the peak value of velocity. However, their effects on the average velocity (or flow rate) are limited. Figure 6.13 shows velocity distributions of pulsating flow with different pressure amplitude parameter ϵ. It can be observed that when ϵ increases, the peak value of velocity of unsheared plug increases, and the average velocity also increases. That means the addition of pulsating fluctuation to a steady pressure gradient will result in enhancement of the flow rate. These results are similar to the results of

previous investigations by Kajiuchi and Saito (1984) on the laminar pulsating flow of an ideal Bingham fluid in a circular pipe. However, if the pressure amplitude is larger than a certain value, flow reversal occurs, Figure 6.14 shows the velocity distributions of pulsating flow with different frequency parameter ξ. When ξ increases, the velocity peak value decreases. The effect of ξ on average velocity is limited.

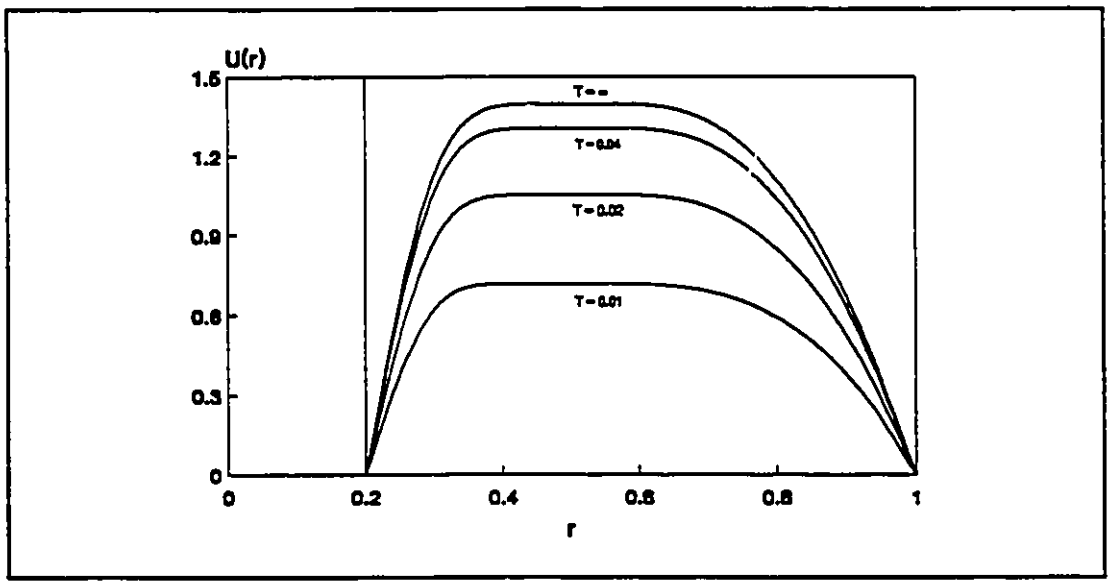

Figure 6.2 Start-up flow in a concentric annulus, velocity profiles Pl=5 n=0.7 s=0.2

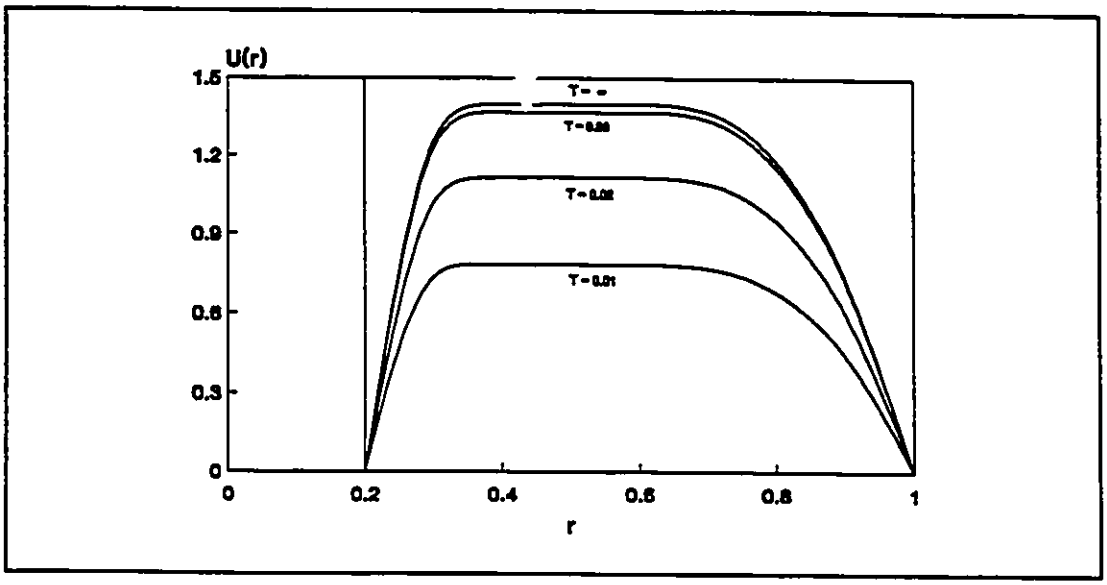

Figure 6.3 Start-up flow in a concentric annulus, velocity profiles Pl=10 n=0.7 s=0.2

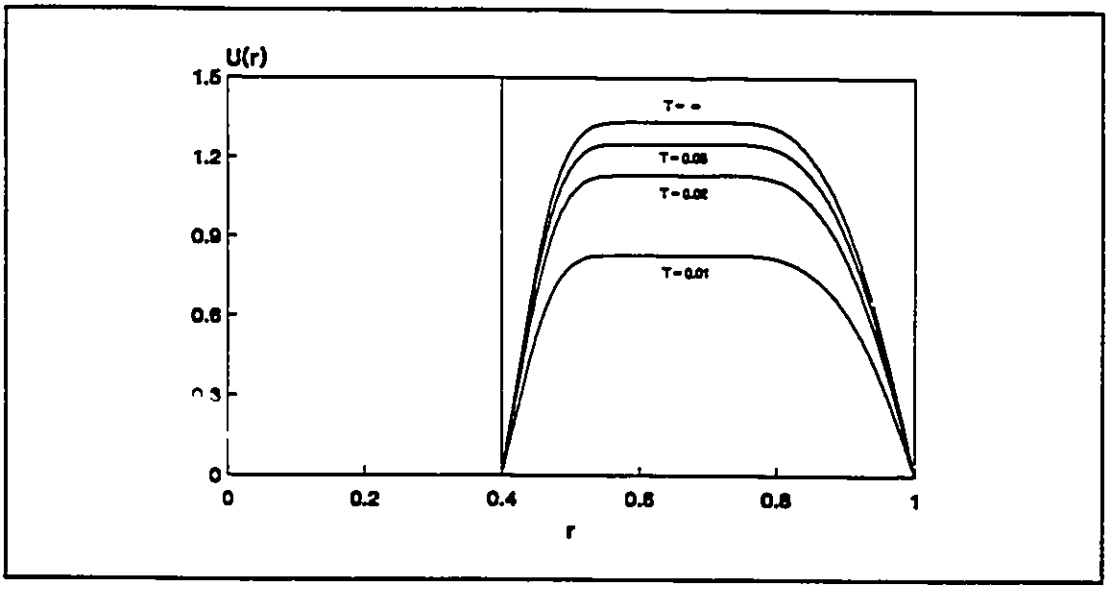

Figure 6.4 Start-up flow in a concentric annulus, velocity profiles Pl=10 n=0.7 s=0.4

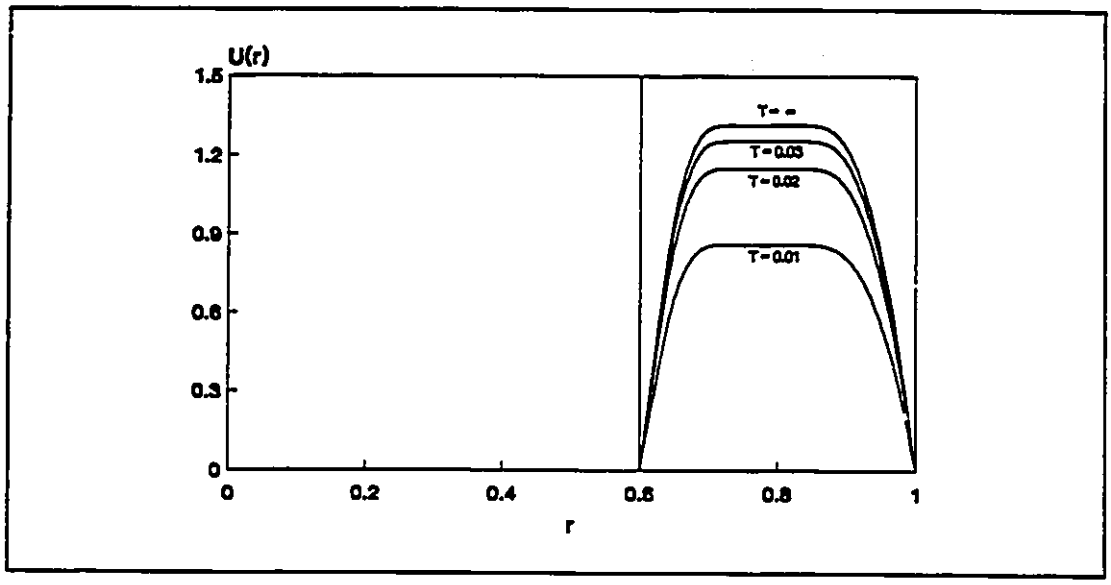

Figure 6.5 Start-up flow in a concentric annulus, velocity profiles Pl=10 n=0.7 s=0.6

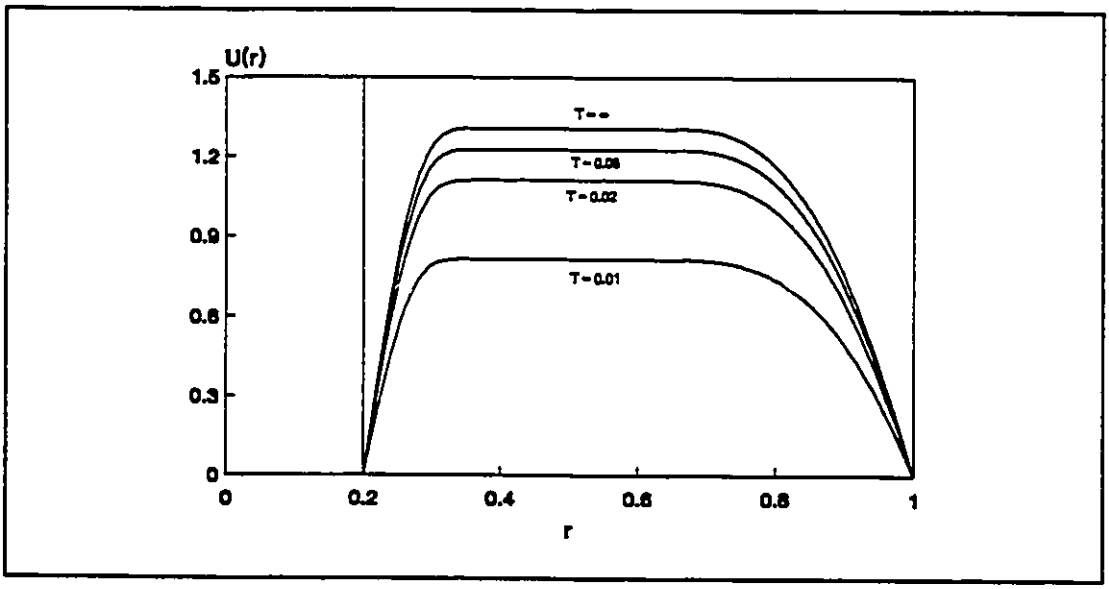

Figure 6.6 Start-up flow in a concentric annulus, velocity profiles Pl=15 n=0.7 s=0.2

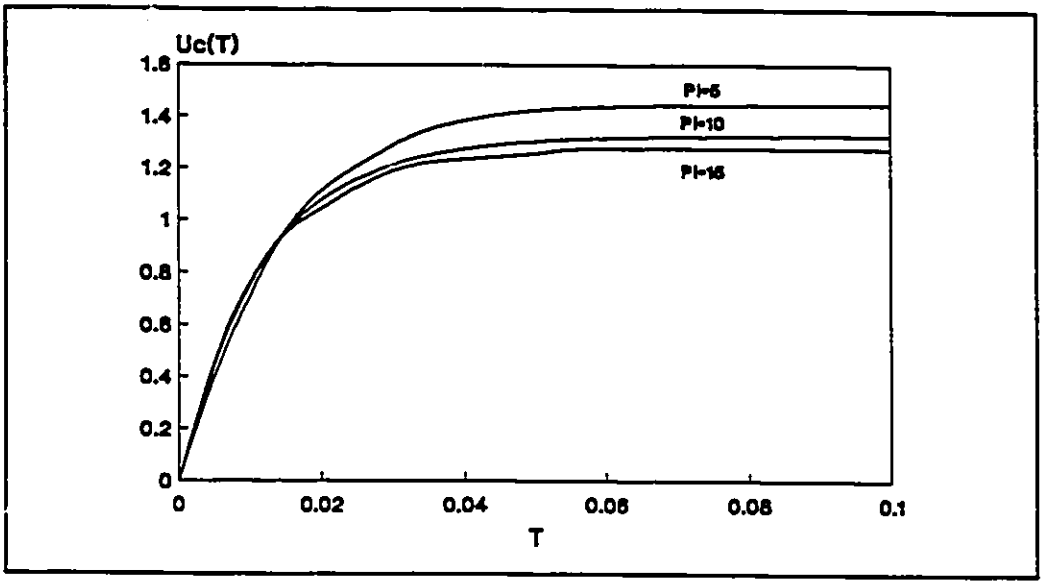

Figure 6.7 Start-up flow in a concentric annulus, unsheared plug velocity profiles n=0.7 s=0.2 with different generalized Bingham number Pl

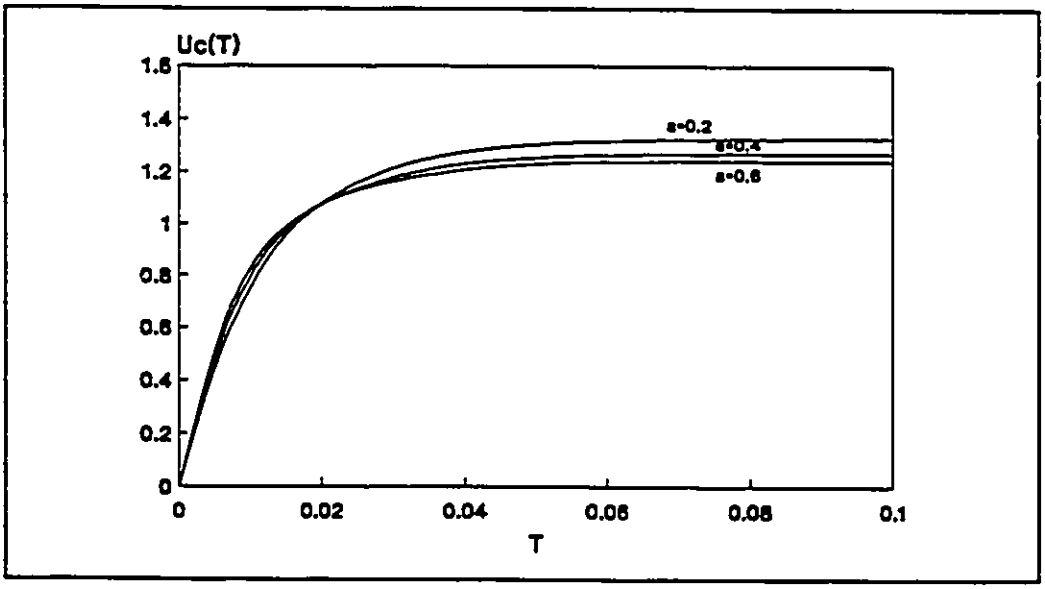

Figure 6.8 Start-up flow in a concentric annulus, unsheared plug velocity profiles Pl=10 n=0.7 with different radius ratio $s=r_i/r_o$

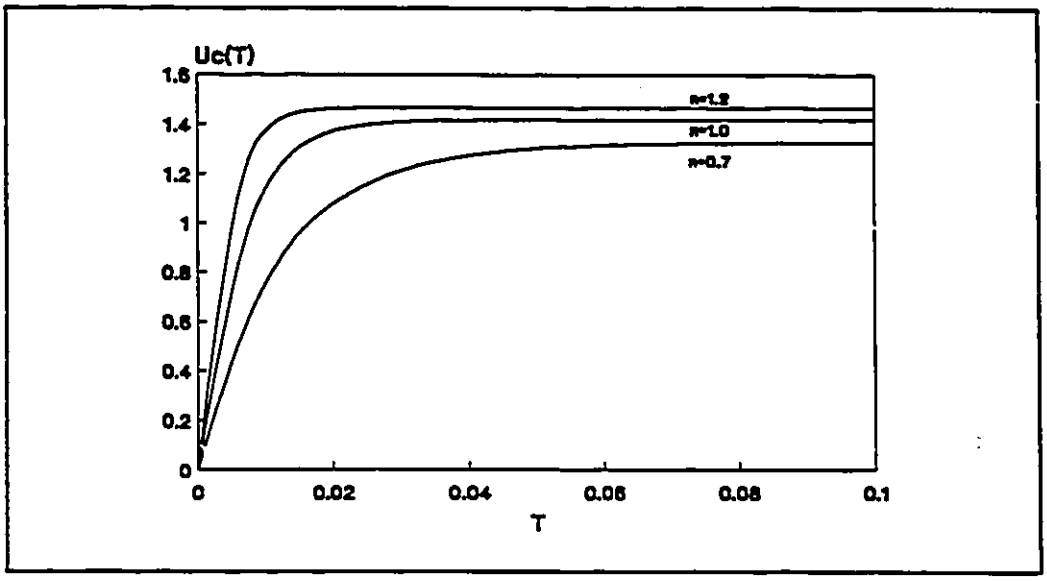

Figure 6.9 Start-up flow in a concentric annulus, unsheared plug velocity profiles Pl=10 s=0.2 with different flow index n

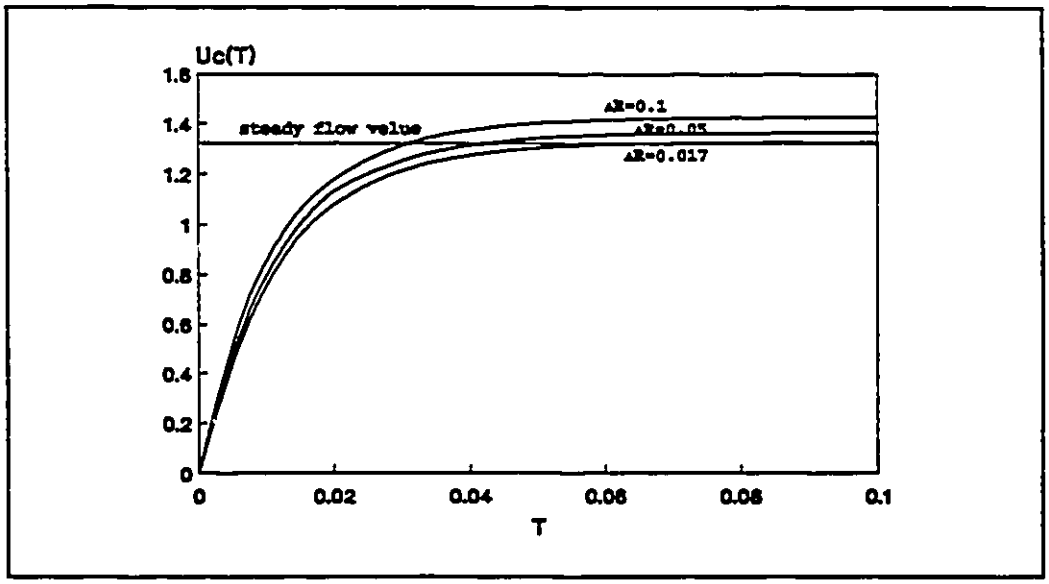

Figure 6.10 Start-up flow in a concentric annulus, unsheared plug velocity profiles Pl=10 n=0.7 s=0.2 with different finite difference grid sizes ΔR

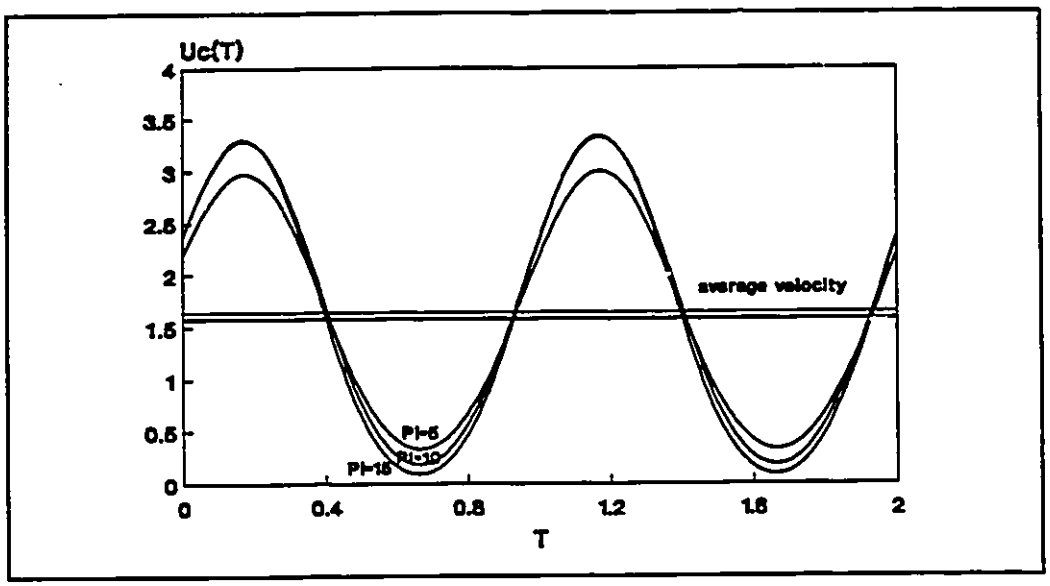

Figure 6.11 Pulsating flow in a concentric annulus, unsheared plug velocity distributions n=0.7 ϵ=0.5 ζ=1 with different generalized Bingham number Pl

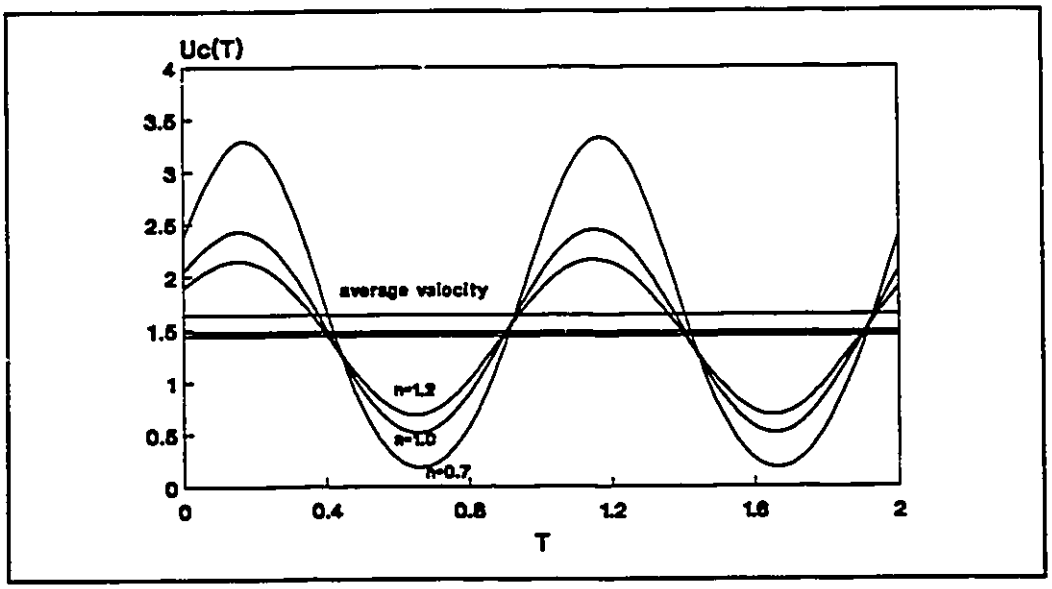

Figure 6.12 Pulsating flow in a concentric annulus, unsheared plug velocity distributions Pl=10 s=0.2 ϵ=0.5 ζ=1 with different flow index n

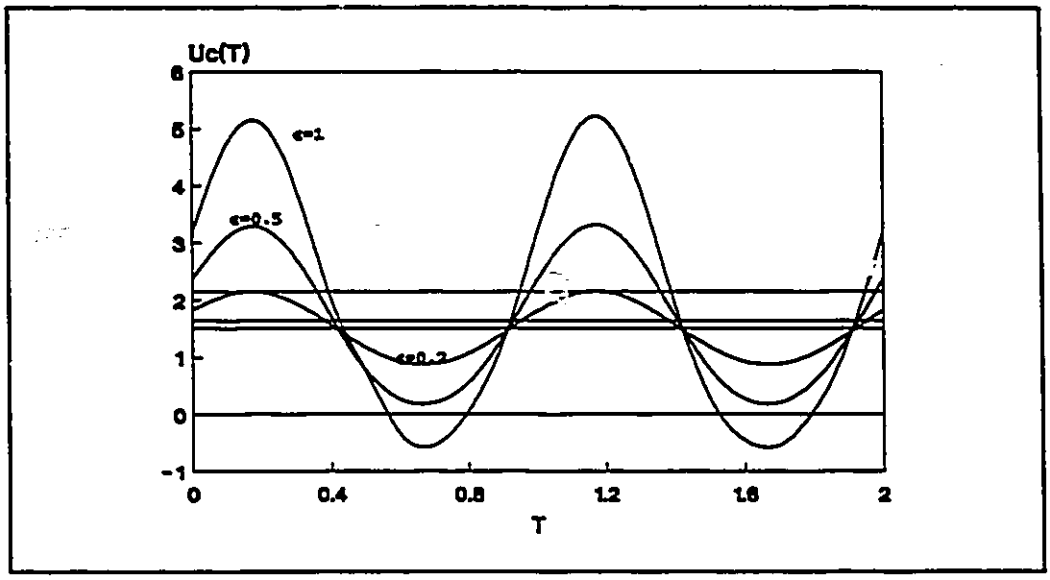

Figure 6.13 Pulsating flow in a concentric annulus, unsheared plug velocity distributions Pl=10 s=0.2 ζ=1 with different pressure amplitude ϵ

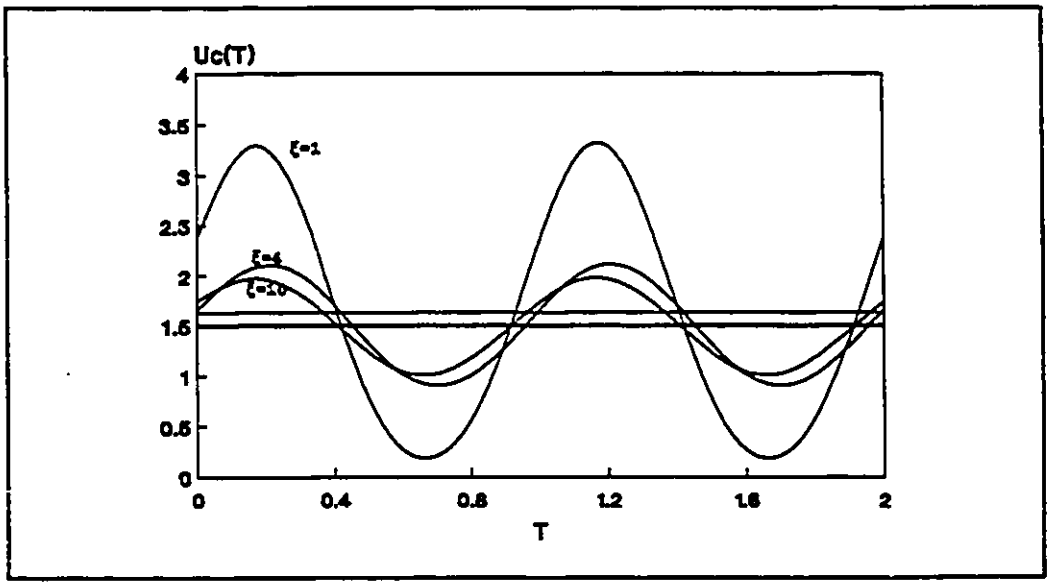

Figure 6.14 Pulsating flow in a concentric annulus, unsheared plug velocity distributions Pl=10 n=0.7 s=0.2 ϵ=0.5 with different frequency parameter ξ

CHAPTER 7

UNSTEADY FLOW OF NON-NEWTONIAN FLUIDS IN AN ECCENTRIC ANNULUS

7.1. Derivation of governing equations

Figure 7.1 shows the geometry of an eccentric annulus: where r_o is the outer cylinder radius, r_i is the inner cylinder radius, and e is the distance between the centres of the inner and outer cylinders. Because the flow in an eccentric annulus is not axisymmetric, it becomes a three dimensional problem. For simplicity, a Cartesian coordinate system will be

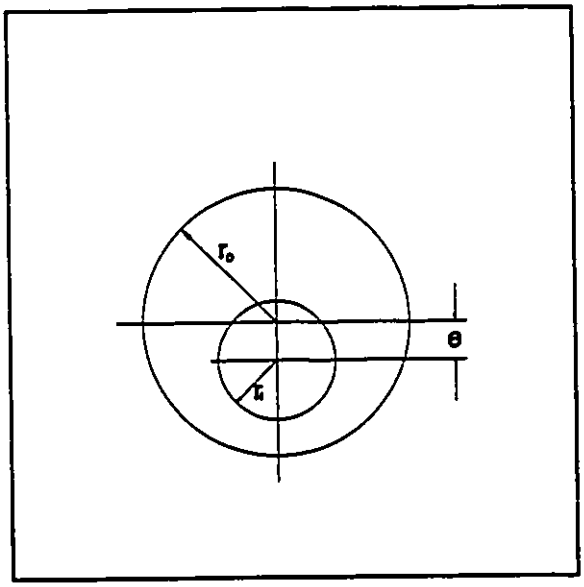

Figure 7.1 Eccentric annulus

used to develop the governing equation of motion. Ignoring the influence of the effect of entry and exit regions, the momentum equation of an incompressible, laminar, unsteady axial flow of a generalized Bingham fluid in an eccentric annulus is given as:

$$\frac{\partial u}{\partial t}=\frac{\partial p}{\partial z}+\frac{\partial}{\partial x}(\mu\frac{\partial u}{\partial x})+\frac{\partial}{\partial y}(\mu\frac{\partial u}{\partial y}) \qquad 7.1$$

where viscosity, μ, is a function of strain rate $\dot{\gamma}$ and defined as:

$$\mu=\frac{\tau}{\dot{\gamma}}$$

for generalized Bingham fluids, the viscosity may be expressed as:

$$\mu=\frac{\tau_0}{\dot{\gamma}}+k\dot{\gamma}^{n-1} \qquad 7.2$$

The definition of strain rate, $\dot{\gamma}$, in Cartesian coordinates is:

$$\dot{\gamma}=\left|\sqrt{(\frac{\partial u}{\partial x})^2+(\frac{\partial u}{\partial y})^2}\right| \qquad 7.3$$

For unsteady flow, the pressure gradient is a function of time. In this chapter, only start-up flow is discussed. The boundary conditions for the flow in an eccentric annulus are the velocity at the inner and outer cylinders is equal to zero. However, it is very difficult to give an expression of the boundary conditions in Cartesian coordinates, it is preferable to use a bipolar coordinate system.

7.2. Dimensional analysis

Equation 7.1 can be made dimensionless by introducing the following nondimensional variables:

$$U=\frac{u}{\bar{u}} \qquad X=\frac{x}{d_h} \qquad Y=\frac{y}{d_h}$$

$$R_i=\frac{r_i}{d_h/4} \qquad R_o=\frac{r_o}{d_h/4} \qquad E=\frac{e}{d_h}$$

$$Re=\frac{\varrho d_h{}^n \bar{u}^{2-n}}{k} \qquad Pl=\frac{\tau_0 d_h{}^n}{k\bar{u}^n}$$

$$f=-\frac{dp}{dz}_s \frac{d_h}{\varrho \bar{u}^2/2} \qquad T=\frac{t\bar{u}}{d_h Re}$$

where Re and Pl are generalized Reynolds number and generalized Bingham number, f is the friction factor, $\bar{u}$ is the average velocity in the annulus, d_h is the hydraulic diameter of the annulus. $d_h = 2(r_o - r_i)$

In terms of these nondimensional variables, equation 7.1 becomes:

$$\frac{\partial U}{\partial T} = \frac{1}{2} fRe + \frac{\partial}{\partial X}\left(\tilde{\mu}\frac{\partial U}{\partial X}\right) + \frac{\partial}{\partial Y}\left(\tilde{\mu}\frac{\partial U}{\partial Y}\right) \qquad 7.4$$

where the dimensionless viscosity may be written as:

$$\tilde{\mu} = \frac{Pl}{\left[\left(\frac{\partial U}{\partial X}\right)^2 + \left(\frac{\partial U}{\partial Y}\right)^2\right]^{1/2}} + \left[\left(\frac{\partial U}{\partial X}\right)^2 + \left(\frac{\partial U}{\partial Y}\right)^2\right]^{\frac{n-1}{2}} \qquad 7.5$$

7.3. Bipolar coordinate transformation

It was mentioned previously that the boundary conditions of the flow in an eccentric annulus are very difficult to handle when expressed in Cartesian coordinates. The geometry of an eccentric annulus, shown in Figure 7.1, is described most easily using the bipolar coordinate system shown in Figure 7.2. In bipolar coordinates, the eccentric annulus is represented by two orthogonal families of circles, ξ and η.

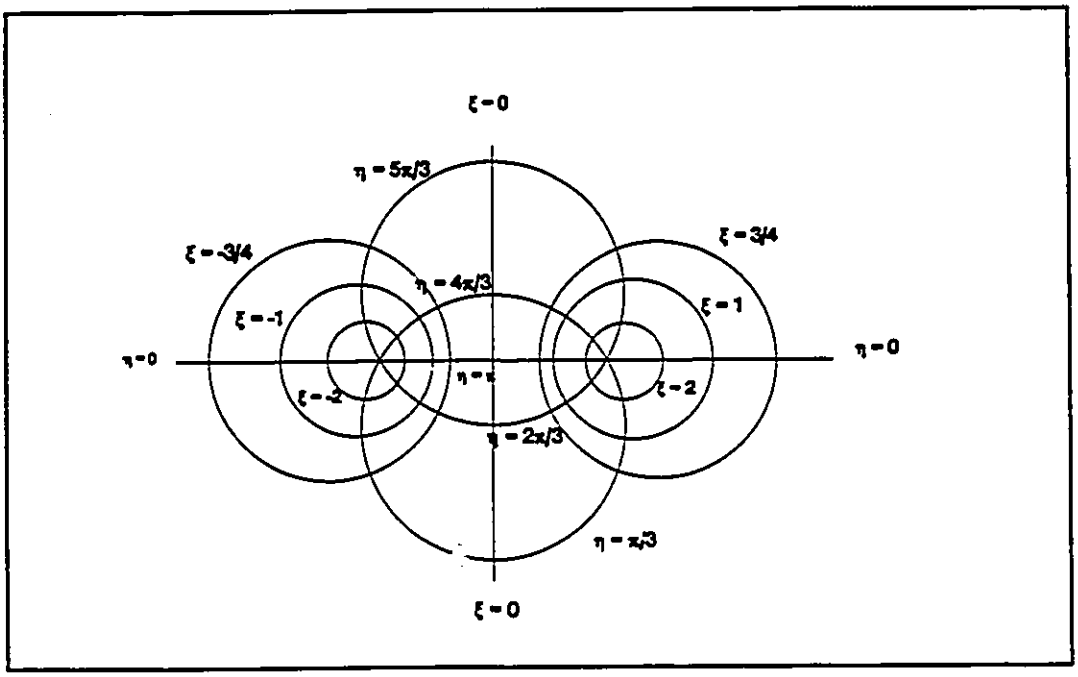

Figure 7.2 Bipolar coordinate system

The ζ axis is perpendicular to the ξ - η plane. This coordinate system is obviously useful, because the walls of the eccentric annulus are represented by two constant values ξ_o and ξ_i (Figure 7.3). The transformation from Cartesian coordinates to bipolar coordinates is given by (Guckes, 1975):

$$X=\frac{a\sinh(\xi)}{\cosh(\xi)-\cos(\eta)} \qquad 7.6$$

$$Y=\frac{-a\sin(\eta)}{\cosh(\xi)-\cos(\eta)} \qquad 7.7$$

$$Z = \zeta \qquad 7.8$$

where $$a = R_i \sinh\xi_i = R_o \sinh \xi_o \qquad 7.9$$

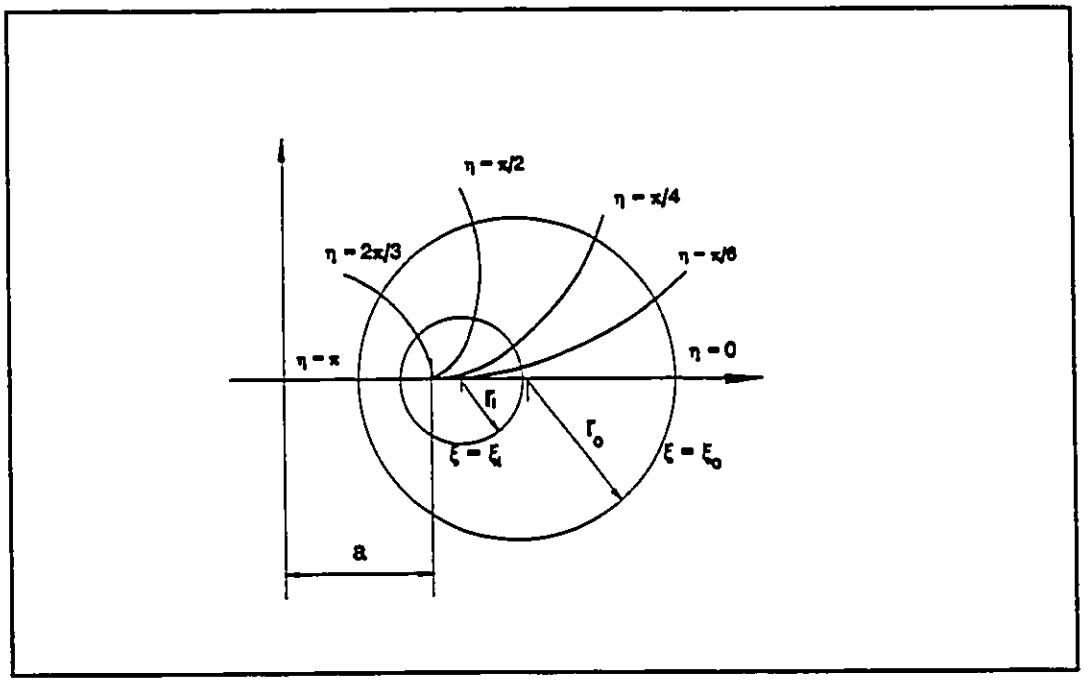

Figure 7.3 Eccentric annulus in bipolar coordinate system

The definitions of ξ_i and ξ_o are given by:

$$\xi_i=\cosh^{-1}\left[\frac{1-(R_i/R_o)^2-(E/R_o)^2}{2R_i/R_oE/R_o}\right] \qquad 7.10$$

$$\xi_o=\cosh^{-1}\left[\frac{1-(R_i/R_o)^2+(E/R_o)^2}{2E/R_o}\right] \qquad 7.11$$

The transformation of the equation of motion into bipolar coordinates is given by equation 7.12. Details of the transformation are provided in Appendix A.

$$\left(\frac{a}{\psi}\right)^2\frac{\partial U}{\partial T}=\frac{1}{2}fRe\left(\frac{a}{\psi}\right)^2+\frac{\partial}{\partial\xi}\left(\tilde{\mu}\frac{\partial U}{\partial\xi}\right)+\frac{\partial}{\partial\eta}\left(\tilde{\mu}\frac{\partial U}{\partial\eta}\right) \qquad 7.12$$

for $\qquad 0 \le \eta \le \pi \quad$ and $\quad \xi_i \le \xi \le \xi_o$

where

$$\tilde{\mu}=\frac{PI}{\frac{\psi}{a}\left[\left(\frac{\partial U}{\partial \xi}\right)^2+\left(\frac{\partial U}{\partial \eta}\right)^2\right]}+\left(\frac{\psi}{a}\right)^{n-1}\left[\left(\frac{\partial U}{\partial \xi}\right)^2+\left(\frac{\partial U}{\partial \eta}\right)^2\right]^{\frac{n-1}{2}} \qquad 7.13$$

and

$$\psi=\cosh(\xi)-\cos(\eta) \qquad 7.14$$

The boundary conditions are:

$$\text{At} \quad \xi = \xi_i \quad \text{and} \quad \xi_o, \quad U = 0$$

$$\text{At} \quad \eta = 0 \quad \text{and} \quad \pi, \quad \partial U/\partial \eta = 0$$

7.4. Finite difference approach

A control volume based upon a finite difference calculation technique was used to solve the momentum equation 7.12. In an eccentric annulus, the velocity profile is symmetric about the axis which goes through the centres of the inner and outer cylinders. Therefore, only one half of the annulus need be calculated. Figure 7.4 shows the network of the grid points in transformed coordinates. The region of the

network is:

$$0 \leq \eta \leq \pi$$

and

$$\xi_i \leq \xi \leq \xi_o$$

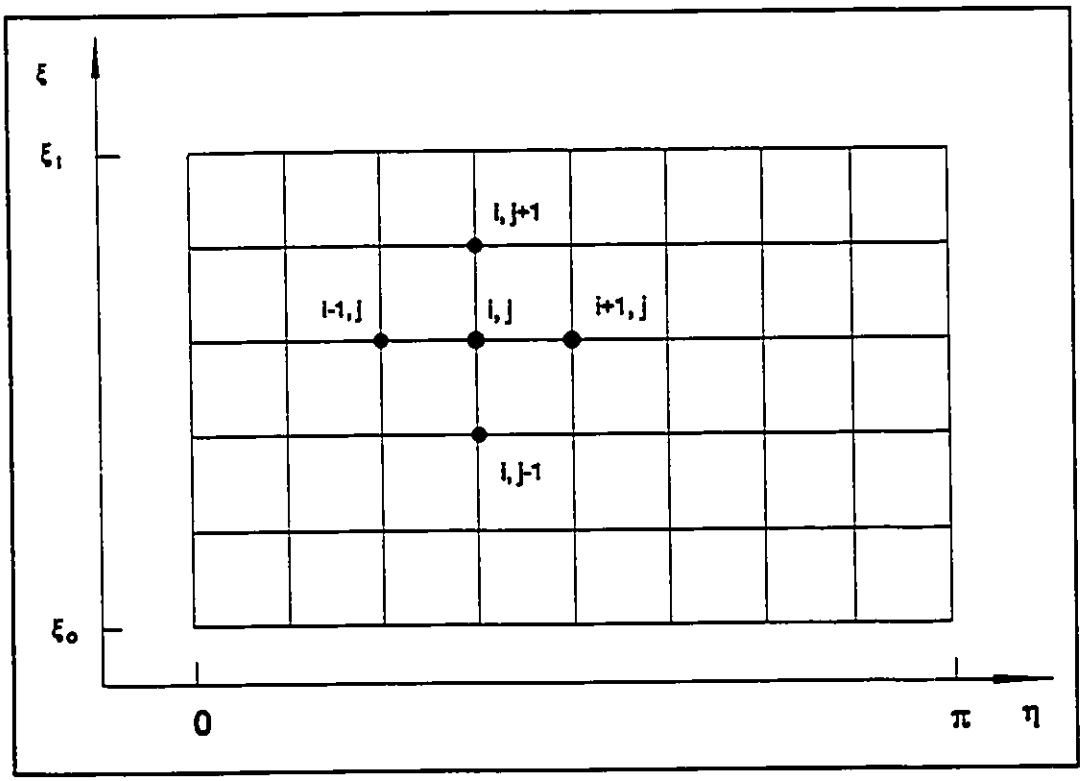

Figure 7.4 Finite difference network in the transformed coordinates

The finite difference representations used for various terms in equation 7.12 at a grid point (i,j) are:

$$\frac{\partial U}{\partial T}=\frac{U_{i,j}^{K+1}-U_{i,j}^{K}}{\Delta T}$$

$$\frac{\partial}{\partial \xi}\left(\tilde{\mu}\frac{\partial U}{\partial \xi}\right)=\frac{1}{\Delta \xi^2}\left[\tilde{\mu}_{i,j+\frac{1}{2}}U_{i,j+1}-\left(\tilde{\mu}_{i,j+\frac{1}{2}}+\tilde{\mu}_{i,j-\frac{1}{2}}\right)U_{i,j}+\tilde{\mu}_{i,j-\frac{1}{2}}U_{i,j-1}\right]$$

$$\frac{\partial}{\partial \eta}\left(\tilde{\mu}\frac{\partial U}{\partial \eta}\right)=\frac{1}{\Delta \eta^2}\left[\tilde{\mu}_{i+\frac{1}{2},j}U_{i+1,j}-\left(\tilde{\mu}_{i+\frac{1}{2},j}+\tilde{\mu}_{i-\frac{1}{2},j}\right)U_{i,j}+\tilde{\mu}_{i-\frac{1}{2},j}U_{i-1,j}\right]$$

Where U^{K+1} represents the velocity at current time, and U^{K} represents the velocity at the previous time interval.

The discretization of the equation of motion (Eqn. 7.12) becomes:

$$A_{i,j}U_{i-1,j}^{K+1}+B_{i,j}U_{i+1,j}^{K+1}+C_{i,j}U_{i,j-1}^{K+1}+D_{i,j}U_{i,j+1}^{K+1}+E_{i,j}U_{i,j}^{K+1}=F_{i,j} \qquad 7.15$$

where

$$A_{i,j}=-\frac{1}{\Delta\eta^2}\tilde{\mu}_{i-\frac{1}{2},j}$$

$$B_{i,j}=-\frac{1}{\Delta\eta^2}\tilde{\mu}_{i+\frac{1}{2},j}$$

$$C_{i,j}=-\frac{1}{\Delta\xi^2}\tilde{\mu}_{i,j-\frac{1}{2}}$$

$$D_{i,j}=-\frac{1}{\Delta\xi^2}\tilde{\mu}_{i,j+\frac{1}{2}}$$

$$E_{i,j}=\frac{a^2}{\psi_{i,j}^2\Delta T}-A_{i,j}-B_{i,j}-C_{i,j}-D_{i,j}$$

$$F_{i,j}=\left(\frac{U_{i,j}^K}{\Delta T}+\frac{1}{2}fRe\right)\frac{a^2}{\psi_{i,j}^2}$$

According to the equation 7.13, a set of discretization equations for the dimensionless viscosity $\tilde{\mu}$s in each coefficient are expressed by the values of velocity at the

faces of the control volume surrounding the grid point (see Figure 7.5).

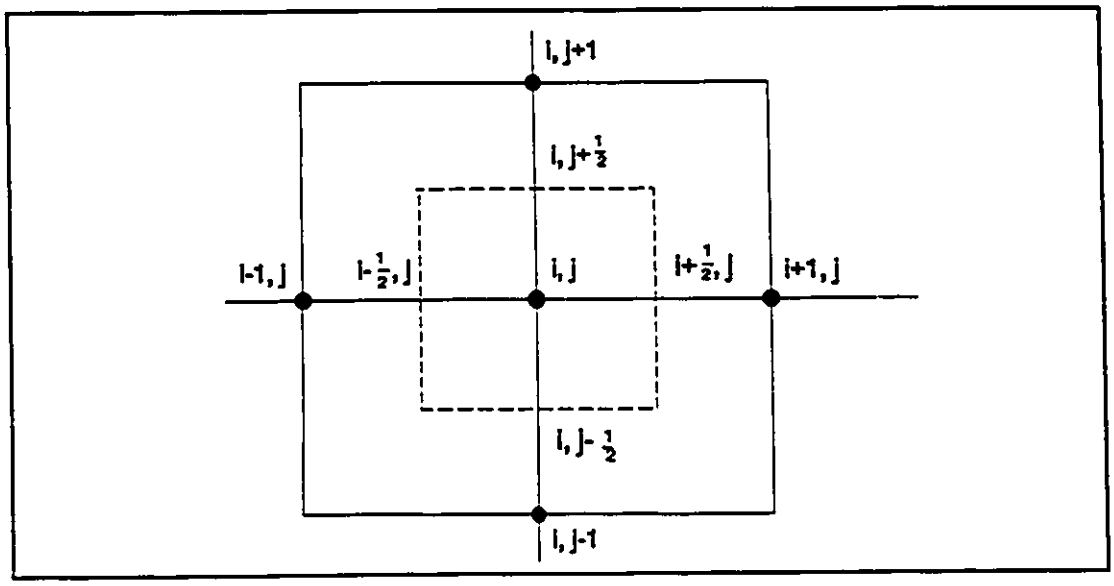

Figure 7.5 Grid point control volume

$$\tilde{\mu}_{i\pm\frac{1}{2},j}=\frac{PI}{\left(\frac{\Psi}{a}\right)_{i\pm\frac{1}{2},j}\left[\left(\frac{\partial U}{\partial \xi}\right)^2_{i\pm\frac{1}{2},j}+\left(\frac{\partial U}{\partial \eta}\right)^2_{i\pm\frac{1}{2},j}\right]^{\frac{1}{2}}}$$

$$+\left(\frac{\Psi}{a}\right)^{n-1}_{i\pm\frac{1}{2},j}\left[\left(\frac{\partial U}{\partial \xi}\right)^2_{i\pm\frac{1}{2},j}+\left(\frac{\partial U}{\partial \eta}\right)^2_{i\pm\frac{1}{2},j}\right]^{\frac{n-1}{2}}$$

$$\tilde{\mu}_{i,j\pm\frac{1}{2}} = \frac{Pl}{\left(\frac{\Psi}{a}\right)_{i,j\pm\frac{1}{2}} \left[\left(\frac{\partial U}{\partial \xi}\right)^2_{i,j\pm\frac{1}{2}} + \left(\frac{\partial U}{\partial \eta}\right)^2_{i,j\pm\frac{1}{2}}\right]^{\frac{1}{2}}}$$

$$+ \left(\frac{\Psi}{a}\right)^{n-1}_{i,j\pm\frac{1}{2}} \left[\left(\frac{\partial U}{\partial \xi}\right)^2_{i,j\pm\frac{1}{2}} + \left(\frac{\partial U}{\partial \eta}\right)^2_{i,j\pm\frac{1}{2}}\right]^{\frac{n-1}{2}}$$

where

$$\left(\frac{\partial U}{\partial \xi}\right)_{i-\frac{1}{2},j} = \frac{1}{4\Delta\xi}\left(U_{i-1,j+1} + U_{i,j+1} - U_{i-1,j-1} - U_{i,j-1}\right)$$

$$\left(\frac{\partial U}{\partial \xi}\right)_{i+\frac{1}{2},j} = \frac{1}{4\Delta\xi}\left(U_{i,j+1} + U_{i+1,j+1} - U_{i,j-1} - U_{i+1,j-1}\right)$$

$$\left(\frac{\partial U}{\partial \eta}\right)_{i,j-\frac{1}{2}} = \frac{1}{4\Delta\eta}\left(U_{i+1,j-1} + U_{i+1,j} - U_{i-1,j-1} - U_{i-1,j}\right)$$

$$\left(\frac{\partial U}{\partial \eta}\right)_{i,j+\frac{1}{2}} = \frac{1}{4\Delta\eta}\left(U_{i+1,j} + U_{i+1,j+1} - U_{i-1,j} - U_{i-1,j+1}\right)$$

$$\left.\frac{\partial U}{\partial \xi}\right|_{i,j-\frac{1}{2}} = \frac{U_{i,j} - U_{i,j-1}}{\Delta \xi}$$

$$\left.\frac{\partial U}{\partial \xi}\right|_{i,j+\frac{1}{2}} = \frac{U_{i,j+1} - U_{i,j}}{\Delta \xi}$$

$$\left.\frac{\partial U}{\partial \eta}\right|_{i-\frac{1}{2},j} = \frac{U_{i,j} - U_{i-1,j}}{\Delta \eta}$$

$$\left.\frac{\partial U}{\partial \eta}\right|_{i+\frac{1}{2},j} = \frac{U_{i+1,j} - U_{i,j}}{\Delta \eta}$$

The boundary conditions are:

At $\xi = \xi_i$ j=1 and ξ_o j=N+1,

U(i,1) = U(i,N+1) = 0

At $\eta = 0$ i=1 and π i=M+1,

U(i-1,j) = U(i+1,j) and U(M+2,j) = U(M,j)

where M and N are the numbers of grid network on η and ξ respectively.

For a non-Newtonian fluid, the viscosity is not a constant but a function of velocity. To solve equation 7.15, an iterative method was used. In iterative calculations, a set of velocities in the network were calculated first by using the viscosity values at a previous time step, then the values of the velocities were used to calculate the viscosities at the current time interval. Velocities were again calculated by using these values of viscosities. These procedures were repeated until the difference between the new and old value of the velocity at every grid point was less than a prescribed small value (in this study: 0.001). The calculations were then repeated at the next time step. Thus the velocity profile development with time was obtained.

7.5 Results and discussion

Velocity profiles of start-up flow of generalized Bingham fluids in an eccentric annulus were obtained using the finite difference method mentioned previously in this chapter. The results are presented on a generalized basis in terms of the ratio of radii of inner and outer cylinders of the annulus, s, and the distance between the centres of the two cylinders. Figures 7.6, 7.9 and 7.12 show the start-up flow velocity profile development of a generalized Bingham fluid (Pl=10, n=.7) with different radius ratio s and eccentricity e.

Comparing with flow in a concentric annulus, when the annulus becomes slightly eccentric, the velocity profile changes considerably. The velocity in the narrowing part of the annulus ($\eta = \pi$) is decreased, and the velocity in the widening part ($\eta = 0$) is increased. The reason being that the resistance to flow is increased as the gap between the two cylinders is reduced. The results show that the difference between the $\eta = 0$ and $\eta = \pi$ is increased when eccentricity e increases or radius ratio s increases. Figures 7.7, 7.10 and 7.13 show the maximum velocity distribution of a generalized Bingham fluid (Pl=10, n=0.7) at different angle η in a start-up flow, which represents velocity distributions at different locations in the annulus. Figures 7.8, 7.11, and 7.14 show the three-dimensional velocity profiles of generalized Bingham fluids in an eccentric annulus at steady state. Because the flow is symmetric about the axis which goes through the centres of inner and outer cylinders, the Figures show only one half of the profiles. The effect of generalized Bingham number Pl on the velocity distribution in an eccentric annulus may be observed in Figure 7.15. When Pl increases, start-up flow reaches steady state more quickly, and the maximum velocities at both the narrow and wider parts in the annulus are smaller. Figure 7.16 shows the comparison of velocity distributions with different eccentricity e. It can be seen that when the eccentricity e increases, the velocity distribution at narrow part ($\eta = \pi$) of the annulus achieves

steady state more quickly; in the wider part (η = 0) it takes more time to become steady. The accuracy of this numerical program was verified by comparing the results of velocity profiles of a Newtonian fluid in an eccentric annulus at steady state (Figure 7.17) with the analysis of Heyda (1959). Using Heyda's equation, for an eccentric annulus with s=0.2 and e=0.2, the ratio of maximum velocities at $\eta=\pi$ and η=0 is 0.63. In this program, that ratio is 0.645. The agreement is good. If the finite difference network had been further refined, the results would have been even better.

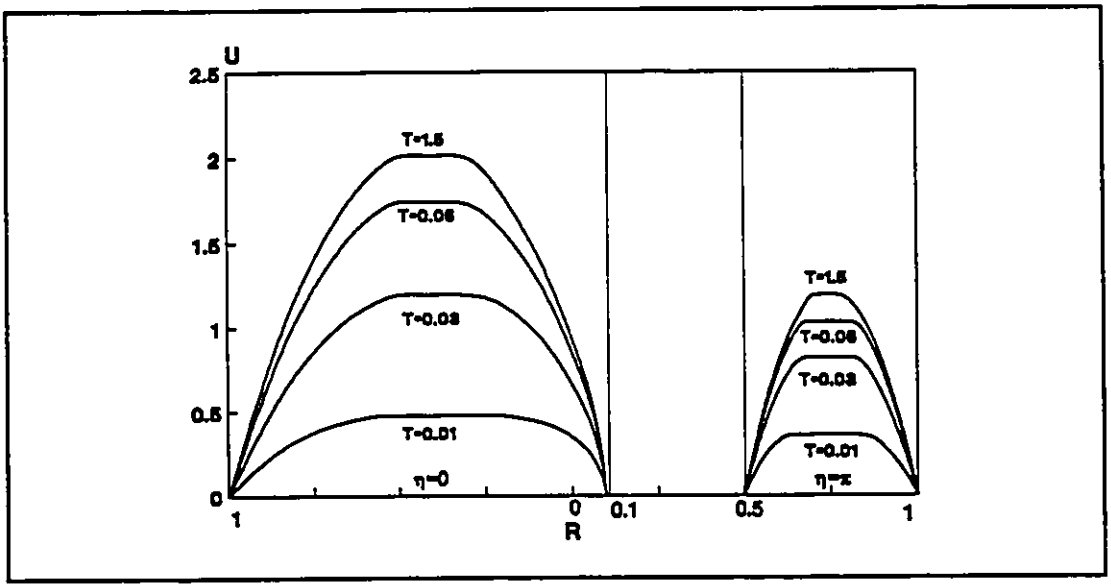

Figure 7.6 Start-up flow in an eccentric annulus, velocity profiles Pl=10 n=0.7 s=0.2 e=0.3

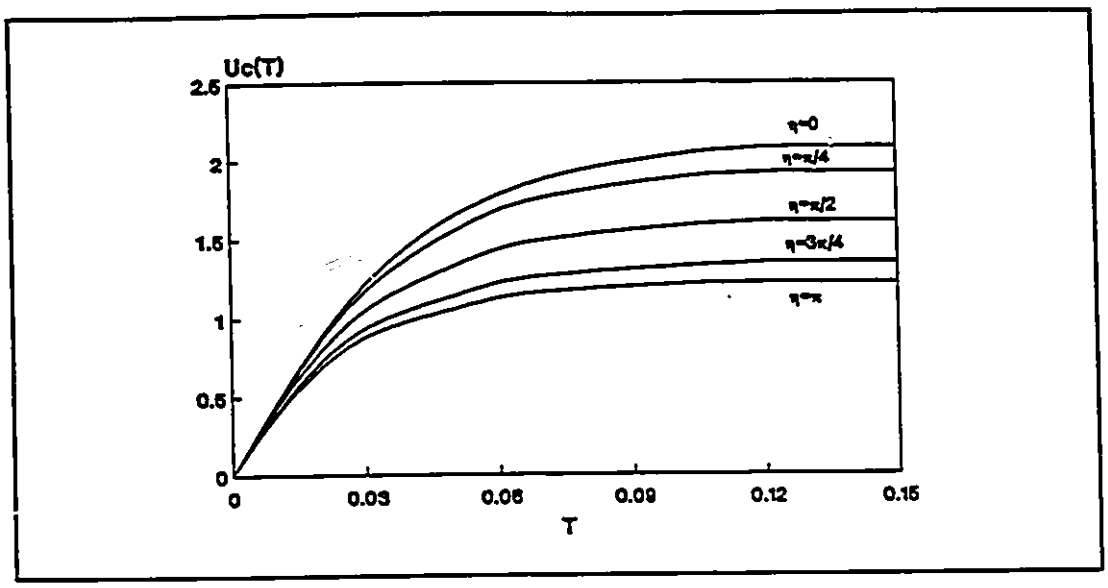

Figure 7.7 Start-up flow in an eccentric annulus, maximum velocity distributions at different angle η Pl=10 n=0.7 s=0.2 e=0.3

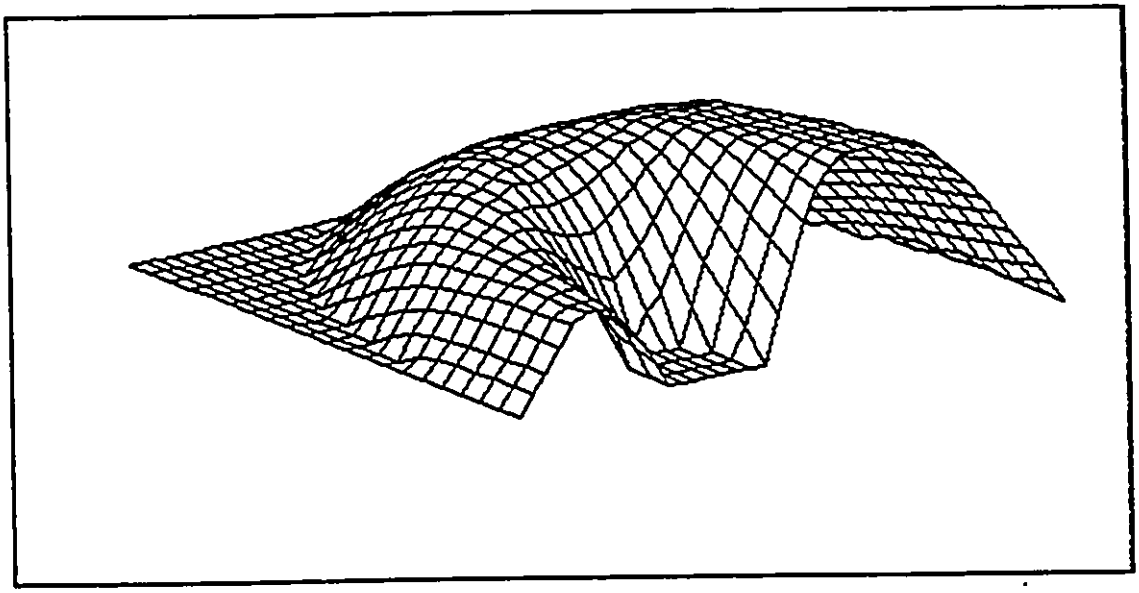

Figure 7.8 Start-up flow in an eccentric annulus, 3-D velocity profile at steady state Pl=10 n=0.7 s=0.2 e=0.3

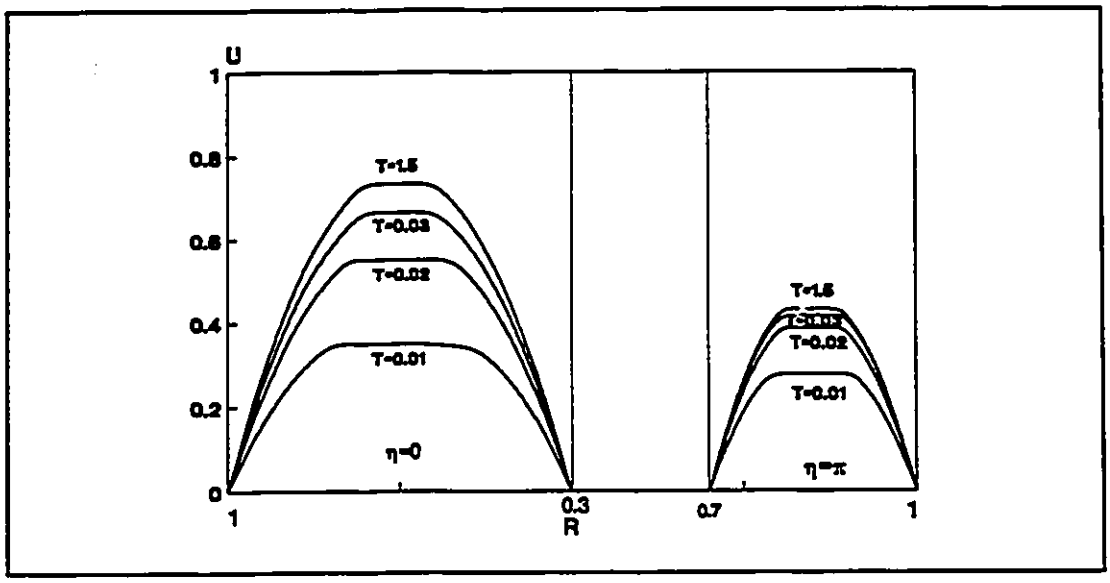

Figure 7.9 Start-up flow in an eccentric annulus, velocity profiles Pl=10 n=0.7 s=0.6 e=0.1

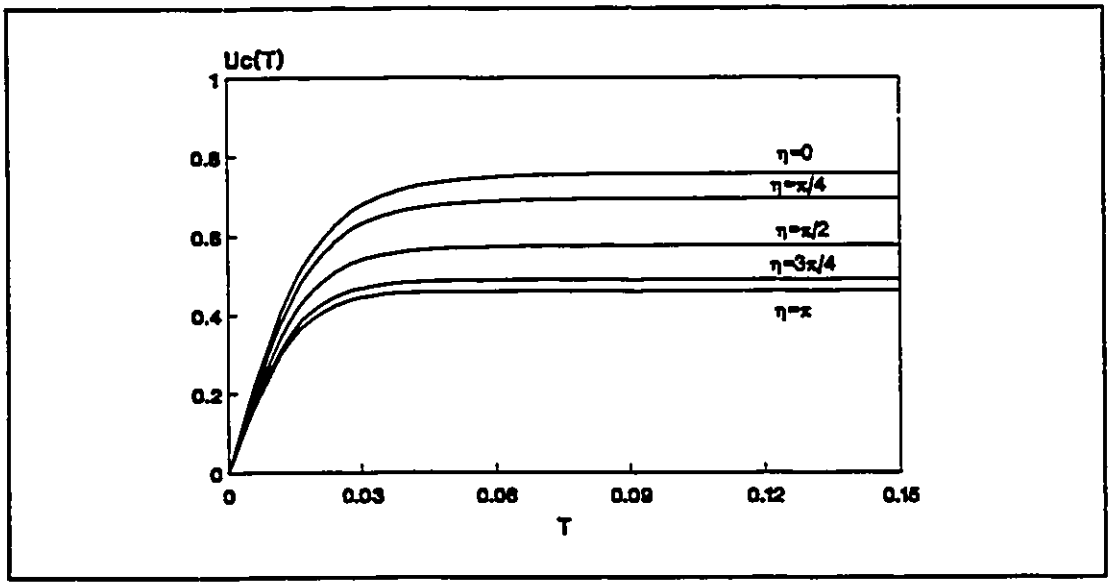

Figure 7.10 Start-up flow in an eccentric annulus, maximum velocity distributions at different angle η Pl=10 n=0.7 s=0.6 e=0.1

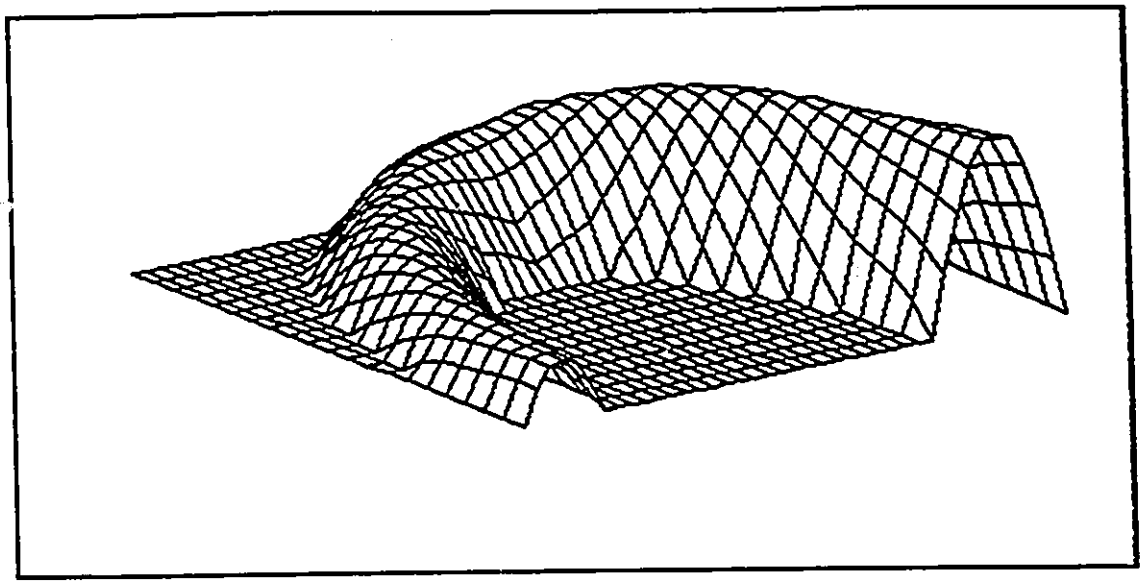

Figure 7.11 Start-up flow in an eccentric annulus, 3-D velocity profile at steady state Pl=10 n=0.7 s=0.6 e=0.2

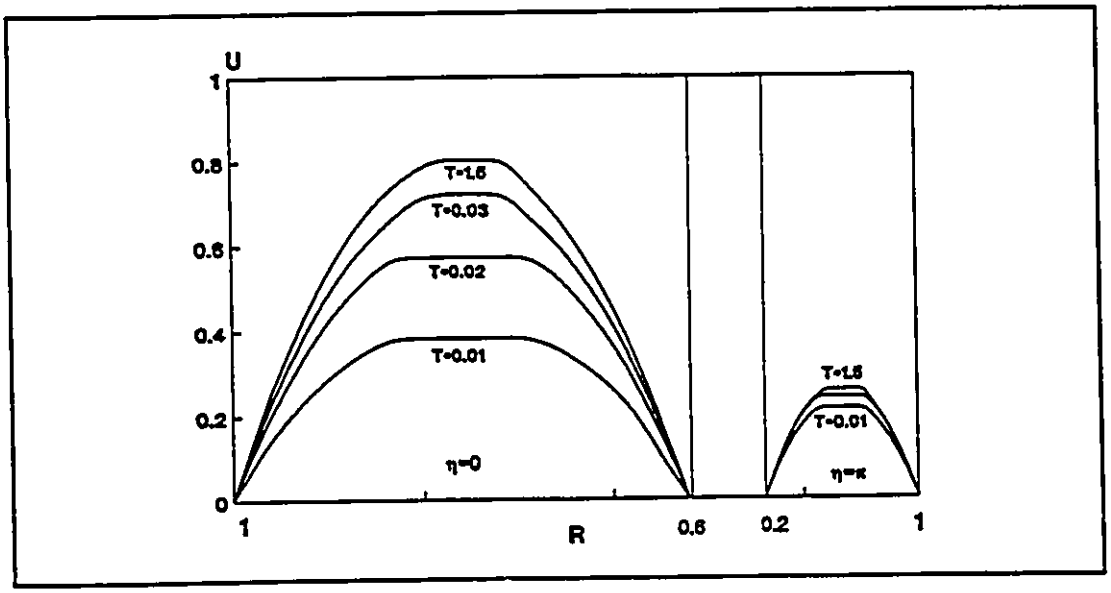

Figure 7.12 Start-up flow in an eccentric annulus, velocity profiles Pl=10 n=0.7 s=0.6 e=0.3

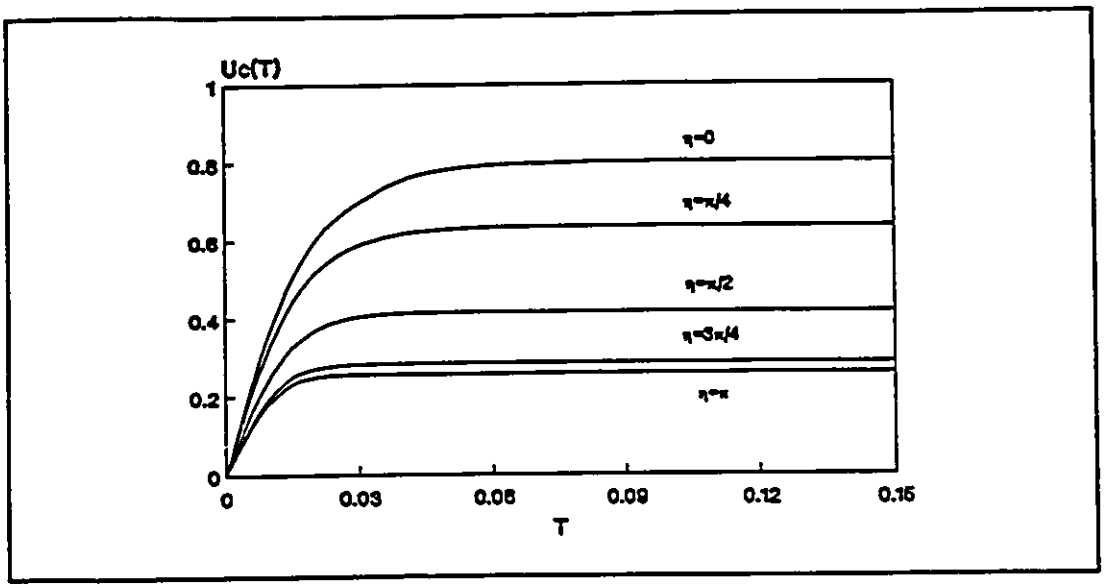

Figure 7.13 Start-up flow in an eccentric annulus, maximum velocity distributions at different angle η Pl=10 n=0.7 s=0.6 e=0.3

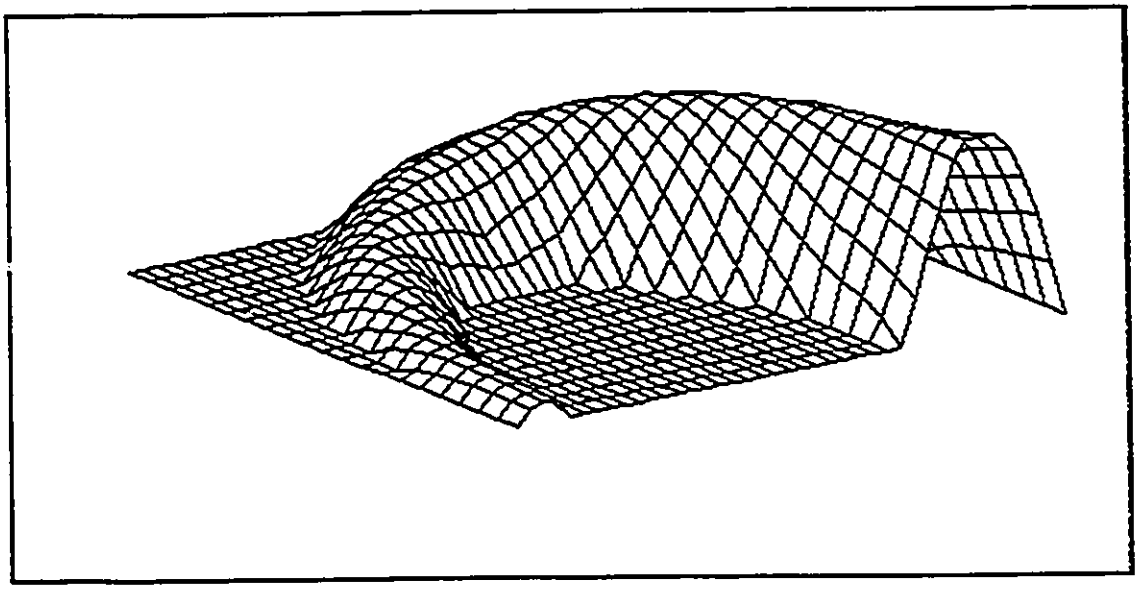

Figure 7.14 Start-up flow in an eccentric annulus, 3-D velocity profile at steady state Pl=10 n=0.7 s=0.6 e=0.1

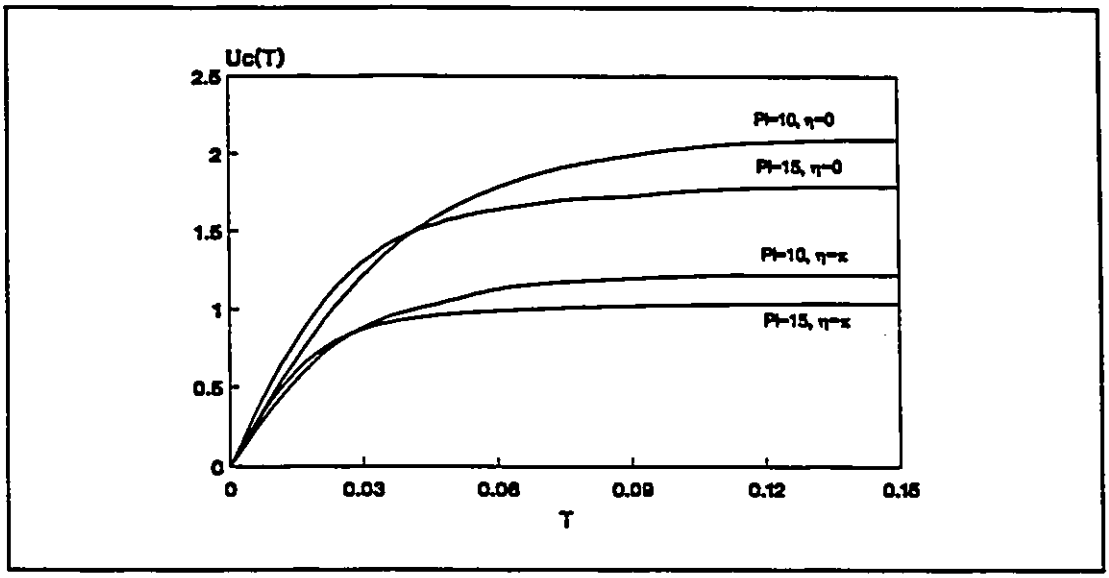

Figure 7.15 Start-up flow in an eccentric annulus, velocity distributions with different Pl n=0.7 s=0.2 e=0.3

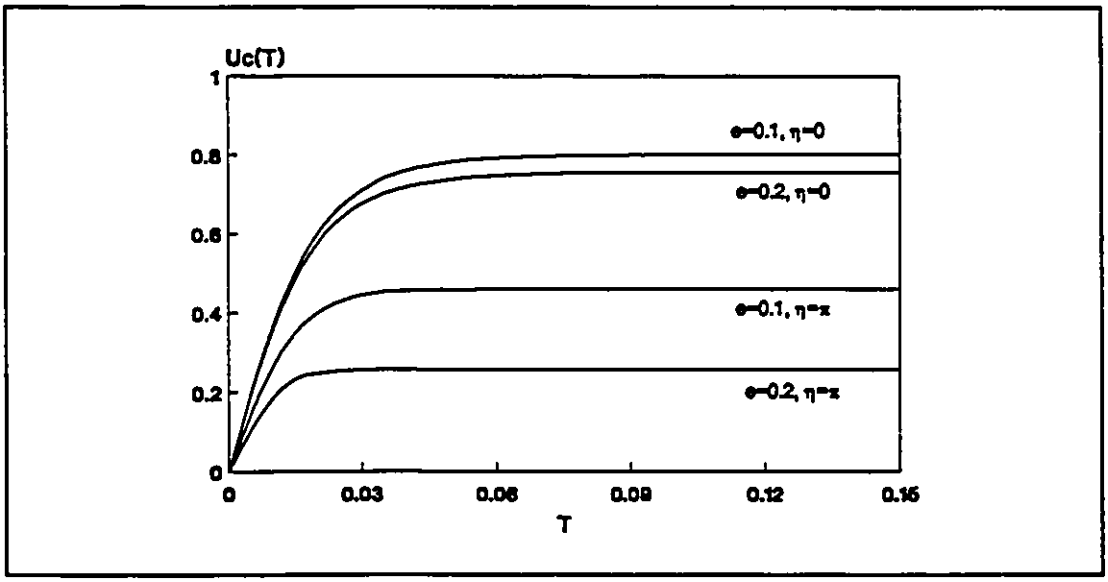

Figure 7.16 Start-up flow in an eccentric annulus, velocity distributions with different eccentricity e Pl=10 n=0.7 s=0.6

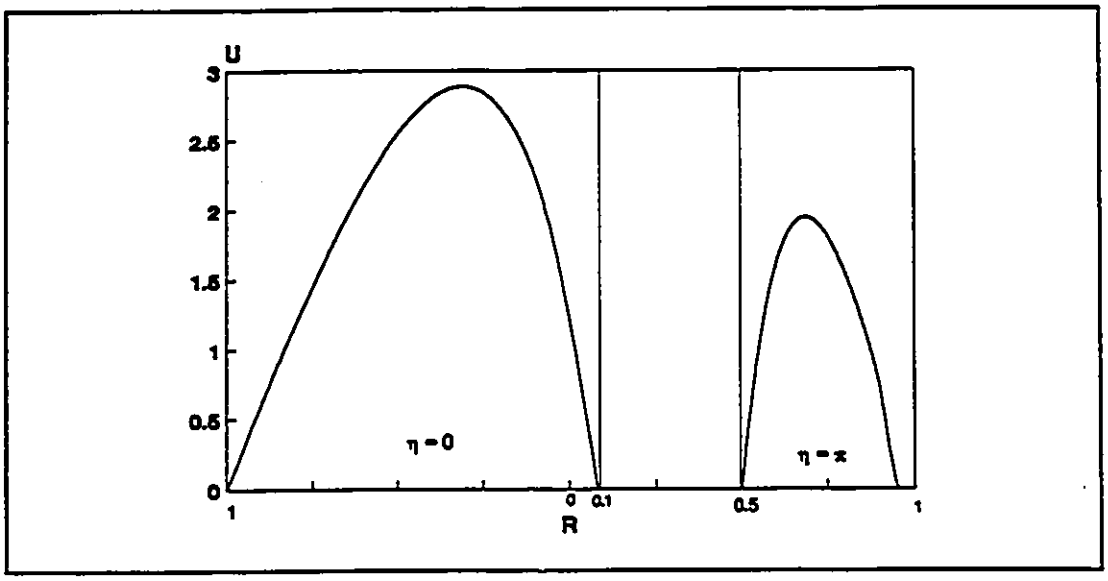

Figure 7.17 Start-up flow of Newtonian fluid in an eccentric annulus, steady state velocity profiles Pl=0 n=1.0 s=0.2 e=0.2

CHAPTER 8

CONCLUSIONS AND RECOMMENDATIONS

8.1. Conclusions

The study that has been presented in previous chapters gives a certain number of important results on the flow of non-Newtonian fluids in both concentric and eccentric annuli. Fully developed flow, unsteady state flow and entrance flow of generalized Bingham fluids in a concentric annulus and unsteady flow in an eccentric annulus were investigated. The following general conclusions can be drawn:

1. Previous studies of non-Newtonian fluid flow did not cover unsteady state flow and entrance flow of generalized Bingham fluids in both concentric and eccentric annuli.

2. A set of mathematical formulations have been developed for fully developed flow of generalized Bingham fluids in a concentric annulus. A numerical scheme was used to treat the equations governing the flow.

3. Typical velocity profiles are presented for fully developed flow of generalized Bingham fluids in a concentric

annulus for values of flow index n=0.7, generalized Bingham number Pl=5, 10, 15 and radius ratio s=0.02, 0.2, 0.4 and 0.6. The influences of the major variables were demonstrated. An unsheared plug existed in the annulus because of the characteristics of yield stress of generalized Bingham fluids.

4. The position of the unsheared plug may be determined by solving the governing equations numerically. It is not symmetric between the inner and outer wall of the annulus, and it is closer to the inner wall. With the radius ratio s decreasing, the plug is shifted further towards the inner wall. The region of the unsheared plug is proportional to the generalized Bingham number Pl. The boundary radii of the plug may be used as boundary conditions to solve entrance flow and unsteady flow problems in a concentric annulus.

5. The equation of motion of entrance flow of generalized Bingham fluids in a concentric annulus has been derived with a set of dimensionless variables. A control volume approach based upon an up-winding finite difference technique was used to solve the governing equations. Velocity and pressure profiles in the entrance region were presented for values of n=0.7, 1.0, and 1.2, Pl=5, 10 and 15, s=0.02, 0.2, 0.4, and 0.6.

6. A graphical summary of the solutions indicates that the entrance length in a concentric annulus increases when radius ratio s or generalized Bingham number Pl decreases.

However, when flow index n increases, the entrance length increases. The pressure drop in the entrance region exhibits similar behaviour to the entrance length with the variables s, n and Pl. The value of maximum velocity (the velocity of the unsheared plug) in a concentric annulus is proportional to n, and is inversely proportional to s and Pl.

7. Mathematical models for start-up flow and pulsating flow have been developed to analyze the flow behaviour of generalized Bingham fluids in a concentric annulus. A set of dimensionless variables were used to derive the equation of motion. A control volume based finite difference marching integration method was used to treat the equations governing the flows. Velocity profiles for start-up flow and pulsating flow are presented with s=0.2, 0.4 and 0.6, n=0.7, 1.0 and 1.2, Pl=5, 10 and 15, pressure amplitude ϵ=0.2, 0.5 and 1 and frequency parameter ξ=1, 4 and 10.

8. Start-up flow in a concentric annulus will quickly become fully developed flow for generalized Bingham fluids. The greater the generalized number Pl,the shorter the time from start to steady state. The radius ratio s has the same effect as Pl. The time of flow from start to steady state is shorter when s is increased. As the flow index n increases from less than unity to larger than unity, the time of flow from start to steady state reduces greatly.

9. Graphical results of pulsating flow of generalized

Bingham fluids in a concentric annulus show that generalized Bingham number Pl and flow index n have marked effects on the velocity profiles and the peak value of velocity. However, their effects on the average velocity are limited. That means changing Pl and n has little effect on the change of flow rate in a pulsating flow.

10. Graphical results of pulsating flow of generalized Bingham fluids in a concentric annulus indicate that the pressure amplitude parameter ϵ and pressure frequency parameter ξ have significant effects on the velocity profiles and the peak value of velocity in pulsating flow. When ϵ increases, the average velocity also increases. That means the addition of a pulsating fluctuation to a steady pressure gradient could result in enhancement of the flow rate in a concentric annulus.

11. The equation of motion for the start-up flow of generalized Bingham fluids in an eccentric annulus has been developed with a set of dimensionless variables. The use of a transform in conjunction with bipolar coordinates enables use of a control volume based finite difference method to solve the three dimensional equation governing the flow.

12. Typical velocity profiles of start-up flow in an eccentric annulus are presented for flow indices n=0.7, generalized Bingham number Pl=10, 15, radius ratio s= 0.2, 0.6 and eccentricity e=0.1, 0.2, and 0.3. When an annulus becomes

slightly eccentric, the velocity profiles are changed dramatically. The velocity in the narrowing part of the annulus is decreased, and the velocity in the widening part is increased. The difference between the narrow part and the wider part increases when eccentricity e increases, or when radius ratio s increases.

13. Graphical results of start-up flow in an eccentric annulus show that when eccentricity e increases,the velocity distribution at the narrow part of an annulus achieves steady state quicker than the wider part. When generalized Bingham number Pl increases, the flow also achieves steady state more quickly.

14. Several computer programs have been developed to carry out the numerical analysis and calculations of the above studies. Good agreements was found with results from previous studies.

8.2. Recommendations

1. The present study is quite general and sufficiently comprehensive to deal with any non-Newtonian fluid flow in an annulus. The main focus was on the theoretical investigation and numerical analysis. Experiments should be conducted to verify the numerical results.

2. For flow in an eccentric annulus, this study only involved the problem of start-up flow, which is a specific

situation in application. For many industrial applications, the governing equations are even more complicated, therefore, further theoretical investigation and numerical analysis needs to be done.

3. For practical applications, the parameters presented in these studies, such as: flow index n and generalized Bingham number Pl, should be used specifically according to the situation. Some experiments may be necessary.

4. The theoretical investigation and numerical analysis reported here may be modified to include problems of heat transfer which have potential applications in many areas of industry.

REFERENCES

Astarita, G. "Letter to The Editor: The engineering reality of the yield stress" J. Rheol 34(2) Feb. (1990)

Balmer, R.T. and Fiorina, M.A., "Unsteady Flow of an Inelastic Power-Law Fluid in a Circular Tube", J. Non-Newtonian Fluid Mech. 7, 189-198 (1980)

Barnes, H.A., Townsend, P. and Walter, K., "Flow of Non-Newtonian Liquids under a Varying Pressure Gradient", Nature, 224, 585-587 (1969)

Batra, R.L. and Jena, B, "Entrance Region Flow of Blood in Concentric Annulus", Int. J. Eng. Sci. Vol. 28, No. 5, 407-419 (1990)

Batra, R.L. and Kandasamy, A., "Entrance Flow of Herschel-Bulkley Fluids in a Duct", Fluid Dynamics Res. 6, 43-50 (1990)

Bhattacharyya, S. and Tiu, c., "Developing Pressure Profiles for Non-Newtonian Flow in an Annular Duct", AIChE. J. 20, No. 1, 154-158 (1974)

Bird, R.B. and Dai, G.C., "The rheology and flow of

viscoplastic materials", Reviews in Chem. Eng. I, 1-70 (1983).

Bodoia, J.R. and Osterle, J.F., "Finite Difference Analysis of Plane Poiseuille and Couette Flow Development", Appl. Sci. Res. 10, 265-276 (1961)

Bogue, D.C., "Entrance Effects and Prediction of Turbulence in Non-Newtonian Flow", Indus. Eng. Chem. 51, No. 7, 874-878 (1959)

Campbell, W.D. and Slattery, J.C., "Flow in the Entrance of a Tube", J. Basic Eng. 41-46 March (1963)

Carlson, G.A. and Hornbeck, R.W., "A Numerical Solution for Laminar Entrance Flow in a Square Duct", J. Appl. Mech. 25-30 March (1973)

Chen, S.S., Fan, L.T. and Hwang, C.L., "Entrance Region Flow of the Bingham Fluid in a Circular Pipe", AIChE. J. 16, No. 2, 293-299 March (1970)

Cho, H.W. and Hyun, J.M., "Numerical Solutions of Pulsating Flow and Heat Transfer Characteristics in a Pipe", Int. J. Heat and Fluid Flow, 11, No. 4, 321-330 Dec. (1990)

Collin, M. and Schowalter, W.R., "Behaviour of Non-Newtonian Fluids in the Entry Region of a Pipe", AIChE. J. 804-809 Nov. (1963)

Duggins, R.K., "The commencement of Flow of a Bingham Plastic Fluid", Chem. Eng. Sci. 27, 1991-1996 (1972)

Edwards, M.F., Nellist, D.A. and Wilkinson, W.L., "Unsteady,

Laminar Flows of Non-Newtonian Fluids in Pipes", Chem. Eng. Sci. 27, 296-306 (1972)

Edwards, M.F., Nellist, D.A. and Wilkinson, W.L., "Pulsating Flow of Non-Newtonian Fluids in Pipes", Chem. Eng. Sci. 27, 545-553 (1972)

Elkouh, A.F., "Approximate Solution for Pulsatile Laminar Flow in a Circular Rigid Tube", J. Fluids Eng. 100, 131-133 March (1978)

Fargie, D. and Martin, B.W., "Developing Laminar Flow in a Pipe of Circular Cross-Section", Proc. Roy. Soc. Lond. A. 321, 461-476 (1971)

Fordham, E.J., Bittleston, S.H. and Tehrani, M.A., "Viscoplastic Flow In Centered Annuli, Pipes, and Slots" Ind. Eng. Chem. Res. 1991,30, 517-524

Fredrickson, A.G. and Bird, R.B., "Non-Newtonian Flow in Annuli", Indus. Eng. Chem. 50, No. 3, 347-352 March (1958)

Gorla, R.S.R. and Madden, P.E., "A Variational Approach to Non-Steady Non-Newtonian Flow in a Circular Pipe", J. Non-Newtonian Fluid Mech. 16, 251-265 (1984)

Guckes, T.L., "Laminar Flow of Non-Newtonian Fluids in an Eccentric Annulus", J. Eng. Indus. ASME 498-506 May (1975)

Gupta, R.C., "Laminar Flow in the Entrance of a Tube", Appl. Sci. Res. 33, 1-10 February (1977)

Gupta, R.C., "Laminar Two-Dimensional Entrance Region Flow of

Power-Law Fluids II", Acta Mechanica 84, 209-215 (1990)

Gupta, R.C., "Laminar Two-Dimensional Entrance Region Flow of Power-Law Fluids", Acta Mechanica 67, 129-137 (1987)

Gupta, S.C. and Garg, V.K., "Developing Flow in a Concentric Annulus", Computer Methods in Appl. Mech. and Eng. 28, 27-35 (1981)

Giicuyener, H.I. and Mehmatoglu, T. "Flow of Yield-Pseudo-Plastic Fluids through a Concentric Annulus" AIChE Journal Vol. 38, No. 7, July (1992)

Haciislamoglu, M. and Langlinais, J., "Non-Newtonian Flow in Eccentric Annuli", 115-123 (1990)

Hanks, R.W., "The Axial Laminar low Of Yield-Pseudoplastic Fluids In a Concentric Annulus" Ind. Eng. Chem. Process Des. Dev., Vol. 18, No. 3, (1979)

Hanks, R.W. and Larsen, K.M., "The Flow of Power-Law Non-Newtonian Fluids in Concentric Annuli", Ind. Eng. Chem. Fundam. 18, No. 1, 33-35 (1979)

Hornbeck, R.W, "Laminar Flow in the Entrance Region of a Pipe", Appl. Sci. Res. Section A, 13, 224-232 (1964)

Iyoho, A.W. and Azar, J.J., "An Accurate Slot-low Model for Non-Newtonian Fluid Flow Through Eccentric Annuli" Society of Petroleum Engineers Journal V. 21, 1981 565-572

Kajiuchi, T. and Saito, A., "Flow Enhancement of laminar Pulsating Flow of Bingham Plastic Fluids", J. Chem. Eng.

Japan, 17, No. 1, 34-38 (1984)

Lin, T. and Shah, V.L., "Numerical solution of heat transfer to yield power-law fluids flowing in the entrance region", Proc. VI Intern. Heat Transfer Conf. 5, 317- 322 (1978)

Liu, J. and Shah, V.L., "Numerical Solution of a Casson Fluid Flow in the Entrance Region of Annular Tubes", Appl. Sci. Res. 31, 213-221 Oct. (1975)

Lundgren, T.S., Sparrow, E.M. and Starr, J.B., "Pressure Drop Due to the Entrance Region in Ducts of Arbitrary Cross Section", J. Basic Eng. 620- 626 Sep. (1964)

Luo, Y. and Peden, J.M., "Flow of Non-Newtonian Fluids through Eccentric Annuli", SPE Produc. Eng. 91-91 Feb. (1990)

Ly, D.P. and Bellet, D., "The Study of Time-dependent Pipe Flows of Inelastic Non-Newtonian Fluids Using a Multiviscous Approximation", J. Non-Newtonian Fluid Mech. 1, 287-304 (1976)

Masliyah, J.H. and Shook, C.A., "Laminar Transient Flow in Pipes", Canadian J. Chem. Eng. 53, 469-475 Oct. (1975)

Matras, Z. and Nowak, Z., "Laminar Entry Length Problem for Power-Law Fluids", Acta Mechanica 48, 81-90 (1983)

McEachern, D.W., "Axial Laminar Flow of a Non-Newtonian Fluid in an Annulus," AICHE J., 12, 328 (1966)

Mckillop, A.A., Harper, J.C., Bader, H.J. and Korayem, A.y., "Variable Viscosity Entrance Region Flow of Non-Newtonian Liquids", Int. J. Heat Mass Transfer Vol. 13, 901-909 (1970)

Mehrotra, A.K. and Patience G.S., "Unified Entry Length for Newtonian and Power-Law Fluids in Laminar Pipe Flow", The Canadian J. Chem. Eng. 68, 529-533 Aug. (1990)

Mishra. P. and Mishra, I. "Flow Behaviour of Power-Law Fluids in an Annulus", AIChE. J. 22, No. 3, 617-619 May (1976)

Mishra, I.M. and Mishra, P., "Linearized Approach for Predicting Loss Coefficients in Entrance Region Flows of Purely Viscous Non-Newtonian Fluids in an Annular Duct", Chem. Eng. J. 14, 41-47 (1977)

Mishra, I.M., Kumar, S. and Mishra, P., "Entrance Region Flow of Bingham Plastic Fluids in Concentric Annulus", Indian J. Tech. 23, 81-87 March (1985)

Mitsuishi, N. and Aoyagi, Y., "Non-Newtonian Fluid Flow in an Eccentric Annulus", J. Chem. Eng. Japan 6, No. 5, 402-408 (1973)

Nakamura, M. and Sawada, T., "Numerical Study on the Unsteady Flow of Non-Newtonian Fluid", J. Biomech. Eng. 112, 100-103 Feb. (1990)

Nakamura, M. and Sawada, T., "An Experiment on the Pulsatile Flow of Bingham Plastic Fluids in a High Reynolds Number Region", JSME Inter. J. series II, 33, No. 1, 56-62 (1990)

Nakamura, M. and Sawada, T., "Numerical Study on the Laminar Pulsatile Flow of Slurries", J. Non-Newtonian Fluid Mech. 22, 191-206 (1987)

Nowak, Z. and Gajdeczko, B., "Laminar Entrance Region Flow of the Bingham Fluid", Acta Mechanica 49, 191-200 (1983)

Otis, D.R., "Laminar Start-Up Flow in a Pipe", J. Appl. Mech. 52, 706-711 Sep. (1985)

Patankar, S.V. and Spalding, D.B., "Heat and Mass Transfer in Boundary Layers", Intertext Book, 2nd Ed., London, (1970)

Patankar, S.V., "Numerical Heat Transfer and Fluid Flow", McGRAW-HILL Book (1980) Patience, G.S. and Mehrotra, A.K., "Laminar Start-Up Flow in Short Pipe Lengths", Canadian J. Chem. Eng. 67, 883-888 Dec. (1989)

Patience, G.S. and Mehrotra, A.K., "Laminar Start-Up Flow In a Pipe", J. Appl. Mech. 54, 243-244 March (1987)

Phan-Thien, N. and Dudek, J., "Pulsating Flow of a Plastic Fluid", Nature, 296, 843-844 April (1982)

Phan-Thien, N. and Dudek, J., "Pulsating Flow Revisited", J. Non-Newtonian Fluid Mech. 11, 147-161 (1982)

Redberger, P.J. and Charles, M.E., Axial Laminar Flow in a Circular Pipe Containing a Fixed Eccentric Core", Canadian J. Chem. Eng. 148-151 August (1962)

Rotem, Z., "Non-Newtonian Flow in Annuli," J. Appl. Mech., 29, 421 (1962)

Round, G.F., "Pulsed Slurry Flow in Pipelines", 1, 307-318 (1981)

Round, G.F. and Ei-Sayed, E., "Pulsating Flows of Solid/Liquid Suspensions. I. Bentonite-Clay/Water Suspensions", J. Pipelines, 5, 95-106 (1985)

Round, G.F. and Ei-Sayed, E., "Pulsating Flows of Solid/Liquid Suspensions. II. Coal/Water Slurries", J. Pipelines, 6, 105-116 (1987)

Schlichting, H. "Boundary-Layer Theory" McGraw-Hill Publishing Company, (1980)

Scott, P.S., Mirza, F. and Vlachopoulos, J. "Finite Element Simulation of Laminar Viscoplastic Flows With Regions of Recirculation" J. Rheology, 32(4) 387-400 (1988)

Shah, V.L. and Farnia, K., "Flow in the Entrance of Annular Tubes", Computers and Fluids, 2, 285-294 (1974)

Shah, V.L. and Soto, R., "Non-newtonian Blood Flow in the Entrance Region of a Tube", Computers and Fluids, 2, 273-284 (1974)

Shah, V.L. and Soto, R.J., "Entrance Flow of a Bingham Fluid in a Tube", Appl. Sci. Res. 30, 271-278 Feb. (1975)

Snyder, W.T. and Goldstein, G.A., "An Analysis of Fully Developed Laminar Flow in an Eccentric Annulus",AIChE. J. 11, No.3, 462-467 May (1965)

Soto, R.J and Shah, V.L., "Entrance Flow of a Yield-Power Law Fluids", Appl. Sci. Res. 32, 73-85 March (1976)

Sparrow, E.M. and Lin, S.H., "The Developing Laminar Flow and

Pressure Drop in the Entrance Region of Annular Ducts", J. Basic Eng. 827-834 Dec. (1964)

Tan, K.L. and Tiu, C., "Entry Flow Behaviour of Viscoelastic Fluids in an Annulus", J. Non-Newtonian Fluid Mech 3, 25-40 (1977/1978)

Tiu, C. and Bhattacharyya, S., "Flow Behaviour of Power-Law Fluids in the Entrance Region of Annuli", Canadian J. Chem. Eng. 51, 47-54 Feb. (1973)

Tosun, I., "Axial Laminar Flow in an Eccentric Annulus: an Approximate Solution", AIChE. J. 30, No. 5, 877-878 Sep. (1984)

Uner, D., Ozgen, C. and Tosun, I., "An Approximate Solution for Non-Newtonian Flow in Eccentric Annuli", Ind. Eng. Chem. Res. 27, 698-701 (1988)

Walton, I.C. and Bittleston, S.H., "The Axial Flow of a Bingham Plastic in a Narrow Eccentric Annulus", J. Fluid Mech. 222, 39-60 (1991)

APPENDIX A

TRANSFORMATION OF THE EQUATION OF MOTION TO BIPOLAR COORDINATES

The dimensionless equation of motion of generalized Bingham fluids in Cartesian coordinates is:

$$\frac{\partial U}{\partial T}=\frac{1}{2}fRe+\frac{\partial}{\partial X}(\tilde{\mu}\frac{\partial U}{\partial X})+\frac{\partial}{\partial Y}(\tilde{\mu}\frac{\partial U}{\partial Y}) \qquad \text{A.1}$$

where the dimensionless viscosity may be written as:

$$\tilde{\mu}=\frac{Pl}{[(\frac{\partial U}{\partial X})^2+(\frac{\partial U}{\partial Y})^2]^{1/2}}+[(\frac{\partial U}{\partial X})^2+(\frac{\partial U}{\partial Y})^2]^{\frac{n-1}{2}} \qquad \text{A.2}$$

The transformation from Cartesian coordinates to bipolar

coordinates are given by (Guckes, 1975):

$$X=\frac{a\sinh(\xi)}{\cosh(\xi)-\cos(\eta)} \qquad \text{A.3}$$

$$Y=\frac{-a\sin(\eta)}{\cosh(\xi)-\cos(\eta)} \qquad \text{A.4}$$

$$Z = \zeta \qquad \text{A.5}$$

where $$a = R_i \sinh\xi_i = R_o \sinh \xi_o \qquad \text{A.6}$$

Taking the derivatives of equations A.3 and A.4 we can get:

$$\frac{\partial X}{\partial \xi}=\frac{a(1-\cosh(\xi)\cos(\eta))}{(\cosh(\xi)-\cos(\eta))^2} \qquad \text{A.7}$$

$$\frac{\partial X}{\partial \eta}=-\frac{a\sinh(\xi)\sin(\eta)}{(\cosh(\xi)-\cos(\eta))^2} \qquad \text{A.8}$$

$$\frac{\partial Y}{\partial \xi}=\frac{a\sinh(\xi)\sin(\eta)}{(\cosh(\xi)-\cos(\eta))^2} \qquad \text{A.9}$$

$$\frac{\partial Y}{\partial \eta}=\frac{a(1-\cosh(\xi)\cos(\eta))}{(\cosh(\xi)-\cos(\eta))^2} \qquad \text{A.10}$$

It can be found:

$$\frac{\partial X}{\partial \xi}=\frac{\partial Y}{\partial \eta} \qquad \text{A.11}$$

$$\frac{\partial X}{\partial \eta}=-\frac{\partial Y}{\partial \xi} \qquad \text{A.12}$$

and

$$\frac{\partial^2 X}{\partial \xi^2}+\frac{\partial^2 X}{\partial \eta^2}=0 \qquad \text{A.13}$$

$$\frac{\partial^2 Y}{\partial \xi^2}+\frac{\partial^2 Y}{\partial \eta^2}=0 \qquad \text{A.14}$$

$$\left(\frac{\partial X}{\partial \xi}\right)^2+\left(\frac{\partial X}{\partial \eta}\right)^2=\frac{a^2}{(\cosh(\xi)-\cos(\eta))^2} \qquad \text{A.15}$$

$$\left(\frac{\partial X}{\partial \xi}\right)^2+\left(\frac{\partial Y}{\partial \eta}\right)^2=\frac{a^2}{(\cosh(\xi)-\cos(\eta))^2} \qquad \text{A.16}$$

$$\frac{\partial^2 U}{\partial X^2}+\frac{\partial^2 U}{\partial Y^2}=\frac{(\cosh(\xi)-\cos(\eta))^2}{a^2}\left[\frac{\partial^2 U}{\partial \xi^2}+\frac{\partial^2 U}{\partial \eta^2}\right] \qquad \text{A.17}$$

$$\frac{\partial \tilde{\mu}}{\partial X}\frac{\partial U}{\partial X}+\frac{\partial \tilde{\mu}}{\partial Y}\frac{\partial U}{\partial Y}=\frac{(\cosh(\xi)-\cos(\eta))^2}{a^2}\left[\frac{\partial \tilde{\mu}}{\partial \xi}\frac{\partial U}{\partial \xi}+\frac{\partial \tilde{\mu}}{\partial \eta}\frac{\partial U}{\partial \eta}\right] \qquad \text{A.18}$$

Substituting equations A.7, to A.18, we can get the dimensionless equation of motion of generalized Bingham fluids in bipolar coordinates:

$$\left(\frac{a}{\psi}\right)^2\frac{\partial U}{\partial T}=\frac{1}{2}fRe\left(\frac{a}{\psi}\right)^2+\frac{\partial}{\partial \xi}\left(\tilde{\mu}\frac{\partial U}{\partial \xi}\right)+\frac{\partial}{\partial \eta}\left(\tilde{\mu}\frac{\partial U}{\partial \eta}\right) \qquad \text{A.19}$$

for $\qquad 0 \le \eta \le \pi \quad$ and $\quad \xi_i \le \xi \le \xi_o$

where

$$\tilde{\mu}=\frac{Pl}{\frac{\Psi}{a}\left[\left(\frac{\partial U}{\partial \xi}\right)^2+\left(\frac{\partial U}{\partial \eta}\right)^2\right]}+\left(\frac{\Psi}{a}\right)^{n-1}\left[\left(\frac{\partial U}{\partial \xi}\right)^2+\left(\frac{\partial U}{\partial \eta}\right)^2\right]^{\frac{n-1}{2}} \qquad \text{A.20}$$

and

$$\Psi=\cosh(\xi)-\cos(\eta) \qquad \text{A.21}$$

APPENAIX B

COMPUTER PROGRAM FOR GENERALIZED BINGHAM FLUIDS FULLY DEVELOPED FLOW IN CONCENTRIC ANNULI

```
C       THIS PROGRAM CALCULATES THE VELOCITY PROFILE OF FULLY
C       DEVELOPED FLOW OF GENERALIZED BINGHAM FLUIDS IN ANNULI.
C       IT ALSO DETERMINDS THE BOUNDARY RADII OF UNSHEARED PLUG.

        DIMENSION V(401),V1(401)
        OPEN(UNIT=6,FILE='ANL.DAT')
        WRITE(*,*)' INPUT  EN, R1, R2, PL, RE,N'
        READ(*,*)EN,R1,R2,PL,RE,N
        WRITE(6,11)EN,R1,R2,PL,RE,N
 11     FORMAT(10X,'EN=',F5.3,3X,'RI=',F5.3,3X,'RO=',
     + F5.3,3X,//,10X,'PL=',F5.2,3X, 'RE=',F7.2,3X,'N=',I2//)

C       EN.........FLOW INDIX
C       R1, R2....INNER AND OUTER RADII OF THE ANNULUS
C       PL.........GENERALIZED BINGHAM NUMBER
C       RE.........REYNOLDS NUMBER
C       N..........NUMBER OF GRID
C       F1.........FRICTION FACTOR
C       RN1,RQ1...INNER AND OUTER BOUNDARY RADII OF UNSHEARED
C       PLUG
C       V..........VELOCITY

        NQ=0
        RI=2*R1/(R2-R1)
        RO=2*R2/(R2-R1)
        RN=0.0
        A=0.01
        B=0.102
        EPS=0.0000001
        N1=1
        XX=1.0E10
        YY=1.0E10
        XA=A
        XB=B
        CALL TT(NQ,XA,EN,RI,RO,RT,PL,RE,RN,RQ)
        CALL TV1(XA,EN,RI,RO,RT,PL,RE,RN,RQ,FA)
```

```
      YA=FA
      CALL TT(NQ,XB,EN,RI,RO,RT,PL,RE,RN,RQ)
      CALL TV1(XB,EN,RI,RO,RT,PL,RE,RN,RQ,FB)
      YB=FB
30    XC=XA-YA*(XA-XB)/(YA-YB)
      CALL TT(NQ,XC,EN,RI,RO,RT,PL,RE,RN,RQ)
      CALL TV1(XC,EN,RI,RO,RT,PL,RE,RN,RQ,FC)
      YC=FC
      IF(YA*YC.GT.0.0)THEN
      XA=XC
      YA=YC
      ELSE
      XB=XC
      YB=YC
      END IF
      DX=ABS(XC-XX)
      DY=ABS(YC-YY)
      IF(DX.LT.EPS.AND.DY.LT.EPS)GO TO 50
      XX=XC
      YY=YC
      GO TO 30
50    F1=XC
      FRE=F1*RE
      T0=8*PL/(F1*RE)
      WRITE(6,71)RI,RO,RN,RQ
71    FORMAT(10X,'RI=',F5.3,3X,'RO=',F5.3,3X,
     + 'RN=',F5.3,3X,'RQ=',F5.3//)
      WRITE(6,72)RN1,RQ1,F1
72    FORMAT(10X,'RN1=',F5.3,3X,'RQ1=',F5.3,3X'f=',f7.4//)
      WRITE(6,73)SLMDA,T0,FRE
73    FORMAT(10X,'LMDA=',F5.3,3X,'T0=',F5.3,
     + 3X,'f*Re=',F10.5,//)
      NQ=1
      DER=(RO-RI)/(N-1)
      V(1)=0.0
      V(N)=0.0
      DO 100 I=1,N-2
      RR=RI+I*DER
      IF(RR.GE.RQ.OR.RR.LE.RN)CALL UU(EN,F1,RR,RI,RO,RT,PL,
     + RE,RN,RQ,U)
      IF(RR.GT.RN.AND.RR.LT.RQ)CALL UU(EN,F1,RQ,RI,RO,RT,PL,
     + RE,RN,RQ,U)
      V(I+1)=U
      V1(I+1)=-F1*RE/128.0*(RR*RR-RO*RO
     + -(RO*RO-RI*RI)*LOG(RR/RO)/ LOG(RO/RI))
100   CONTINUE
      DO 111 I=1,N
      RR=R1+((R2-R1)/(N-1))*(I-1)
      WRITE(6,76)I,RR,I,V(I),I,V1(I)
76    FORMAT(10X,'RR(',I2,')=',F5.3,3X,'V(',I2,')=',F8.4,3X,
     + 'V1(',I2,')=',F8.4/)
111   CONTINUE
```

```
      STOP
      END

      SUBROUTINE UU(EN,X,RR,RI,RO,RT,PL,RE,RN,RQ,U)
      F1(R)=ABS(A1+B1/R+C1*R)**(1/EN)
      F2(R)=ABS(A2+B2/R+C2*R)**(1/EN)
      A1=-PL/(X*RE)/(4**EN)
      A2=-A1
      C1=-1.0/4**(EN+2)
      C2=C1
      B1=RN*RN/4**(EN+2)+PL*RN/(X*RE)/(4**EN)
      B2=RQ*RQ/4**(EN+2)-PL*RQ/(X*RE)/(4**EN)
      EPS=0.000001
      N=1
      P=1.0E10
      IF(RR.GE.RQ) GO TO 201
      T1=(F1(RI)+F1(RR))/2
100   H1=(RR-RI)/N
      S1=T1
      DO 200 K=0,N-1
      S1=S1+F1(RI+K*H1)
200   CONTINUE
      IF(ABS(P-S1).LT.EPS) GO TO 500
      P=S1
      N=N+N
      IF(N.GT.10000) GO TO 500
      GO TO 100
201   T2=(F2(RO)+F2(RR))/2
300   H2=(RO-RR)/N
      S2=T2
      DO 400 K=0,N-1
      S2=S2+F2(RR+K*H2)
400   CONTINUE
      S1=S2
      H1=H2
      IF(ABS(P-S1).LT.EPS) GO TO 500
      P=S1
      N=N+N
      IF(N.GT.10000)GO TO 500
      GO TO 300
500   U=(X*RE)**(1/EN)*S1*H1
      RETURN
      END

      SUBROUTINE TV(NQ,RR,EN,X,RI,RO,RT,PL,RE,RN,V)
      F1(R)=ABS(A1+B1/R+C1*R)**(1/EN)
      F2(R)=ABS(A2+B2/R+C2*R)**(1/EN)
      RQ=RN+8*PL/X/RE
      IF(RQ.GE.RO)RQ=RO-0.1*RO
      IF(RN.LE.RI)RN=RI+0.1*RI
      IF(NQ.EQ.0)RR=RN
      A1=-PL/(X*RE)/(4**EN)
```

```
      A2=-A1
      C1=-1.0/4**(EN+2)
      C2=C1
      B1=RN*RN/4**(EN+2)+PL*RN/(X*RE)/(4**EN)
      B2=RQ*RQ/4**(EN+2)-PL*RQ/(X*RE)/(4**EN)
      EPS=0.000001
      N=1
      P=1.0E10
      T1=(F1(RR)+F1(RI))/2
      T2=(F2(RO)+F2(RQ))/2
100   H1=(RR-RI)/N
      H2=(RO-RQ)/N
      S1=T1
      S2=T2
      DO 200 K=0,N-1
      S1=S1+F1(RI+K*H1)
      S2=S2+F2(RQ+K*H2)
200   CONTINUE
      F=S1*H1+S2*H2
      IF (ABS(P-F).LT.EPS) GO TO 500
      P=F
      N=N+N
      IF(N.GT.10000)GO TO 500
      GO TO 100
500   IF(EN.EQ.1)EE=1.0
      V=ABS(X*RE)**(1/EN)*(S2*H2-S1*H1)
      V1=ABS(X*RE)**(1/EN)*S1*H1
      V2=ABS(X*RE)**(1/EN)*S2*H2
      IF(NQ.EQ.1)V=V1
      RETURN
      END

      SUBROUTINE TT(NQ,X,EN,RI,RO,RT,PL,RE,RN,RQ)
      IF(RN.LE.RI)XA=RI
      IF(RN.GT.RI)XA=RN
      XB=RI+(RO-RI)/2
      RR=0.0
      EPS=0.000001
      XX=1.0E10
      YY=1.0E10
      CALL TV(NQ,RR,EN,X,RI,RO,RT,PL,RE,XA,FFA)
      YA=FFA
      IF(YA.EQ.0.0) GO TO 53
      CALL TV(NQ,RR,EN,X,RI,RO,RT,PL,RE,XB,FFB)
      YB=FFB
      IF(YB.EQ.0.0) GO TO 55
30    XC=XA-YA*(XA-XB)/(YA-YB)
      CALL TV(NQ,RR,EN,X,RI,RO,RT,PL,RE,XC,FFC)
      YC=FFC
      IF(YA*YC.GT.0.0) THEN
      XA=XC
      YA=YC
```

```
      ELSE
      XB=XC
      YB=YC
      END IF
      DX=ABS(XC-XX)
      DY=ABS(YC-YY)
      IF(DX.LT.EPS.AND.DY.LT.EPS) GO TO 50
      XX=XC
      YY=YC
      GO TO 30
53    XC=XA
      GO TO 50
55    XC=XB
50    RN=XC
      RQ=8*PL/(X*RE)+RN
      RETURN
      END

      SUBROUTINE TV1(X,EN,RI,RO,RT,PL,RE,RN,RQ,Q)
      F(R)=(R*R*ABS(A1+B1/R+C1*R)**(1/EN))
      D(R)=(R*R*ABS(A2+B2/R+C2*R)**(1/EN))
      A1=-PL/(X*RE)/(4**EN)
      A2=-A1
      B1=RN*RN/4**(EN+2)+PL*RN/(X*RE)/(4**EN)
      B2=RQ*RQ/4**(EN+2)-PL*RQ/(X*RE)/(4**EN)
      C1=-1./4**(EN+2)
      C2=C1
      EPS=0.000001
      N=1
      P=1.0E10
      T1=(F(RN)+F(RI))/2.0
      T2=(D(RO)+D(RQ))/2.0
100   H1=(RN-RI)/N
      H2=(RO-RQ)/N
      S1=T1
      S2=T2
      DO 200 K=0,N-1
      S1=S1+F(RI+K*H1)
      S2=S2+D(RQ+K*H2)
200   CONTINUE
      FF=-S1*H1+S2*H2
      IF(ABS(P-FF).LT.EPS) GO TO 500
      P=FF
      N=N+N
      IF(N.GT.10000)GO TO 500
      GO TO 100
500   CONTINUE
      Q=-(RO*RO-RI*RI)/(ABS(X*RE)**(1/EN))-S1*H1+S2*H2
      Q1=(S2*H2-S1*H1)*(ABS(X*RE)**(1/EN))
      RETURN
      END
```

APPENDIX C

COMPUTER PROGRAM FOR GENERALIZED BINGHAM FLUIDS DEVELOPING FLOW IN CONCENTRIC ANNULI

```
C     THIS PROGRAM CALCULATES THE VELOCITY AND PRESSURE PROFILES
C     OF DEVELOPING FLOW OF GENERALIZED BINGHAM FLUIDS IN ANNULI

      DIMENSION U(151),V(151),U0(151),V0(151),D(151),RR(151),
     + P(150,151),B1(150)
      OPEN(UNIT=6,FILE='ANL1.DAT',STATUS='NEW')
      OPEN(UNIT=7,FILE='ANL2.DAT',STATUS='NEW')
      WRITE(*,*)' INPUT RN,PL,EN'
      READ(5,*)RN,PL,EN
      WRITE(6,77)RN,PL,EN
77    FORMAT(/////,35X,'USING FINITE DIFFERENCE METHOD TO
     + CALCULATE',//,30X,'DEVELOPING FLOW OF NON-NEWTONIAN
     + FLUIDS IN A PIPE',/////,40X,'REYNOLDS NUMBER=',F6.0,//,
     + 40X,'PLASTICITY NUMBER=',F4.0,//,
     + 40X,'NON-NEWTONIAN INDEX=',F4.1,//)
      WRITE(*,*)'INPUT DELX,DELR,IW,IR,XMAX,NR,W,R1,R2,F1'
      READ(5,*) DELX,DELR,IW,IR,XMAX,NR,W,R1,R2,F1
      DELR=(R1-R2)/(NR-1)
      WRITE(6,78)DELX,DELR,IW,IR,XMAX,NR
78    FORMAT(20X,'DELX=',F6.5,5X,'DELR=',F5.4,5X,
     +  'IW=',I4,5X,'IR=',I2
     + ,5X,'XMAX=',F3.2,5X,'NR=',I4,//)
      WRITE(*,*)'INPUT RP,RQ'
      READ(5,*)RP,RQ
      WRITE(6,79)RP,RQ,R1,R2
79    FORMAT(20X,'RP=',F5.3,5X,'RQ=',F5.3,5X,'R1=',F5.3,5X,
     + 'R2=',F5.3,//)

C     EN.........FLOW INDIX
C     R1, R2....INNER AND OUTER RADII OF THE ANNULUS
C     PL.........GENERALIZED BINGHAM NUMBER
C     RE.........REYNOLDS NUMBER
C     N..........NUMBER OF GRID
C     F1.........FRICTION FACTOR
C     RN1,RQ1...INNER AND OUTER BOUNDARY RADII OF UNSHEARED
C     PLUG
C     V..........VELOCITY
```

```
      DO 50 I=1,NR,IR
50    RR(I)=R1-(I-1)*DELR
      WRITE(6,2)(RR(I),I=1,NR,IR)
2     FORMAT(///,35X,'VELOCITY PROFILE OF DEVELOPING FLOW',
     + ////,15X,11(5X,'R=',F3.1),/,10(5X,'R=',
     +  F3.1),/,10(5X,'R=',F3.1)
     +  ,/,10(5X,'R=',F3.1),/,11(5X,'R=',F3.1),//)
      RATIO=8*PL/RN/F1
      DO 100 I=1, NR
      U0(I)=NR/(NR-2)
      V0(I)=0.0
      U(I)=0.0
      V(I)=0.0
      D(I)=0.0
100   CONTINUE
      U0(1)=0.0
      U0(NR)=0.0
      P0=0.0
      J=0
      MC=0
      X=0.0
      UT=20.0
      IM=0
300   J=J+1
      MC=MC+1
      X=J*DELX
      IF(IM.EQ.1) GO TO 900
      IF(X.GT.XMAX) GO TO 900
      CALL DEVL1(F1,RN,PL,P0,EN,NR,RP,RQ,DELR,DELX,
     + D,E,U0,V0,U,V,RATIO,P1,IM,W,R1)
      P0=P1
      UM=0.0
      DO 400 I=1,NR
      U0(I)=U(I)
      V0(I)=V(I)
      IF(U(I).GT.UM)UM=U(I)
400   CONTINUE
      IF(MC.NE.IW) GO TO 300
      MC=0
      WRITE(6,3)X,P0,(U(I),I=1,NR,IR)
3     FORMAT(3X,'X=',F8.4,5X,'P1=',F8.4,/,8X,
     +  'U(R)=',5X,10(F8.4,2X),/
     +  ,10(F8.4,2X),/,10(F8.4,2X),/,11(F8.4,2X),//)
      UT=U(NR)
      U1=0.0
      GO TO 300
900   STOP
      END

      SUBROUTINE DEVL1(F1,RN,PL,P0,EN,NR,RP,RQ,DELR,DELX,
     + D,E,U0,V0,U,V,RATIO,P1,IM,W,R1)
      DIMENSION U0(151),V0(151),U(151),V(151),D(151),
```

```
     + W1(151),W2(151),P(150,151),B1(150),R(151),U1(151),V1(151),
     +  U11(101)
        DO 5 I=1,NR-1
        DO 5 J=1,NR
        P(I,J)=0.0
5       CONTINUE
        PP=0.0
        IF(PL.EQ.0.0)RATIO=0.0
        IF(PL.NE.0.0)RATIO=8*PL/(RN*F1)
        DO 30 I=1,NR
        R(I)=R1-(I-1)*DELR
        IF(ABS(RP-R(I)).LE.(0.5*DELR))I1=I
        IF(ABS(RQ-R(I)).LE.(0.5*DELR))I2=I
        PP=PP+U0(I)*R(I)
30      CONTINUE
        IF(RP.EQ.RQ)I2=I1
        U(1)=0.0
        V(1)=0.0
        U(NR)=0.0
        V(NR)=0.0
        DO 11 I=1,NR
        U1(I)=U0(I)
        V1(I)=V0(I)
11      CONTINUE
17      D(1)=(U1(1)-U1(2))/DELR
        D(NR)=(U1(NR-1)-U1(NR))/DELR
10      DO 20 I=2,NR-1
        D(I)=(U1(I-1)-U1(I+1))/(2*DELR)
20      CONTINUE
        DO 21 I=1,NR
        IF(EN.EQ.1.0) GO TO 12
        IF(EN.NE.1.0.AND.D(I).EQ.0.0) GO TO 14
        IF(EN.NE.1.0.AND.D(I).NE.0.0) GO TO 18
12      W1(I)=4.0
        W2(I)=4.0
        GO TO 21
14      W1(I)=0.0
        W2(I)=0.0
        GO TO 21
18      W1(I)=4**EN*ABS(D(I))**(EN-1)
        W2(I)=4**EN*ABS(D(I))**(EN-1)*(1+(EN-1))
21      CONTINUE
29      RR=0.0
        DO 33 I=I1,I2
        RR=RR+R(I)
33      CONTINUE
        I0=I2-I1
        II=NR-I2
        NI=NR
        I3=NR
        IF(PL.EQ.0.0) GO TO 44
        DO 40 I=1,I1-1
```

```
      P(1,I)=R(I+1)
      P(I+1,I)=U1(I+1)/DELX+2*W2(I+1)/(DELR*DELR)
      IF(I+2.LT.I1+1)P(I+2,I)=-W1(I+2)/(2*DELR*R(I+2))
     +  +V1(I+2)/(2*DELR)-
     +  W2(I+2)/(DELR*DELR)
      P(I+1,I+1)=-V1(I+1)/(2*DELR)+W1(I+1)/(2*DELR*R(I+1))-
     + W2(I+1)/(DELR*DELR)
      P(I+1,I3-1)=1/DELX
      P(I+1,I3)=P0/DELX+U1(I+1)*U0(I+1)/DELX-PL/R(I+1)
40    CONTINUE
      P(1,I3)=PP
      DO 41 I=I1,I2-1
      P(1,I)=R(I+1)
      P(I+1,I-1)=1
      P(I+1,I)=-1
41    CONTINUE
      DO 43 I=I2,I3-2
      P(1,I)=R(I+1)
      IF(I+1.LE.I3-1)P(I+1,I-1)=-W1(I+1)/(2*DELR*R(I+1))+
     +  V1(I+1)/(2*DELR)-W2(I+1)/(DELR*DELR)
      IF(I+1.LE.I3-1)P(I+1,I)=U1(I+1)/DELX+2*W2(I+1)/(DELR*DELR)
      IF(I+1.LE.I3-2)P(I+1,I+1)=-V1(I+1)/(2*DELR)+W1(I+1)/
     +  (2*DELR*R(I+1))-W2(I+1)/(DELR*DELR)
      IF(I+1.LE.I3-1)P(I+1,I3-1)=1/DELX
      IF(I+1.LE.I3-1)P(I+1,I3)=P0/DELX+U1(I+1)*U0(I+1)/DELX
     +  +PL/R(I+1)
43    CONTINUE
      GO TO 49
44    DO 45 I=1,I3-2
      P(1,I)=R(I+1)
      P(I+1,I)=U1(I+1)/DELX+2*W2(I+1)/(DELR*DELR)
      P(I+1,I+1)=-V1(I+1)/(2*DELR)+W1(I+1)/(2*DELR*R(I+1))-
     +  W2(I+1)/(DELR*DELR)
      P(I+1,I3-1)=1/DELX
      P(I+1,I3)=P0/DELX+U1(I+1)*U0(I+1)/DELX-PL/R(I+1)
45    CONTINUE
      P(1,I3)=PP
49    CALL SLN2(I3-1,P,B1)
      DU=0.0
      DO 50 I=2,I3-1
      U(I)=B1(I-1)
      DU1=ABS(U(I)-U0(I))
      IF(DU.LT.DU1)DU=DU1
50    CONTINUE
      P1=B1(I3-1)
      PP1=0.0
      SS=0.0
      DO 69 I=1,NR+1
      DO 69 J=1,NR+1
      P(I,J)=0.0
69    CONTINUE
      I4=NR-3-I0
```

```
      DO 70 I=1,I1-2
     IF(I+2.LT.I1)P(I,I+1)=-1.0
     IF(I+2.LT.I1)P(I+1,I)=1.0
     IF(I+2.LE.I1)P(I,I)=2*DELR/R(I+1)
     P(I,I4+1)=DELR*(U0(I+1)-U(I+1))/DELX
 70  CONTINUE
     DO 71 I=I1-1,I4
     P(I,I)=2*DELR/R(I+1+I0)
     P(I,I+1)=-1.0
     P(I+1,I)=1.0
     P(I,I4+1)=DELR*(U0(I+1+I0)-U(I+1+I0))/DELX
 71  CONTINUE
     CALL SLN2(I4,P,B1)
     DO 77 I=2,I1-1
     V(I)=B1(I-1)
 77  CONTINUE
     DO 78 I=I1,I2
     V(I)=0.0
 78  CONTINUE
     DO 79 I=I1-1,I4
     V(I+II+2)=B1(I)
 79  CONTINUE
1001 RETURN
     END


     SUBROUTINE SLN2(N,A,X)
     DIMENSION A(150,151),X(151)
     DO 111 K=1,N
     S=0.0
     DO 222 I=K,N
     IF(ABS(A(I,K)).GT.ABS(S)) THEN
     S=A(I,K)
     I0=I
     ENDIF
 222 CONTINUE
     IF(I0.EQ.K) GO TO 888
     DO 777 J=K,N+1
     T=A(K,J)
     A(K,J)=A(I0,J)
     A(I0,J)=T
 777 CONTINUE
 888 S=1/S
     DO 100 J=K+1,N+1
     A(K,J)=A(K,J)*S
 100 CONTINUE
     DO 333 I=K+1,N
     DO 333 J=K+1,N+1
     A(I,J)=A(I,J)-A(I,K)*A(K,J)
 333 CONTINUE
 111 CONTINUE
     DO 555 K=N,1,-1
```

```
      C=A(K,N+1)
      DO 444 J=K+1,N
      C=C-A(K,J)*X(J)
  444 CONTINUE
      X(K)=C
  555 CONTINUE
      RETURN
      END
```

APPENDIX D

COMPUTER PROGRAM FOR GENERALIZED BINGHAM FLUIDS

UNSTEADY FLOW IN CONCENTRIC ANNULI

```
C       PROGRAM PULSATING FLOW OF NON-NEWTONIAN FLUIDS
        DIMENSION U(141),U0(141),D(141),RR(141)
        OPEN(UNIT=6,FILE='UANL.DAT')
        OPEN(UNIT=8,FILE='U0.DAT')
        WRITE(*,*)'INPUT RN,PL,EN,F1'
        READ(5,*)RN,PL,EN,F1
        WRITE(6,*)RN,PL,EN,F1
77      FORMAT(/////,35X,'USING FINITE  DIFFERENCE
     +  METHOD  TO  CALCULATE',
     +  //,30X,'PULSATING  FLOW  OF  NON-NEWTONIAN
     +  FLUIDS  IN  ANNULI',
     +  /////,40X,'REYNOLDS NUMBER=',F6.0,//,
     +  40X,'PLASTICITY NUMBER=',F4.0,//,
     +  40X,'NON-NEWTONIAN INDEX=',F4.1,//,
     +  40X,'FRICTION FACTOR=',F8.5,//)
        WRITE(*,*)'INPUT R1,R2,RP,RQ'
        READ(5,*)R1,R2,RP,RQ
        WRITE(*,*)R1,R2,RP,RQ
        WRITE(*,*)'INPUT DELT,IW,IR,TMAX,NR,W,NCO,AMP,OM,XI'
        READ(5,*) DELT,IW,IR,TMAX,NR,W,NCO,AMP,OM,XI
        DELR=(R1-R2)/(NR-1)
        WRITE(6,*)DELT,DELR,IW,IR,TMAX,NR,NCO,AMP,OM,XI
78      FORMAT(20X,'DELT=',F6.5,5X,'DELR=',F7.5,5X,
     +  'IW=',I4,5X,'IR=',I2,/
     +  ,5X,'TMAX=',F5.3,5X,'NR=',I3,3X,'NCO=',I2,
     +  'AMP=',F5.3,'OM=',F5.3,'XI=',F5.3//)

C       EN.........FLOW INDIX
C       R2, R1....INNER AND OUTER RADII OF THE ANNULUS
C       PL.........GENERALIZED BINGHAM NUMBER
C       RN.........REYNOLDS NUMBER
C       N..........NUMBER OF GRID
C       F1.........FRICTION FACTOR
C       RQ,RP.....INNER AND OUTER BOUNDARY RADII OF UNSHEARED
C       PLUG
C       V..........VELOCITY
```

```
      DO 50 I=1,NR,IR
50    RR(I)=R1-(I-1)*DELR
      WRITE(6,*)(RR(I),I=1,NR,IR)
2     FORMAT(///,35X,'VELOCITY PROFILE OF PULSATING FLOW
     + IN ANNULI',
     + ////,15X,11(5X,'R=',F3.1),//)
      RATIO=8*PL/RN/F1
      PI=4*ATAN(1.0)
      DO 100 I=1, NR
      U0(I)=0.0
      U(I)=0.0
      D(I)=0.0
100   CONTINUE
      U0(1)=0.0
      U0(NR)=0.0
      J=0
      MC=0
      T=0.0
      UT=20.0
      IM=0
300   J=J+1
      MC=MC+1
      T=J*DELT
      IF(IM.EQ.1) GO TO 900
      IF(T.GT.TMAX) GO TO 900
      IF(NCO.EQ.0)B=1.0
      IF(NCO.EQ.1)B=1+AMP*SIN(2*PI*OM*T)
      CALL DEVL1(B,F1,RN,PL,EN,NR,RP,RQ,DELR,DELT,
     + D,U0,U,RATIO,IM,W,R1,XI)
      DO 400 I=1,NR
      U0(I)=U(I)
400   CONTINUE
      IF(MC.NE.IW) GO TO 300
      MC=0
      WRITE(6,*)T,(U(I),I=1,NR+1,IR)
      UT=U(NR)
      U1=0.0
      GO TO 300
900   STOP
      END


      SUBROUTINE DEVL1(B,F1,RN,PL,EN,NR,RP,RQ,DELR,DELX,
     + D,U0,U,RATIO,IM,W,R1,XI)
      DIMENSION U0(141),U(141),D(141),
     + W1(141),W2(141),P(140,141),B1(141),R(141),U1(141)
      DO 5 I=1,NR-1
      DO 5 J=1,NR
      P(I,J)=0.0
5     CONTINUE
      IF(PL.EQ.0.0)RATIO=0.0
      W=1.0
```

```
      IF(PL.NE.0.0)RATIO=8*PL/(RN*F1)
      DO 30 I=1,NR
      R(I)=R1-(I-1)*DELR
      IF(ABS(RP-R(I)).LE.(0.5*DELR))I1=I
      IF(ABS(RQ-R(I)).LE.(0.5*DELR))I2=I
30    CONTINUE
      IF(RP.EQ.RQ)I2=I1
      U(1)=0.0
      U(NR)=0.0
      DO 11 I=1,NR
      U1(I)=U0(I)
11    CONTINUE
17    D(1)=(U1(1)-U1(2))/DELR
      D(NR)=(U1(NR-1)-U1(NR))/DELR
10    DO 20 I=2,NR-1
      D(I)=(U1(I-1)-U1(I+1))/(2*DELR)
20    CONTINUE
      DO 21 I=1,NR
      IF(EN.EQ.1.0) GO TO 12
      IF(EN.NE.1.0.AND.D(I).EQ.0.0) GO TO 14
      IF(EN.NE.1.0.AND.D(I).NE.0.0) GO TO 18
12    W1(I)=1.0
      W2(I)=1.0
      GO TO 21
14    W1(I)=0.0
      W2(I)=0.0
      GO TO 21
18    W1(I)=ABS(D(I))**(EN-1)
      W2(I)=ABS(D(I))**(EN-1)*(1+(EN-1))
21    CONTINUE
29    RR=0.0
      I0=I2-I1
      II=NR-I2
      I3=NR
      IF(PL.EQ.0.0) GO TO 44
      DO 40 I=1,I1-1
      P(I,I)=XI/(DELX*4**(EN+2))+2*W2(I+1)/(DELR*DELR)
      IF(I+2.LT.I1+1)P(I+1,I)=-W1(I+2)/(2*DELR*R(I+2))
     +-W2(I+2)/(DELR*DELR)
      P(I,I+1)=W1(I+1)/(2*DELR*R(I+1))-
     +W2(I+1)/(DELR*DELR)
      P(I,I3-1)=F1*RN*B/(2**(2*EN+3))
     ++XI*U0(I+1)/(DELX*4**(EN+2))
     +-PL/R(I+1)/(4**EN)
40    CONTINUE
      DO 41 I=I1,I2-1
      P(I,I-1)=1
      P(I,I)=-1
41    CONTINUE
      DO 43 I=I2,I3-2
      IF(I+1.LE.I3-1)P(I,I-1)=-W1(I+1)/(2*DELR*R(I+1))
     +-W2(I+1)/(DELR*DELR)
```

```
      IF(I+1.LE.I3-1)P(I,I)=XI/(DELX*4**(EN+2))
     +  +2*W2(I+1)/(DELR*DELR)
      IF(I+1.LE.I3-2)P(I,I+1)=W1(I+1)/
     +  (2*DELR*R(I+1))-W2(I+1)/(DELR*DELR)
      IF(I+1.LE.I3-1)P(I,I3-1)=XI*U0(I+1)/(DELX*4**(EN+2))
     +  +PL/R(I+1)/(4**EN)
     +  +F1*RN*B/(2**(2*EN+3))
43    CONTINUE
      GO TO 49
44    DO 45 I=1,I3-2
      P(I,I)=XI/DELX/(4**(EN+1))+2*W2(I+1)/(DELR*DELR)
      IF(I+2.LT.I3)P(I+1,I)=-W1(I+2)/(2*DELR*R(I+2))-
     +  W2(I+2)/(DELR*DELR)
      P(I,I+1)=W1(I+1)/(2*DELR*R(I+1))-
     +  W2(I+1)/(DELR*DELR)
      P(I,I3-1)=XI*U0(I+1)/DELX/(4**(EN+1))
     +  +F1*RN*B/(2**(2*EN+3))
45    CONTINUE
49    CALL SLN2(I3-2,P,B1)
      DU=0.0
      DO 50 I=1,I3-2
      U(I+1)=B1(I)
      DU1=ABS(U(I)-U0(I))
      IF(DU.LT.DU1)DU=DU1
50    CONTINUE
1001  RETURN
      END


      SUBROUTINE SLN2(N,A,X)
      DIMENSION A(140,141),X(141)
      DO 111 K=1,N
      S=0.0
      DO 222 I=K,N
      IF(ABS(A(I,K)).GT.ABS(S)) THEN
      S=A(I,K)
      I0=I
      ENDIF
222   CONTINUE
      IF(I0.EQ.K) GO TO 888
      DO 777 J=K,N+1
      T=A(K,J)
      A(K,J)=A(I0,J)
      A(I0,J)=T
777   CONTINUE
888   S=1/S
      DO 100 J=K+1,N+1
      A(K,J)=A(K,J)*S
100   CONTINUE
      DO 333 I=K+1,N
      DO 333 J=K+1,N+1
      A(I,J)=A(I,J)-A(I,K)*A(K,J)
```

```
333     CONTINUE
111     CONTINUE
        DO 555 K=N,1,-1
        C=A(K,N+1)
        DO 444 J=K+1,N
        C=C-A(K,J)*X(J)
444     CONTINUE
        X(K)=C
555     CONTINUE
        RETURN
        END
```

APPENDIX E

COMPUTER PROGRAM FOR GENERALIZED BINGHAM FLUIDS

UNSTEADY FLOW IN ECCENTRIC ANNULI

```
C       PROGRAM UNSTEADY FLOW IN ECCENTRIC ANNULI
        DIMENSION A(30,30),B(30),U0(30,30),U(30,30)
     +  ,U1(30,30),X(30,30),Y(30,30),FI(30,30),DX1(30,30),
     +  DY1(30,30),DX2(30,30),DY2(30,30),
     +  DX3(30,30),DY3(30,30),DX4(30,30),DY4(30,30),UX1(30,30),
     +  UY1(30,30),UX2(30,30),UY2(30,30),XM1(30,30),YM1(30,30),
     +  FX1(30,30),FY1(30,30),FX2(30,30),FY2(30,30),
     +  UA(30,30),UB(30,30),UC(30,30),
     +  UE(30,30),UD(30,30),UF(30,30)
        OPEN(8,FILE='YF.DAT')
        OPEN(9,FILE='X.DAT')
        OPEN(10,FILE='Y.DAT')
        OPEN(11,FILE='U.DAT')
        WRITE(*,*)' INPUT RE,PL,EN,F1,DELT,TMAX,N,
     +  RI,RO,E,IN,IW'
        READ(5,*)RE,PL,EN,F1,DELT,TMAX,N,
     +  RI,RO,E,IN,IW
        WRITE(8,1)
 1      FORMAT(//5X,'FD SOLUTION OF THE ECCENTRIC FLOW ',//)
        WRITE(8,2)RE,PL,EN,F1,RI,RO,E,DELT,N,IN
 2      FORMAT(//
     +  5X,'RE=',F7.2,5X,'PL=',F5.2,//
     +  5X,'EN=',F5.2,5X,'F1=',F7.3,//
     +  5X,'RI=',F5.2,5X,'RO=',F5.2,//
     +  5X,'E=',F5.2,5X,'DELT=',F6.4,//
     +  5X,'N=',I3,5X,'IN=',I3,////)
        R1=2*RI/(RO-RI)
        R2=2*RO/(RO-RI)
        E=2*E/(RO-RI)
        XX1=(1-R1*R1/R2/R2-E*E/R2/R2)/(2*E*R1/R2/R2)
```

```
      XX2=(1-R1*R1/R2/R2+E*E/R2/R2)/(2*E/R2)
      X1=LOG(XX1+SQRT(XX1*XX1-1))
      X2=LOG(XX2+SQRT(XX2*XX2-1))
      WRITE(*,*)'X1=',X1,'X2=',X2
      Y1=0.0
      Y2=3.1415926
      A1=R1*(EXP(X1)-EXP(-X1))/2
      WRITE(*,*)'A1=',A1
      FLOATN=N
      DELY=(Y2-Y1)/N
      DELX=(X1-X2)/N
      DO 10 J=1,N+1
      DO 10 I=1,N+1
      X(I,J)=X2+DELX*(I-1)
      Y(I,J)=Y1+DELY*(J-1)
      FI(I,J)=(EXP(X(I,J))+EXP(-X(I,J)))/2-COS(Y(I,J))
      FX1(I,J)=(EXP(X(I,J)+0.5*DELX)+EXP(-X(I,J)-0.5*DELX))/2
     +-COS(Y(I,J))
      FX2(I,J)=(EXP(X(I,J)-0.5*DELX)+EXP(-X(I,J)+0.5*DELX))/2
     +-COS(Y(I,J))
      IF(I.EQ.1) FX2(I,J)=FI(I,J)
      IF(I.EQ.N+1)FX1(I,J)=FI(I,J)
      FY1(I,J)=(EXP(X(I,J))+EXP(-X(I,J)))/2-COS(Y(I,J)+0.5*DELY)
      FY2(I,J)=(EXP(X(I,J))+EXP(-X(I,J)))/2-COS(Y(I,J)-0.5*DELY)
      A(I,J)=0.0
      B(I)=0.0
      U(I,J)=0.0
      U0(I,J)=0.0
      U1(I,J)=0.0
10    CONTINUE
      T=0.0
      IP=0
      VIS=0.01
      MT=0
      MM=0
      IM=0
      DU0M=0.0
      N1=0
800   T=T+DELT
      MM=MM+1
      MT=MT+1
      IM=0
      IF(T.GT.TMAX) GO TO 1000
700   IM=IM+1
      DUM=0.0
      DIM=0.0
      DO 21 J=1,N+1
      DO 21 I=2,N
      IF(PL.EQ.0.0.AND.EN.EQ.1.0)GOTO 18
      DX1(I,J)=(U1(I+1,J)-U1(I,J))/DELX
      DX2(I,J)=(U1(I,J)-U1(I-1,J))/DELX
      IF(J.NE.1.AND.J.NE.N+1) THEN
```

```
      DX3(I,J)=(U1(I+1,J)+U1(I+1,J+1)-U1(I-1,J)
     +  -U1(I-1,J+1))/4/DELX
      DX4(I,J)=(U1(I+1,J-1)+U1(I+1,J)-U1(I-1,J-1)
     +  -U1(I-1,J))/4/DELX
      DY1(I,J)=(U1(I+1,J+1)+U1(I,J+1)-U1(I,J-1)
     +  -U1(I+1,J-1))/4/DELY
      DY2(I,J)=(U1(I,J+1)+U1(I-1,J+1)-U1(I,J-1)
     +  -U1(I-1,J-1))/4/DELY
      DY3(I,J)=(U1(I,J+1)-U1(I,J))/DELY
      DY4(I,J)=(U1(I,J)-U1(I,J-1))/DELY
      ENDIF
      IF(J.EQ.1) THEN
      DX3(I,J)=(U1(I+1,J)+U1(I+1,J+1)-U1(I-1,J)
     +  -U1(I-1,J+1))/4/DELX
      DX4(I,J)=(U1(I+1,J+1)+U1(I+1,J)-U1(I-1,J+1)
     +  -U1(I-1,J))/4/DELX
      DY1(I,J)=0.0
      DY2(I,J)=0.0
      DY3(I,J)=(U1(I,J+1)-U1(I,J))/DELY
      DY4(I,J)=(U1(I,J)-U1(I,J+1))/DELY
      ENDIF
      IF(J.EQ.N+1) THEN
      DX3(I,J)=(U1(I+1,J)+U1(I+1,J-1)-U1(I-1,J)
     +  -U1(I-1,J-1))/4/DELX
      DX4(I,J)=(U1(I+1,J-1)+U1(I+1,J)-U1(I-1,J-1)
     +  -U1(I-1,J))/4/DELX
      DY1(I,J)=0.0
      DY2(I,J)=0.0
      DY3(I,J)=(U1(I,J-1)-U1(I,J))/DELY
      DY4(I,J)=(U1(I,J)-U1(I,J-1))/DELY
      ENDIF

      DDX1=SQRT(DX1(I,J)*DX1(I,J)+DY1(I,J)*DY1(I,J))
      IF(DDX1.LE.VIS)THEN
      UX1(I,J)=
     +  ABS(PL*A1/FX1(I,J)/1.0)+ABS(FX1(I,J)/A1)**(EN-1)*
     +  VIS**(EN-1)
      ELSE
      UX1(I,J)=ABS(PL*A1/FX1(I,J)/1.0)
     +  +(ABS(FX1(I,J)/A1))**(EN-1)*DDX1**(EN-1)
      ENDIF

      DDX2=SQRT(DX2(I,J)*DX2(I,J)+DY2(I,J)*DY2(I,J))
      IF(DDX2.LE.VIS)THEN
      UX2(I,J)=
     +  ABS(PL*A1/FX2(I,J)/1.0)+ABS(FX2(I,J)/A1)**(EN-1)*
     +  VIS**(EN-1)
      ELSE
      UX2(I,J)=ABS(PL*A1/FX2(I,J)/1.0)
     +  +(ABS(FX2(I,J)/A1))**(EN-1)*DDX2**(EN-1)
      ENDIF
```

```
      DDY1=SQRT(DX3(I,J)*DX3(I,J)+DY3(I,J)*DY3(I,J))
      IF(DDY1.LE.VIS)THEN
      UY1(I,J)=
     +ABS(PL*A1/FY1(I,J)/1.0)+ABS(FY1(I,J)/A1)**(EN-1)*
     +VIS**(EN-1)
      ELSE
      UY1(I,J)=ABS(PL*A1/FY1(I,J)/1.0)
     ++(ABS(FY1(I,J)/A1))**(EN-1)*DDY1**(EN-1)
      ENDIF

      DDY2=SQRT(DX4(I,J)*DX4(I,J)+DY4(I,J)*DY4(I,J))
      IF(DDY2.LE.VIS)THEN
      UY2(I,J)=
     +ABS(PL*A1/FY2(I,J)/1.0)+ABS(FY2(I,J)/A1)**(EN-1)*
     +VIS**(EN-1)
      ELSE
      UY2(I,J)=ABS(PL*A1/FY2(I,J)/1.0)
     ++(ABS(FY2(I,J)/A1))**(EN-1)*DDY2**(EN-1)
      ENDIF
18    IF(PL.EQ.0.0.AND.EN.EQ.1.0) THEN
      UX1(I,J)=1.0
      UX2(I,J)=1.0
      UY1(I,J)=1.0
      UY2(I,J)=1.0
      ENDIF
      UA(I,J)=-UX2(I,J)/(DELX*DELX)
      UB(I,J)=-UX1(I,J)/(DELX*DELX)
      UC(I,J)=-UY2(I,J)/(DELY*DELY)
      UD(I,J)=-UY1(I,J)/(DELY*DELY)
      UE(I,J)=A1*A1/(FI(I,J)*FI(I,J))*(1/DELT)
     +-UA(I,J)-UB(I,J)-UC(I,J)-UD(I,J)
      UF(I,J)=(U0(I,J)/DELT+F1*RE/2)*A1*A1/(FI(I,J)*
     +FI(I,J))
21    CONTINUE
      DO 100 J=1,N+1
      DO 30 I=1,N-1
      A(I,I)=UE(I+1,J)
      IF(I+1.LT.N)A(I,I+1)=UB(I+1,J)
      IF(I+1.LT.N)A(I+1,I)=UA(I+2,J)
      IF(J.NE.1.AND.J.NE.N+1)A(I,N)=-UC(I+1,J)*U1(I+1,J-1)
     +-UD(I+1,J)*U1(I+1,J+1)+UF(I+1,J)
      IF(J.EQ.1)A(I,N)=-(UC(I+1,J)+UD(I+1,J))*U1(I+1,J+1)+
     +UF(I+1,J)
      IF(J.EQ.N+1)A(I,N)=-(UC(I+1,J)+UD(I+1,J))*U1(I+1,J-1)
     ++UF(I+1,J)
      IF(I.NE.1.AND.I.NE.N-1)THEN
      IF(A(I,I+1).EQ.0.0)THEN
      A(I,I)=1.0
      A(I,I-1)=-1.0
      A(I,N)=0.0
      ENDIF
      ENDIF
```

```
30      CONTINUE
        CALL SLN(N-1,A,B)
        DO 50 I=1,N-1
        U(I+1,J)=B(I)
        DU=ABS(U(I,J)-U1(I,J))
        DU0=ABS(U(I,J)-U0(I,J))
        IF(DU0.GT.DU0M)DU0M=DU0
        IF(DU.GT.DUM)DUM=DU
50      CONTINUE
100     CONTINUE
        DO 60 J=1,N+1
        DO 60 I=2,N+1
        IF(ABS(U(I,J)-U(I-1,J)).LT.0.02)U(I,J)=U(I-1,J)
        U1(I,J)=U(I,J)
60      CONTINUE
        WRITE(*,*)'IM=',IM,'DUM=',DUM
        IF(DUM.GT.0.01)GOTO 700
191     DO 210 I=1,N+1
        DO 210 J=1,N+1
        U0(I,J)=U(I,J)
210     CONTINUE
        IF(MT.NE.IN) GO TO 800
        MT=0
        WRITE(8,295)T
295     FORMAT(//,5X,F6.4)
        DO 300 J=1,N+1,5
        WRITE(*,*)(U(I,J),I=1,N+1)
        WRITE(8,297)(U(I,J),I=1,N+1)
297     FORMAT(//,5X,6(F7.4,2X),//,5X,5(F7.4,2X))
300     CONTINUE
        IF(DU0M.LT.0.000001)GOTO 1000
        GOTO 800
1000    DO 1100 I=1,N+1,IW
        DO 1100 J=1,N+1,IW
        XM1(I,J)=A1*SINH(X(I,J))/(COSH(X(I,J))-COS(Y(I,J)))
        YM1(I,J)=-A1*SIN(Y(I,J))/(COSH(X(I,J))-COS(Y(I,J)))
1100    CONTINUE
        DO 1200 I=1,N+1,IW
        DO 1200 J=1,N+1,IW
        WRITE(9,*)XM1(I,J),YM1(I,J),U(I,J)
1200    CONTINUE
        STOP
        END

        SUBROUTINE SLN(N,TT,B)
        DIMENSION TT(30,30), B(30)
        DO 333 K=1,N-1
        DO 333 I=K+1,N
        DO 333 J=K+1,N+1
        TT(I,J)=TT(I,J)-TT(I,K)*TT(K,J)/TT(K,K)
333     CONTINUE
        B(N)=TT(N,N+1)/TT(N,N)
```

```
      DO 555 K=N-1, 1, -1
      C1=0.0
      DO 444 J=K+1,N
      C1=C1+TT(K,J)*B(J)
444   CONTINUE
      B(K)=(TT(K,N+1)-C1)/TT(K,K)
555   CONTINUE
      RETURN
      END
```